THE 4TH INTERNATIONAL WORKSHOP ON SIMULATION FOR ENERGY, SUSTAINABLE DEVELOPMENT & ENVIRONMENT

SEPTEMBER 26-28 2016

CYPRUS

EDITED BY

AGOSTINO BRUZZONE
JANOS SEBESTYEN JANOSY
LETIZIA NICOLETTI
GREGORY ZACHAREWICZ

PRINTED IN RENDE (CS), ITALY, SEPTEMBER 2016

ISBN 978-88-97999-72-0 (paperback)
ISBN 978-88-97999-80-5 (PDF)

ISBN 978-88-97999-72-0 (paperback)
ISBN 978-88-97999-80-5 (PDF)

THE 4ND INTERNATIONAL WORKSHOP ON SIMULATION FOR ENERGY, SUSTAINABLE DEVELOPMENT & ENVIROMENT, SESDE 2016

SEPTEMBER 26-28 2016, CYPRUS

ORGANIZED BY

DIME – UNIVERSITY OF GENOA

LIOPHANT SIMULATION

SIMULATION TEAM

IMCS – INTERNATIONAL MEDITERRANEAN & LATIN AMERICAN COUNCIL OF SIMULATION

DIMEG, UNIVERSITY OF CALABRIA

MSC-LES, MODELING & SIMULATION CENTER, LABORATORY OF ENTERPRISE SOLUTIONS

MODELING AND SIMULATION CENTER OF EXCELLENCE (MSCOE)

LATVIAN SIMULATION CENTER – RIGA TECHNICAL UNIVERSITY

LOGISIM

LSIS – LABORATOIRE DES SCIENCES DE L'INFORMATION ET DES SYSTEMES

MIMOS – MOVIMENTO ITALIANO MODELLAZIONE E SIMULAZIONE

MITIM PERUGIA CENTER – UNIVERSITY OF PERUGIA

BRASILIAN SIMULATION CENTER, LAMCE-COPPE-UFRJ

MITIM - MCLEOD INSTITUTE OF TECHNOLOGY AND INTEROPERABLE MODELING AND SIMULATION – GENOA CENTER

M&SNET - MCLEOD MODELING AND SIMULATION NETWORK

Latvian Simulation Society

Ecole Superieure d'Ingenierie en Sciences Appliquees

Facultad de Ciencias Exactas. Ingegneria y Agrimensura

University of La Laguna

CIFASIS: CONICET-UNR-UPCAM

INSTICC - Institute for Systems and Technologies of Information, Control and Communication

National Russian Simulation Society

CEA - IFAC

University of Bordeaux

University of Cyprus

I3M 2016 Industrial Sponsors

CAL-TEK SRL

LIOTECH LTD

MAST SRL

SIM-4-FUTURE

I3M 2016 Media Partners

Inderscience Publishers – International Journal of Simulation and Process Modeling

INDERSCIENCE PUBLISHERS – INTERNATIONAL JOURNAL OF CRITICAL INFRASTRUCTURES

INDERSCIENCE PUBLISHERS – INTERNATIONAL JOURNAL OF ENGINEERING SYSTEMS MODELLING AND SIMULATION

INDERSCIENCE PUBLISHERS – INTERNATIONAL JOURNAL OF SERVICE AND COMPUTING ORIENTED MANUFACTURING

IGI GLOBAL – INTERNATIONAL JOURNAL OF PRIVACY AND HEALTH INFORMATION MANAGEMENT

HALLDALE MEDIA GROUP: MILITARY SIMULATION AND TRAINING MAGAZINE

HALLDALE MEDIA GROUP: THE JOURNAL FOR HEALTHCARE EDUCATION, SIMULATION AND TRAINING

SAGE
SIMULATION TRANSACTION OF SCS

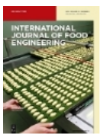

DE GRUYTER
INTERNATIONAL JOURNAL OF FOOD ENGINEERING

EDITORS

AGOSTINO BRUZZONE
MITIM-DIME, UNIVERSITY OF GENOA, ITALY
agostino@itim.unige.it

JANOS SEBESTYEN JANOSY
MTA EK CENTRE FOR ENERGY RESEARCH HUNGARIAN ACADEMY OF SCIENCES, HUNGARY
jjs@sunserv.kfki.hu

LETIZIA NICOLETTI
CAL-TEK SRL
l.nicoletti@cal-tek.eu

GREGORY ZACHAREWICZ
IMS UNIVERSITÉ BORDEAUX 1, FRANCE
Gregory.zacharewicz@ims-bordeaux.fr

THE INTERNATIONAL MULTIDISCIPLINARY MODELING AND SIMULATION MULTICONFERENCE, I3M 2016

GENERAL CO-CHAIRS

AGOSTINO BRUZZONE, *MITIM-DIME, UNIVERSITY OF GENOA, ITALY*
YURI MERKURYEV, *RIGA TECHNICAL UNIVERSITY, LATVIA*

PROGRAM CHAIR

FRANCESCO LONGO, *DIMEG, UNIVERSITY OF CALABRIA, ITALY*

THE 4TH INTERNATIONAL WORKSHOP ON SIMULATION FOR ENERGY, SUSTAINABLE DEVELOPMENT & ENVIRONMENT, SESDE 2016

GENERAL CHAIR

JANOS SEBESTYEN JANOSY, *MTA EK CENTRE FOR ENERGY RESEARCH HUNGARIAN ACADEMY OF SCIENCES, HUNGARY*

PROGRAM CHAIR

GREGORY ZACHAREWICZ, *IMS UNIVERSITÉ BORDEAUX 1, FRANCE*

SESDE 2016 International Program Committee

Michael Affenzeller, *Upper Austria UAS, Austria*
Matteo Agresta, *University of Genoa, Italy*
Angelo Algieri, *University of Calabria, Italy*
Agostino Bruzzone, *University of Genoa, Italy*
Daniel Buchbinder, *Alterna, Guatemala*
Riccardo Di Matteo, *University of Genoa, Italy*
Stephan Hutterer, *Upper Austria University of Applied Sciences, Austria*
Janos Sebestyen Janosy, *MTA EK Centre for Energy Research Hungarian Academy of Sciences, Hungary*
Luis Le Moyne, *University of Bourgogne, France*
Arnis Lektauers, *Riga Technical University, Latvia*
Francesco Longo, *University of Calabria, Italy*
Gianluca Maglione, *University of Genoa, Italy*
Marina Massei, *University of Genoa, Italy*
Pietropaolo Morrone, *University of Calabria, Italy*
Letizia Nicoletti, *Cal-Tek Srl, Italy*
Antonio Padovano, *University of Calabria, Italy*
Gregory Zacharewicz, *IMS Université Bordeaux 1, France*

Tracks and Workshop Chairs

Simulation pro Energy, Environment and Development - SpEED
Chair: Angelo Algieri, University of Calabria, Italy

Transportations
Co-Chairs: Arnis Lektauers, Riga Technical University. Latvia; Luis Le Moyne, University of Bourgogne, France

"Smart Grid Planning, Optimization and Control - SPOC"
Chairs: Michael Affenzeller, Upper Austria University of Applied Sciences, Austria; Stephan Hutterer, Upper Austria University of Applied Sciences, Austria

Sustainable Land Use and Transport Adopting M&S
Chair: Daniel Buchbinder, Alterna, Guatemala

Consumerism
Chair: Daniel Buchbinder, Alterna, Guatemala

Sustainability
Chair: Daniel Buchbinder, Alterna, Guatemala

CHAIRS' MESSAGE

It is our pleasure to welcome all of you in Larnaca (Cyprus) for the International Workshop on Simulation for Energy, Sustainable Development & Environment (SESDE 2016).

As part of the International Multidisciplinary Modeling & Simulation Multi-conference (I3M), SESDE takes care of all the Modeling & Simulation theories, methodologies and applications related to Energy, Sustainability and Environmental Issues.

The articles included in the SESDE 2016 proceedings look in different directions and applications areas. Among others, the selected articles deal with design of hybrid electric vehicles, forest ecosystems assessment, renewable energy systems, electrical systems in standalone buildings, water and carbon footprint of extended supply chains, disasters prevention in urban areas.

Even if SESDE is a small workshop, it has the unquestionable advantage to bring together scientists that share the same research interests and discuss similar problems. Furthermore, having access to all the I3M sessions, the SESDE attendees may exchange new ideas and experience a full multidisciplinary framework.

As General and Program Chairs of SESDE, we are grateful not only to the authors but also to the International Program Committee Members as well as to the Reviewers and to the I3M Internal Staff. Their continuous support makes our workshop "sustainable"!

Again, welcome to SESDE 2016 and welcome to Larnaca where we hope we can share thoughts and ideas for a better world.

Janos Sebestyen Janosy
MTA EK Centre for Energy Research
Hungarian Academy of Sciences, Hungary

Gregory Zacharewicz,
Ims Université Bordeaux 1
France

ACKNOWLEDGEMENTS

The SESDE 2016 International Program Committee (IPC) has selected the papers for the Conference among many submissions; therefore, based on this effort, a very successful event is expected. The SESDE 2016 IPC would like to thank all the authors as well as the reviewers for their invaluable work.
A special thank goes to Prof. Loucas S. Louca from University of Cyprus as local organizer and to all the organizations, institutions and societies that have supported and technically sponsored the event.

I3M 2016 INTERNAL STAFF

MATTEO AGRESTA, *SIMULATION TEAM, ITALY*
LUIGI BRUNO, *DIMEG, UNIVERSITY OF CALABRIA*
AGOSTINO G. BRUZZONE, *DIME, UNIVERSITY OF GENOA, ITALY*
ALESSANDRO CHIURCO, *DIMEG, UNIVERSITY OF CALABRIA, ITALY*
RICCARDO DI MATTEO, *SIMULATION TEAM, ITALY*
CATERINA FUSTO, *, CAL-TEK SRL, ITALY*
FRANCESCO LONGO, *DIMEG, UNIVERSITY OF CALABRIA, ITALY*
GIANLUCA MAGLIONE, *SIMULATION TEAM, ITALY*
MARINA MASSEI, *LIOPHANT SIMULATION, ITALY*
LETIZIA NICOLETTI, *, CAL-TEK SRL, ITALY*
ANTONIO PADOVANO, *DIMEG, UNIVERSITY OF CALABRIA, ITALY*
LUCA ROTUNDO, *DIMEG, UNIVERSITY OF CALABRIA, ITALY*
CATALDO RUSSO, *CAL-TEK SRL, ITALY*
GIUSEPPE SPEZZANO, *DIMEG, UNIVERSITY OF CALABRIA, ITALY*
MARCO VETRANO, *CAL-TEK SRL, ITALY*

This International Workshop is part of the I3M Multiconference: the Congress leading **Simulation around the World and Along the Years**

Index

MULTI-ARCHITECTURE / MULTI-APPLICATION MODELLING APPROACH FOR HYBRID ELECTRIC VEHICLE USING ENERGETIC MACROSCOPIC REPRESENTATION

Daniela CHRENKO[(a)], Shiyu GAN[(b)], Phillipe BOUILLOT[(c)], Luis LE MOYNE[(d)]

[(a,b,d)]ID-MOTION DRIVE EA 1859, Univ. Bourgogne Franche Comté, F58027, Nevers, France
[(b,c)]SODEMO Moteurs, Technopole du Circuit BP 37, 58470 Magny-Cours, France

[(a)]daniela.chrenko@u-bourgogne.fr, [(b)]shiyu.gan@sodemo.com, [(c)]philippe.boulliot@sedomo.com,
[(d)]luis.le-moyne@u-bourgogne.fr

ABSTRACT
Hybrid vehicles are among the most promising solutions for a sustainable mobility. Among the multitude of hybrid architectures three architectures seem to be equally promising (series, parallel and series/parallel) and it is possible to find them in a multitude of applications like motor bikes, city- and family-cars as well as busses. Each application needs an adapted control strategy. The most important tool in the development of control strategies is a well configured model. This article presents a multi-architecture/multi-application model for hybrid vehicles using energetic macroscopic representation and inversion based control design. This approach is successfully used to evaluate the power split and fuel consumption of different vehicles on different driving cycles.

Keywords: hybrid electric vehicles (HEVs), hybrid architecture, energetic macroscopic representation (EMR), energy management

1. INTRODUCTION
The limitation of crude oil resources and the global warming due to greenhouse gas emissions emphasis the need to develop more fuel efficient and cleaner solutions for all sectors of road transportation. Hybrid Vehicles are among the most promising approaches to maintain our mode of personal and individual transportation. A hybrid electric vehicle (HEV) uses two or more different energy sources, storages or converters from which at least one has to deliver its energy in electric form (Guzzella & Sciarretta 2010). Goal of hybridization is to use all propulsion components in their best efficiency regions in order to improve the global efficiency of a vehicle. The large definition of HEVs leads to a multitude of technical solutions with regard to degree of hybridization as well as hybridization architecture and for the moment no solutions shows a considerable advantage. At the same time individual transportation is a broad field not only dominated by the multitude of cars existing, but compromising also two wheelers (scooters and motor bikes) and in a broader sense busses and race cars as technology showcase.
In the product development modeling gets more and more important as it allows the acceleration of multiple aspects of the development as for example the component dimensioning, packaging and design. The entire automotive V-development process (Prechelt n.d.) is accompanied by models with a different degree of detail. Amongst them, the vehicle model is an important tool for the development of system control, especially the energy management. As the advantage of hybridization is strongly linked to the global efficiency, a well-adapted system control is required. Moreover, hybrid system energy management development requires the availability of a system model that can be run in real time, therefore a tradeoff has to be made between model accuracy and calculation time (Kutter & Bäker 2010).
Goal of this work is to develop a generic approach that is capable to represent different hybrid architectures in one single model parameterized accordingly and to use this approach in order to develop energy management strategies.
Energetic Macroscopic Representation (EMR) is a representation tool, capable to visualize complex systems and well adapted for inversion based control design.
In the following section different vehicle architectures and control approaches are presented. Section 3 introduces EMR, the development of a generic hybrid vehicle model and inversion based control design. Results of this approach for different vehicles are discussed in section 4. Conclusions and Perspectives are given in section 5.

2. HYBRID VEHICLE ARCHITECTURES
Hybrid vehicles can be classified according to the degree of hybridization into Micro-HEV, Mild-HEV and Full-HEV (Marc et al. 2010) or according to the power train architecture as Series-HEV, Parallel-HEV and Complex-HEV. If a hybrid electric vehicle can be recharged by connecting a plug to an external electric power source, it can be called a plug-in HEV. Likewise, if an electric vehicle contains a range extender (it is usually an ICE) in order to increase the electric vehicle driving autonomy, we can call this type of vehicle an Extended-range electric vehicle (EREV) (Tingting 2011).

2.1. Architectures
Series Hybrid: In series hybrids, only the electric motor drives the drivetrain, and a smaller ICE works with a generator to power the electric motor or to recharge the batteries. They also usually have a larger

battery pack than parallel hybrids, making them more expensive. Once the battery charge is low, the combustion engine can continously generate power at its optimum settings. As soon as the battery charge is sufficient, the combustion engine is switched off making the hybrid system efficient in extensive city driving (Asus et al. 2013). The series hybrid structure has always been used in the frequent start/stop driving situation such as the city bus, Volvo B5L and Gemini 2 HEV are commercially available series full-HEV (Wikipedia n.d.).

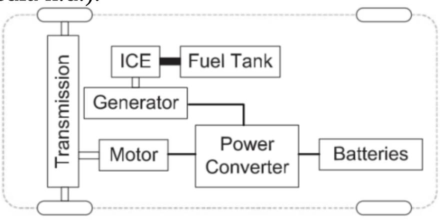

Figure 1: Series Hybrid Configuration

Parallel Hybrid: In parallel full-HEV, the ICE (internal combustion engine) and EM (electric machine) are mechanical coupled and can both deliver power in parallel to the wheel. A parallel HEV is capable of improving the overall efficiency to 43.4% (Tie & Tan 2013). Parallel full-HEV, compared to series HEV, have a lower battery capacity. One of the advantages of parallel full-HEV is that the EM and ICE complement each other during driving. This makes the parallel full-HEV a more desirable vehicle under both highway-driving and city-driving conditions. As compared to series full- HEV, parallel full-HEV has higher efficiency due to smaller EM and battery size. (Tie & Tan 2013).
Honda Insight, Honda Civic Hybrid and Ford Escape are commercially available parallel full-HEV.

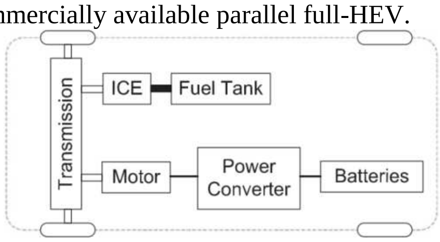

Figure 2: Parallel Hybrid Configuration

Series-Parallel Hybrid: The series–parallel full-HEV drive train employs two power couplers that are mechanically powered and electrically powered. Although it possesses the advantage of series full-HEV and parallel full-HEV, it is relatively more complicated and costly. For the Series-parallel hybrid vehicle, there are 2 possible approaches for the transmission: Electric-Variable-Transmission (EVT) and Planetary-gear-set (Ifak & Iml 2015). The objective of these 2 combinations is to operate ICE at the optimum working point which means at its optimum rotational speed and torque. For series–parallel full-HEV, they are more flexible with regard to their control strategies than the other two configurations.

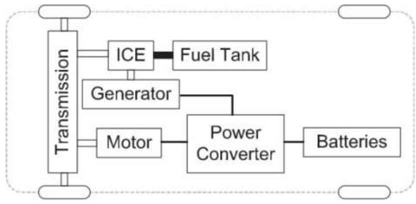

Figure 3: Series-Parallel Hybrid Configuration

Toyota Prius, Lexus LS 600h, Lexus CT 200h and Nissan Tino are commercially available series–parallel full-HEV (Ifak & Iml 2015).
Complex Hybrid: A multitude of other hybrid architectures exist as for example the electric turbocharging (e-Turbo) used in Formula 1 race cars or Le Mans prototypes (Le Mans 2012). Those other architectures are classified as complex hybrids.

2.2. Control Strategies

The energy management strategy of a hybrid vehicle is extremely important as it decides how and when energy will be provided by the various sources of HEV. A control strategy for a PHEV does not necessarily provide maximum fuel savings over all driving demand (Amjad et al. 2010). *Zhang et al.* present an extensive overview of the state of the art control strategies for Hybrid vehicles and classify them in detail which include rule based strategies and optimization based strategies (Zhang et al. 2015). In rule based control strategies, the determined and fuzzy logic strategies have been considered. And in optimization based control strategies, transient and global strategies are included. A similar work has been provided by *Chrenko et al.* (Chrenko et al. 2015).

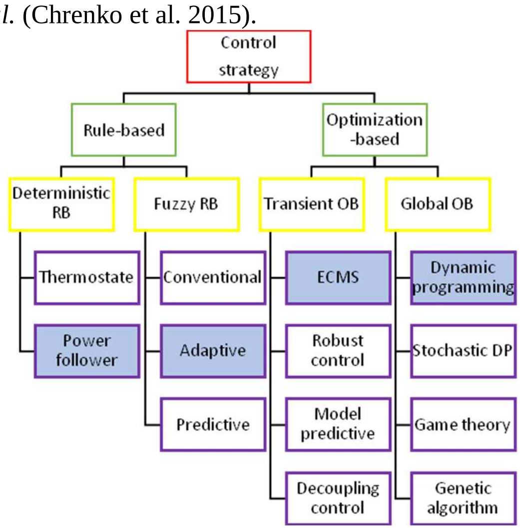

Figure 4: Classification of Control Strategies

Rule based strategies: The primary aspect involved in rule-based power management approaches is their effectiveness to instantly control the power flow in every kind of hybrid powertrain. The rules are determined by heuristics, intuition, human expertise and actually mathematical models and normally, without a priori familiarity with a predefined driving period. These strategies can possibly be classified into deterministic and also fuzzy rule based approaches. The main idea associated with rule based strategies is to move the actual ICE operating point as close as possible to some predetermined value for each and every instant in time in the vehicle operation. If the best efficiency should be used, the vehicle operation points will be forced in the vicinity of the best point of efficiency at a particular engine speed. The resulting power differences, which can be positive or negative, are contributed simply by EM (Asus et al. 2014).

Optimization Based Strategies: In optimization-based control strategies, the reference of the optimal torques and optimal gear ratios can be found by minimizing a cost function of fuel consumption and/or emissions. Global Optimization strategy needs the information of the whole driving cycle which includes the driving speed, acceleration, stop numbers and times, as well as the traffic conditions. The **global OB** can be a good reference for other control strategies. However, with global OB control techniques, real-time energy management is not directly possible.

However, on the basis of an instantaneous cost function, a control strategy based on a real time optimization can be obtained. This instantaneous cost function relies on the system variables at the current time only and also, to maintain the battery SOC with a certain range of variation, it should include equivalent fuel consumption. This control strategy is referred to as **transient OB**.

3. ENERGETIC MACROSCIPIC REPRESENTATION (EMR)

3.1. Introduction

Based on the energy-flow analysis in multi-physics systems, a new representation has been developed by a French research team from the L2EP (a laboratory from University for Sciences and Technologies of Lille) namely Energetic Macroscopic Representation (EMR). Such a representation has been used to propose a synthetic description of electromechanical conversion system, but can be today extended to other types of conversion system where the energy flows have to be managed between more than two sources of different nature (electrical, thermal engine, electrochemical source), through complex paths (Barrade & Bouscayrol 2011).

EMR representation is a synthetic graphical tool based on the principle of action and reaction between connected elements. Components can be internally described by causal ordering graphs, or other descriptions such as transfer functions, Petri nets, state models, bond-graphs (Lhomme et al. 2004). EMR representation allows an upgrade of dedicated sub-models, like the battery model, without the need to change the rest of the model.

The EMR is not only useful for the synthetic representation of complex systems but also for the deduction of an Inversed Based Control scheme (IBC) which is directly obtained from the EMR through specific inversion rules. The IBC leads to a control structure with a maximum number of operations and measurements. Then the final control implements results from simplifications applied on the IBC.

The EMR is based on three kinds of elements which describe the physical state of a component.

Source elements (green oval pictograms) produce state variables (outputs). They can be either generators or receptors. They are disturbed by reactions of other elements.

Conversation elements ensure energy conversion without energy accumulation (power converter, gear box, etc…). They have eventually tuning inputs (red pins) to adjust the conversion between input (action) and output (reaction) variables. Depending on the nature of the conversion, they are depicted by rectangular or circular pictograms. The rectangular pictogram is used for mono-physical conversion (eg. electrical to electrical). The rectangular pictogram is used for multi-physical conversion (eg. chemical to mechanical).

Coupling elements allow the representation of energy distribution (parallel connection of electrical branches for example). They do not have any tuning pin. The energy distribution is then only defined by their internal description.

Accumulation elements (orange rectangular pictograms with an oblique bar) connect other elements, thanks to energy storage, which induces at least one state variable.

All these elements are connected through exchange vectors according to the principle of action and reaction. For energy conversion systems, specific association rules have been defined to build their EMR. The names of variables are associated with originating devices.

From the EMR of a system, one can deduce a control structure, which is composed of a maximum of control operations and measurements. This method is the so called **maximum control structure (MCS)**. Continuous lines are associated with the inversion of action variables while dotted lines are related to the rejection of disturbance variables. All control blocks are depicted by blue parallelograms because they handle only information.

A control structure has to inverse the global functions of the power system. In the MCS approach, the global control structure is decomposed into several control blocks. Each block has to inverse one power element of the EMR. Conversion elements are inverted directly. Accumulation elements need controllers in order to solve the inversion problem of their state variables. All the inputs of power elements, which are not used in the inversion chain, become disturbance inputs. So they are directly rejected in order to minimize their influence.

A tuning chain is defined from the technical requirements. It connects the chosen tuning input of the global system to the wished action output through action inputs of power elements. The other inputs therefore become disturbances. In most electric drive applications, the static converter is chosen as the tuning element.

Then a control chain is obtained by inversion of the tuning chain: from the reference variable to the tuning variable. All the variables are initially considered as measurable. So, the control chain links to control blocks, which are inversions of power elements connected by the tuning chain. It is obvious that the MCS is the most complete control strategy. In real cases, control structures can be deduced from the MCS by simplifications or by taking into account estimations of non-measurable variables. *Locment et al.* (Locment & Sechilariu 2010) developed an EVs charging system with photovoltaic grid-connected model using EMR which allows the EVs feeding at the same time as PV energy production. Then a corresponding Maximum Control Structure (MCS) is deduced from the EMR, through specific inversion rules: direct inversion (without controller) for items that do not vary over time, indirect inversion (with controller) for items that vary over time.

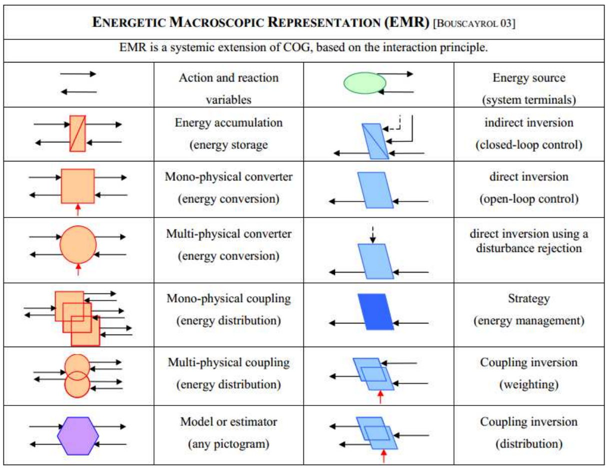

Figure 5: EMR blocks introduction

3.2. Representation of HEVs

Chrenko et al. (Chrenko et al. 2007; Chrenko et al. 2008) use EMR to model fuel cell systems which includes its basic elements and its inversion, the Maximum Control Structure (MCS) in order to develop a fuel cell based auxiliary power unit capable of trigeneration (electricity, heat and refrigeration). She used the model based control development of fuel cell systems because often model based control approaches are rather focused on details of the system than on the overall system.

Allègre et al. (Allègre et al. 2013) realize a hybrid energy storage system (HESS) and flexible control scheme by using EMR. The HESS is composed by batteries and super-capacitors and four energy management strategies have been proposed to control the system. They compare 4 types of strategies because they want to evaluate the characteristics on different criteria: electric consumption, sizing and the lifetime of the batteries.

Martinez et al. (Solano Martinez et al. 2012) develop the different EMR control systems for a multiple architecture heavy duty hybrid vehicle and present different energetic configurations using the available power and energy sources. Their objective is to test the different energetic configurations using various power and energy sources: Fuel cell system, Super-capacitors, Flywheels and ICE. Therefore they chose to use EMR representation to design control structures.

Chen et al. use just one EMR model for different hybrid vehicle architectures (series, parallel and series-parallel). She used EMR to represent different components of the hybrid vehicle, and then switches the model to different architectures by changing the parameters' values. The main objective of this article is to provide a control strategy for an HEV using an Electric Variable Transmission (EVT). A simple deterministic rule based control strategy has been used and the final simulation results prove that EVT could not only satisfy the vehicle performance but also optimize ICE operation and fuel consumption is reduced compared to a conventional vehicle.

Lhomme et al. (Lhomme et al. 2008) build two EMR models to describe 2 states of a clutch, locked or slipping. Author chose to use EMR to represent the clutch working system because certain difficulties arise when attempting to model a clutch by traditional methods due to its nonlinear behavior. In the simulation, two models are used—one for the clutch slipping and another for the clutch locked. Both models are connected using a switch selector to respect the criteria that are necessary to ensure the physical energy flow that is required during the commutation between both models. And the simulation result shows that the switched causal modeling allows the clutch to be simulated without difficulty and with a relatively short computation time.

Liukkonen et al. (Liukkonen & Suomela 2012) design a method for an energy management scheme of a series hybrid powertrain which provides maximal use of the battery, ultra-capacitor, and fuel cell source. Authors describe an energy management algorithm for the dimensioning of the powertrain components.

Silva et al. (Silva et al. 2012) used EMR to model and control an electric vehicle because they want to use both functional (Bond graph model) and structural (EMR model) approaches in the same simulation environment in order to analyze the behavior of the vehicle and its control.

Asus et al. (Asus et al. 2014) used EMR to improve the energy management in a series hybrid race car using different control strategies.

3.3. Multi Architecture Simulation Approach

3.3.1 Modeling Approach

Goal is to provide a generic approach for a multi-architecture / multi-application modeling and control approach for hybrid vehicles. Therefore, the EMR-Model is divided into 2 parts which include the "Source of Vehicle" and the "Coupling Switch". "Source of Vehicle" includes the energy source sub-models and energy flow transmission as well as conversion sub models. The desired driving cycle data will be

introduced in this part of the model with help of the reference command signals which are provided by “Coupling Switch”.
Figure 6 represents the EMR model structure of the “source of vehicle” which includes source of environment, chassis, wheel and transmission. This part does not change for different architectures. By changing the mass of vehicle, frontal surface, drag force coefficient, etc., it is possible to adapt the model to the type of vehicles simulated.

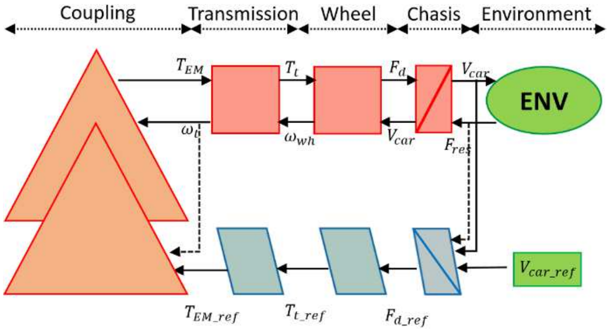

Figure 6: EMR of vehicle environment

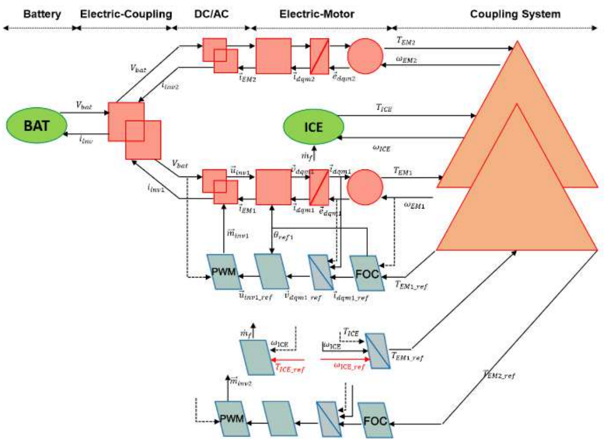

Figure 7: EMR of energy sources

Figure 7 represents the EMR model structure before torque coupling system, which includes the power sources: EM1, EM2, and ICE. The inputs of these power sources are rotational speed and their outputs are torque. They are controlled by their inversion based blocks. For different simulated vehicle, the power sources’ parameters as well as the engine fuel map and motor efficiency maps can be modified. For different architectures, not all of these power sources are needed. If the power source is not used in the selected architecture, its reference torque and rotational speed will be set to 0.
The coupling system plays an important role to describe different vehicle architectures.
For the series hybrid system, there is no connection between ICE and transmission, ICE is connected to EM2 (which works as generator). This generator only charges the battery. EM1 is the only propulsion element. Therefore the output torque of EM1 is connected directly to the transmission.

For the parallel hybrid system, EM2 will not be used and both ICE and EM1 drive the vehicle. Therefore, the torque is the sum of EM1 torque and ICE torque.
For the Series-parallel hybrid vehicle, there are 2 possible combinations: EVT and Planetary-gear-set. EM1 is connected to the transmission in order to drive vehicle. During braking, EM1 will work as a generator to recover the energy. ICE can help EM1 to drive the vehicle, or can be connected to EM2 to charge the battery.

3.3.2 System control

For the moment two different rule based control approaches have been used for the energy management.
For Series hybrid vehicle, the control strategy is realized by several lookup tables which are used to control the battery charging. The battery can be charged by regenerative braking or using the ICE based range extender.
For Parallel hybrid vehicle, the control strategy is realized using a state flow tool. Based on the inputs (battery SOC, required torque of vehicle and speed of transmission system) the output variables (torque split ratio between T_{ICE} and T_{req}) will be evaluated using 6 different modes based on SOC and T_{req}.
For Series Parallel hybrid architecture with planetary gear transmission, the control strategy is also realized by state flow as well. There are 4 working modes which include:

- mode0: Electric mode,
- mode1: E-CVT mode,
- mode2: Hybrid mode
- mode3: Regenerative braking mode.

During the braking, the wheel torque is split into two parts which include *regenerative electric braking* where the energy is used to recharge the batteries and *mechanic braking* where the energy is dissipated.

4. SIMULATION RESULTS

As presented before the availability of an easy to use global vehicle model is crucial for the development of the system control. Therefore a GUI (graphic user interface) has been developed which gives the possibility to choose between different vehicle types, different driving cycles and different hybrid architectures by simple clics. For the moment the approach developed by the authors provides the possibility to study 828 predefined combinations of cycle, vehicle and architecture are available. Moreover, it gives the possibility to start the simulation and represent the most important results graphically. Furthermore, it gives the possibility to adapt all parts of the vehicle individually. It is even possible to estimate the behavior of an internal combustion engine ICE that is especially designed for this case. Therefore the approach of *Asus et al.* (Asus et al. 2012). The user interface is presented in **Erreur ! Source du renvoi introuvable.**, which is developed by authors in order to facilitate the simulation for different vehicles in

different driving cycles._The user interface consists of three parts, the left part is used to select the simulated vehicle, driving cycle and the hybrid structure, the middle part is used to display the vehicles and the parameters of their power system, the right part is used to plot the results, both 2d and 3d figures can be plotted. Furthermore, with the help of the other two cooperating GUIs, it is possible for the users to customize the driving cycle as well as engine parameters.
The most interesting reference point would be the behavior of a C-segment medium car like Toyota Prius for example.
Figure 9 presents the power split inside a C-segment medium series-parallel hybrid car on a motorway cycle. It can be seen, that the power needed by the car is a combination of the power delivered by the battery through the electric motor 1 (EM1). The internal combustion engine ICE is only used during start and around 300s. The fuel consumption on this cycle is equivalent to143g of gasoline fuel, which would be equivalent to 1.2L/100km.

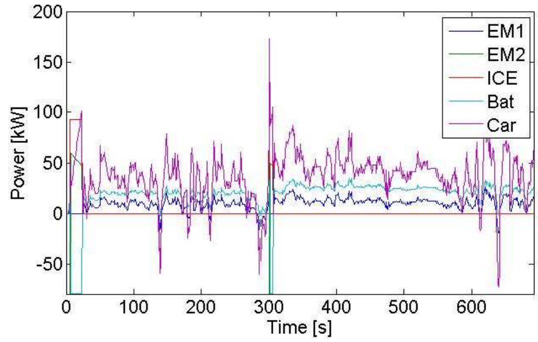

Figure 9: Power demand of C-segment medium car on motorway

A comparison of fuel consumption for different hybrid architectures of is presented in Table 1. It seems that the results for the same architecture and different driving cycles are comparable. However, the results for the different architectures have to be checked carefully. The low fuel consumption for series/parallel architecture can be described by the extensive use of the battery.

Table 1: Comparison of fuel consumption of C-segment middle class car in L/100km

	Urban	Extra-urban	Motorway
Series	2.95	5.35	6.43
Parallel	3.19	5.27	5.51
Series/Parallel	3.78	4.39	7.03

Furthermore, the model gives the possibility to compare the fuel consumption for different types of vehicles. **Erreur ! Référence non valide pour un signet.** presents the fuel consumptions of different series hybrid vehicles on different driving cycles. It can be seen that the fuel consumption increases from urban to extra urban driving cycle and from extra-urban to motorway driving cycle. This is understandable as the mean power demand increases with the driving cycles.

Table 2: Comparison of fuel consumption of different vehicles in L/100km

	Urban	Extra-urban	Motorway
Motorbike	0.93	2.29	4.51
Small Car (A-segment)	3.05	4.43	5.97
Medium Car (C-segment)	3.68	5.08	7.74
Bus	28.87	27.7	35.8

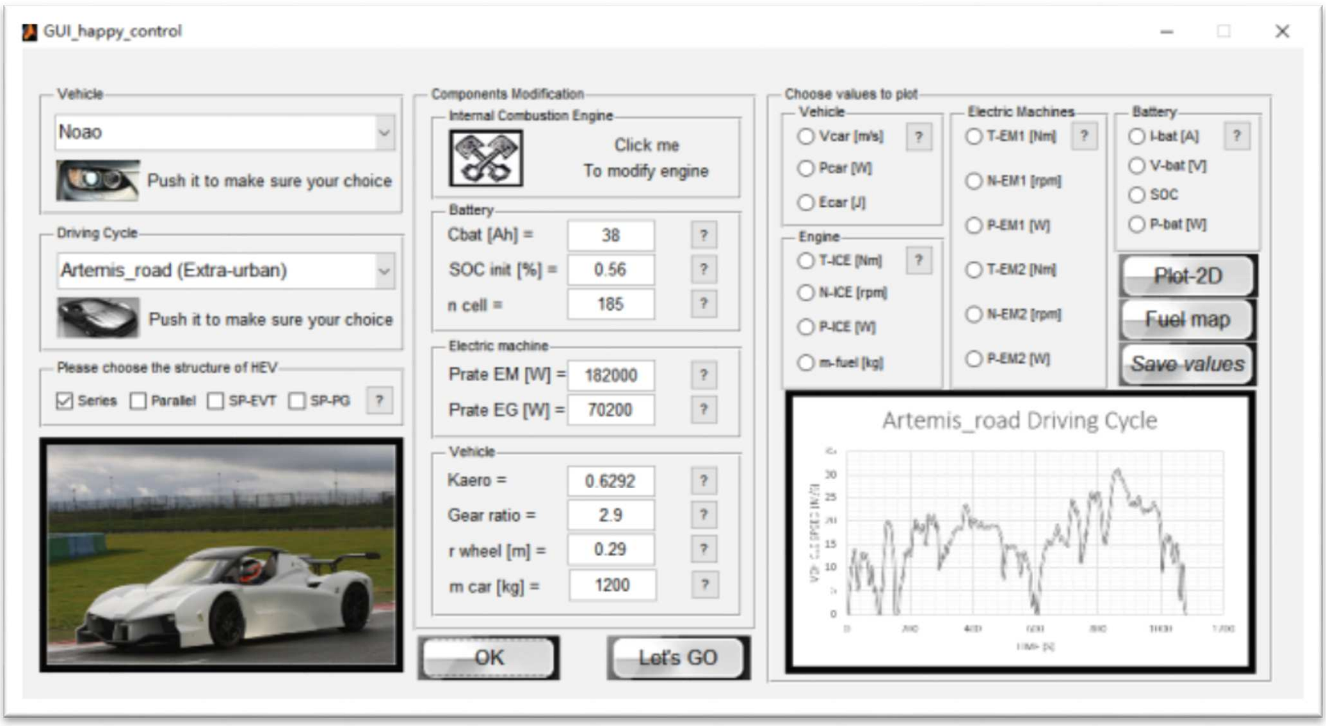

Figure 8: Graphic User Interface (GUI)

5. CONCLUSIONS AND PERSPECTIVES

This work presents a unified multi-architecture / multi-application approach to simulate different hybrid vehicles using REM. Such a tool is required as nowadays several hybrid architectures exist in parallel and they are used for a multitude of vehicle applications from scooter, over vehicle, to busses. In order that the hybrid vehicle shows a real advantage with regard to conventional architectures, it is necessary to develop a well-adapted control. Therefore, it is interesting that EMR allows developing the control strategy by an inversion based approach. Different control strategies (rule based and optimization based) can be applied on hybrid vehicles.

In this example, a GUI was developed providing easy access to different hybrid architectures and control strategies. Different architectures of a middle class car are modeled using rule based control. Furthermore, different vehicle types like a scooter and a bus are modeled. Modeling results show coherent results and the capability of a single generic model to cover this multitude of applications.

In the following the approach will be checked carefully, different control strategies will be developed and results will be compared to real world data.

REFERENCES

Allègre, A.-L., Trigui, R. & Bouscayrol, A., 2013. Flexible real-time control of a hybrid energy storage system for electric vehicles. *IET Electrical Systems in Transportation*, 3(3), pp.79–85.

Amjad, S., Neelakrishnan, S. & Rudramoorthy, R., 2010. Review of design considerations and technological challenges for successful development and deployment of plug-in hybrid electric vehicles. *Renewable and Sustainable Energy Reviews*, 14(3), pp.1104–1110.

Asus, Z. et al., 2014. Model and Control Strategy Simulation of a Racing Series Hybrid Car. In *IEEE Vehicular Power and Propulsion Conference (VPPC)*. Combeira, Portugal.

Asus, Z. et al., 2013. Optimization of Racing Series Hybrid Electric Vehicle using Dynamic Programming. In *SESDE*. Athens, Greece.

Asus, Z. et al., 2012. Simple method of estimating consumption of internal combustion engine for hybrid application. *2012 IEEE Transportation Electrification Conference and Expo, ITEC 2012*.

Barrade, P. & Bouscayrol, A., 2011. Energetic Macroscopic Representation - An Energy-Flow Based Methodology dedicated for the control of multiphysics systems.

Chen, K., Bouscayrol, A., Berthon, A., et al., 2009. Global modeling of different vehicles. , (June), pp.80–89.

Chen, K., Bouscayrol, A., Delarue, P., et al., 2009. Simulation of an Unified Control Scheme for Different Hybrid Electric Vehicles. , pp.3842–3847.

Cheng, Y. et al., 2009. Global Modeling And Control Strategy Simulation. , (June), pp.73–79.

Chrenko, D. et al., 2015. Novel Classification of Control Strategies for Hybrid Electric Vehicles.

Chrenko, D., Pera, M.-C. & Hissel, D., 2008. Inversion based control of a diesel fed low temperature fuel cell system. *2008 13th International Power Electronics and Motion Control Conference*, pp.2156–2163. Available at: http://ieeexplore.ieee.org/lpdocs/epic03/wrapper.htm?arnumber=4635585.

Chrenko, D., Péra, M.-C. & Hissel, D., 2007. Fuel Cell System Modeling and Control with Energetic Macroscopic Representation. In *IEEE ISIE*. Vigo, Spain.

Guzzella, L. & Sciarretta, A., 2010. *Vehicle Propulsion Systems - Introduction to Modeling and Optimization*, Springer.

Ifak, S.N. & Iml, H.V., 2015. Models and Methods for the Evaluation and the Optimal Application of Battery Charging and Switching Technologies for Electric Busses. , (Iml).

Kutter, S. & Bäker, B., 2010. Predictive online control for hybrids: Resolving the conflict between global optimality, robustness and real-time capability. In *IEEE Vehicle Power and Propulsion Conference*. IEEEXplore, pp. 1–7.

Lhomme, W. et al., 2008. Switched Causal Modeling of Transmission With Clutch in Hybrid Electric Vehicles. *IEEE Transactions on Vehicular Technology*, 57(4), pp.2081–2088. Available at: http://ieeexplore.ieee.org/lpdocs/epic03/wrapper.htm?arnumber=4383362.

Lhomme, W., Bouscayrol, a. & Barrade, P., 2004. Simulation of a series hybrid electric vehicle based on energetic macroscopic representation. *2004 IEEE International Symposium on Industrial Electronics*, (May), pp.1525–1530 vol. 2. Available at: http://ieeexplore.ieee.org/lpdocs/epic03/wrapper.htm?arnumber=1572040.

Liukkonen, M. & Suomela, J., 2012. Design of an energy management scheme for a series-hybrid powertrain. *2012 IEEE Transportation Electrification Conference and Expo (ITEC)*, pp.1–6. Available at: http://ieeexplore.ieee.org/lpdocs/epic03/wrapper.htm?arnumber=6243507.

Locment, F. & Sechilariu, M., 2010. Energetic Macroscopic Representation and Maximum Control Structure of electric vehicles charging photovoltaic system. *2010 IEEE Vehicle Power and Propulsion Conference*, pp.1–6.

Le Mans, 2012. Règlement Technique pour Prototype 2012 2012 Technical Regulations for Prototype.

Marc, N. et al., 2010. Sizing and fuel consumption evaluation methodology for hybrid light duty vehicles. In *25th World Battery, Hybrid and Fuel Cell Electric Symposium and Exhibition (EVS)*.

Shenzhen, China.
Prechelt, L., V-Modell XT. , pp.1–38.
Silva, L.I., Bouscayrol, a. & De Angelo, C.H., 2012. Modeling and control of an electric vehicle combining bond graph and Energetic Macroscopic Representation. *2012 IEEE Vehicle Power and Propulsion Conference*, (4), pp.973–977. Available at: http://ieeexplore.ieee.org/lpdocs/epic03/wrapper.htm?arnumber=6422769.
Solano Mart'\inez, J. et al., 2012. A survey-based type-2 fuzzy logic system for energy management in hybrid electrical vehicles. *Information Sciences*, 190, pp.192–207.
Tie, S.F. & Tan, C.W., 2013. A review of energy sources and energy management system in electric vehicles. *Renewable and Sustainable Energy Reviews*, 20, pp.82–102. Available at: http://linkinghub.elsevier.com/retrieve/pii/S1364032112006910.
Tingting, D., 2011. Design Method and Control Optimization of an Extended Range Electric Vehicle. , 15(1).
Wikipedia, Volvo B5LH.
Zhang, P., Yan, F. & Du, C., 2015. A comprehensive analysis of energy management strategies for hybrid electric vehicles based on bibliometrics. *Renewable and Sustainable Energy Reviews*, 48(205), pp.88–104. Available at: http://dx.doi.org/10.1016/j.rser.2015.03.093.

MODELING MECHANICAL DAMAGE TO CORN SEEDS

Feizollah Shahbazi[(a)]

[(a),] *Lorestan University, Faculty of Agriculture, Department of Biosystems Engineering ,Khoram, Iran.*

[(a)] shahbazi.f@lu.ac.ir

ABSTRACT

The experiments were conducted at moisture contents of 7.60 to 25% (wet basis) and at the impact energies of 0.1, 0.2 and 0.3 J, using an impact damage assessment device. The results showed that impact energy, moisture content, and the interaction effects of these two variables significantly influenced the percentage physical damage in corn seeds (p<0.01). Increasing the impact energy from 0.1 to 0.3 J caused a significant increase in the mean values of damage from 23.73 to 83.49%. The mean values of physical damage decreased significantly by a factor of 1.92 (from 83.75 to 43.56%), with increase in the moisture content from 7.6 to 20%. However, by a higher increase in the moisture from 20 to 25%, the mean value of damage showed a non-significant increasing trend. There was an optimum moisture level about 17 to 20%, at which seed damage was minimized. An empirical model developed composed of seed moisture content and energy of impact developed for accurately description the percentage physical damage to corn seeds. It was found that the model has provided satisfactory results over the whole set of values for the dependent variable.

Keywords: Mechanical damage, harvesting, handling, processing, impact, corn**.**

1. INTRODUCTION

Harvesting and postharvest operations on modern grain farms, such as corn, negatively influenced quality of seeds. Harvesters and other machines that used during harvesting, transporting, drying and conveying operations cause significant mechanical damage to seeds i.e. skin rupture, seed fracture etc. The damage resulted from mechanical interaction between biological material (seeds) and steel, rubber etc. (working elements of machines). Most authors admit that damage to seeds occurs mainly in the course of harvest and transport, where the seeds are subject to accidental impact (Baryeh, 2002).

The mechanical resistance to the impact damage of seeds among other mechanical and physical properties, plays a very important role in the design of harvesting and other processing machines (Baryeh, 2002). The value of this basic information is necessary, because during operations, in these sets of equipment, seeds are subjected to impact loads which may cause mechanical damage. Impact damage of seeds depends on a number factors such as velocity of impact, seed structural features, seed variety, seed moisture content, stage of ripeness, fertilization level and incorrect settings of the particular working subassemblies of the machines (Shahbazi, 2011; Shahbazi *et al*., 2011a). Among above factors, the seed moisture content and impact energy are important factors influencing the damage. Some researchers found a significant influence of the impact velocity and moisture content upon the seed damage and found that the damage increases significantly as the energy of the impact increases and as the moisture content decreases (Khazaie *et al*., 2008; Khazaie, 2009; Shahbazi *et al*., 2011a and b). Impact damage to seeds has been the subject of much research due to the loss in product quality incurred during harvesting, handling and processing. Researchers have used different impact damage assessment devices to conduct impact tests on seeds and simulate the impact loads that seed would be subjected (Sosnowski, 2006; Khazaie, 2009; Shahbazi *et al*., 2011a and b).

Because of the complex nature of impact damage to seeds, accurate designing, controlling and adjusting of threshers, harvesters, conveyors, and other processing systems is difficult. This necessitates the accurate design and the use of automatic system for controlling and adjusting of harvesters and other processing systems. Automatic control needs to have practical data for those involved in equipment and methods for handling seeds and a more powerful prediction model to be able to estimate the effects of several independent variables on several dependent ones. During the last decade, various forms of multiple linear regression models have been widely considered to estimate the mechanical damage to seeds, based on the machine and crop parameters (Sosnowski and Kuzniar, 1999; Baryeh, 2002; Szwed and Lukaszuk, 2007; Khazaie, 2009; Shahbazi *et al*., 2001a and b; Shahbazi, 2011).

Information relating the amount of corn seeds impact damage to energy of impact and seed moisture content and modeling the damage to seeds is limited. In light of above facts, the objectives of this study were to: (1)-Evaluate the impact damage to corn seeds and determine the effects of impact energy and seed moisture content on the percentage of physical damage to seeds. (2)-Develop empirical models that explain the relationship between percentage of seed physical damage and the experimental variables for corn seeds and evaluate the predictive performance of the models.

2. MATERIALS AND METHODS

Samples of corn seeds at optimum maturity were harvested by hand in Lorestan province, Iran and cleaned in an air screen cleaner. The initial moisture content was 7.60% (wet basis), determined with ASAE S352.2 for edible beans (*ASAE Standards,* 1988). Higher moisture content samples were prepared by adding calculated amounts of distilled water, then sealing in polyethylene bags, and storing at 5ºC for 15 days. Samples were warmed to room temperature before each test and moisture content was verified. Sample mass was recorded with a digital electronic balance having an accuracy of 0.001 g.

The laboratory apparatus used to impact seeds, operated in a way similar to the impacting energy instruments used by Kim *et al*. (2002), Oluwole *et al*. (2007), Shahbazi *et al*. (2012) and Shahbazi (2014). An aluminum drop bar (800mm length; 25mm external diameter; 0.2kg) was inserted into a steel tube (750mm length; 27mm internal diameter; 29mm external diameter). The steel tube had 4 mm diameter holes drilled at 5 cm intervals from 5 to 60 cm. The drop height of the aluminum bar was manually controlled by a pin inserted in the hole in the middle of a steel tube. The impact energy on seed was depending on the mass and drop height of the aluminum bar.

In this study, the effects of impact energy (at: 0.1, 0.2 and 0.3 J) and seed moisture content (at: 7.60, 12.5, 15, 17.5, 20 and 25% wet basis) were studied on percentage of physical damage in corn seeds. The range of seeds moisture is from 7.6 to 25% as this includes the normal range of moisture levels during harvesting and postharvest processing for seeds (Khazaei, 2009). Energy of impact ranged from 0.1, 0.2 and 0.3 J, including those happening in harvesters, separator, conveyors, storing system, and other processing systems (Shahbazi *et al*., 20014). The factorial experiment was conducted as a randomized design with three replicates. For each impact test, 100 seeds were selected randomly from each sample and impacted by using the impact device. After each test, visual evaluation of the microscopic structural analysis of the seed (before and after the impact) was used to analysis the character of damage on the corn seed. Damaged seeds include the broken, cracked, and bruised seeds were accurately identified and sorted by visual inspection. A handheld magnifying glass was used to augment the visual inspection. The percentage of seed damage was calculated as:

$$Seed\ \ Damage\ \ (SD) = \frac{(Weight\ of\ damaged\ seeds)}{(Weight\ of\ total\ seeds(damaged + undamaged))} \times 100 \quad (1)$$

Experimental data were analyzed using analysis of variance (ANOVA) and the means were separated at the 5% significance level applying Duncan's multiple range tests in SPSS 17 software. The nonlinear regression program of SAS (SAS, 2001), was used to find and fit the best general models to the data and develop empirical models that explain the relationship between percentage of seed damage and the experimental variables.

3. RESULTS AND DISCUSSION

Analysis of variance indicated that moisture content and impact energy (independent variables) created significant effects on the physical damage of corn seeds at 1% significance level (P<0.01). Impact energy had a larger influence than moisture content within the range studied. In addition, the interaction effect of the moisture content × impact energy significantly influenced the physical damage of bean seeds at 1% significance level

3.1. Effect of Moisture Content

The effect of moisture content on the level of damage to the tested seeds of corn is presented in Fig 1. As follows from the relation presented in the figure, the percentage of damaged seeds decreases with increase in their moisture content. This may be related to a change in their elasticity at higher moisture level, which causes greater absorption of energy during the impact. Many researchers have also reported similar results for the other crops (Sosnowski and Kuzniar, 1999; Parde *et al*., 2002; Szwed and Lukaszuk, 2007; Khazaei *et al*., 2008; Khazaei, 2009). With increasing the moisture content from 7.6 to 20%, the mean values of the percentage damage significantly decreased from 83.75 to 43.56% (by a factor of 1.92). However, by a higher increase in the moisture from 20 to 25%, the mean values of damage showed a non-significant increasing trend (Fig 1).

The relation of damage rate presented in Fig 1 is non-linear, and the appearance of minimum values of damage rate at a certain moisture content range is a feature characteristic for the tested seeds. The shape of the graph in the figure show that the changes in seed damage rate plots quadratic function with fairly significantly differing coefficients at variable moisture for corn seeds. The extent of damage of impacted seeds decreased with increasing moisture and reached a minimum at moisture level of about17.5 to 20%. Further increase in seed moisture, however, caused an increase in the amount of damaged seeds. According to numerous studies, there exists a certain optimum level of moisture content for each variety at which, under the effect of impact forces, there occurs a minimum of damage to the seeds (Szwed and Lukaszuk, 2007). Therefore, In the case of corn seeds that optimum level of moisture is about 17-20%.

Fig 2 shows the corn seeds physical damage variation with seed moisture content for various impact energies. As follows from the figure, for all the impact energies considered, the percentage of the seed damage decreases with increase in their moisture content. These results confirm that, as the moisture content has significant effects on the elastic properties of materials of plant origin, it also has a bearing on the effects of impact damage. At higher moisture contents, the elasticity of seeds will increase, which causes that their firmness increase, thus, causes greater absorption of energy during impact and increases the resistance to damage. On the other hand, at lower moisture contents, the seeds are more brittle, thus, more prone to physical damage caused by impact (Khazaei *et al*., 2008; Khazaei, 2009).

As shown in Fig 2 the rates of increase in percent damage to seeds by decrease in their moisture content are not the same for all the levels of impact energies. The effect of moisture content on the damage is stronger at higher impact energies than at lower ones. At the critical range of the tests, when the moisture content decreased from 20 to 7.6%, the maximum rate of increase in the damage to seeds was obtained for the impact energy of 0.3 J, which was equal to 24.01% (from 100% to 75.99%). Corresponding values are equal to 57.43 and 39.13%, for the same moisture range at 0.1 and 0.2 J impact energies, respectively. Fig 2 indicates that for all the impact energies, relations of damage rate are non-linear with seed moisture content. Regression analysis was used to find and fit the best general models to the data. Results showed that the percentage damage to seeds was a quadratic function of their moisture content, at all the impact energies considered. Szwed and Lukaszuk (2007) observed similar behavior for other crops. The equations representing the relationship between the percentage damage to seeds and moisture content for each impact energy and their coefficients of determination (R^2) are presented in Figure 2. As follows from the relations, the effect of moisture is stronger for the higher levels of energy than in the case of the lower ones (higher values at variable M^2).

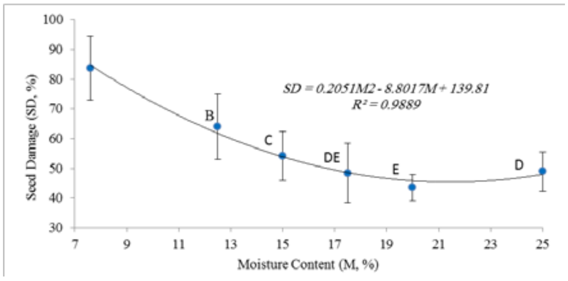

Figure 1: Effects of moisture content on percentage damage to corn seeds. Averages with the same letter have no significant difference at the 5% significance level.

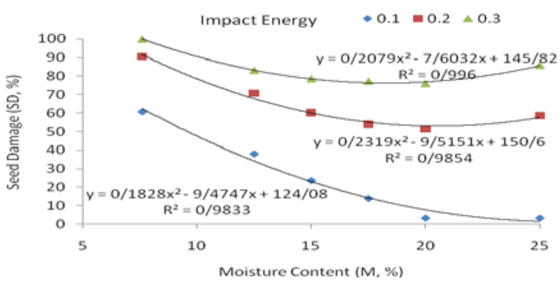

Figure 2: Corn seeds impact damage variation with seed moisture content for different impact energies.

3.2. Effect of Impact Energy

The results of Duncan's multiple range tests for comparing the mean values of the damage to corn seeds at different impact energies is shown in Fig 3. It is evident that seed damage increased, as a quadratic function, with increasing impact energy. For all the levels of impact energy, the differences between the mean values of the damage are significant (*P=0.05*). With increasing the impact energy from 0.1to 0.3 J, the mean value of the damage increased about 59.75% (from 23.73 to 83.49%). The corresponding value for increasing the impact energy from 0.1 to 0.2 J and from 0.2 to 0.3 J, were about 40.49 and 19.25%, respectively. Similar results about incrasing the seeds damage with impact energy, have been reported by other researchers (Khazaei *et al*., 2008; Shahbazi, 2011; Shahbazi *et al*., 2011a and b). Shahbazi *et al.* (2012) found that increasing the impact energy from 0.05 to 0.1 J caused an increase in the percentage breakage of seeds from 18.68 to 35.21% and from 44.78 to 71.61% for wheat and triticale seeds, respectively.

In Fig 4 the percentage damage to seeds is plotted against the energy of impact. The figure reveals that, at all the seed moisture contents considered, the seed damage increases as the impact energy increases. Due to the significant interaction effect between impact energy and moisture content, the rates of increase in damage are not the same for all levels of moisture contents. The effect of impact energy on the damage is stronger at lower moisture contents than at higher ones. In Fig 4 the lowest damage among the combinations was found to be 3.36% occurred in the 0. 1J impact energy with the moisture content of 20%, while the greatest damage was obtained as 100%, occurred in the impact energy of 0.3 J with the moisture content of 7.6%. At 7.6% seed moisture content, percentage damage increased from 60.79 to 100% with increasing in the impact energy from 0.1 to 0.3 J. Corresponding percentage damages were from 38.15 to 83.20%, 23.77 to 78.59%, 14.00 to 77.25, 3.36 to 75.99, and from 3.38 to 18.14% for the same energy range, at 12.5, 15, 17.5, 20 and 25% moisture contents, respectively. The seed damage was related to the energy of impact in the range of 0.1 to 0.3 J, by regression analysis. The results showed that the percentage physical damage to seeds was a quadratic function of the energy of impact, at all the moisture contents considered. The equations representing the relationship between the percentage damage to seeds (*SD*, %) and impact energy (*IE*, J) for each moisture content (*M*, %) and their coefficients of determination (R^2) are presented in Table 1.

For the optimum level of moisture content of 20% in Figs 3 and 4, the percentage damage to seeds were 3.36, 51.33 and 75.99% at impact energies of 0.1, 0.2 and 0.3 J, respectively, shown that at energies lower than 0.1 J, the seed damage is lower than 10%.

Based on the above fact, the limitation of impact energy to 0.1 J could be considered in the case of designing or adjusting the threshing and other mechanisms for handling or processing the corn seeds.

It suggests that the radius and speed of the machine parts should be such that will not allow the impact energy of 0.1 J to be exceeded; higher energy than 0.1 J will damage seeds. However, considering the mass of the seed, m (kg), which absorbs the impact energy, in the machine, the impact velocity, V (m s^{-1}), in such machine to cause the same amount of energy, could be determined:

$$\tfrac{1}{2} mV^2 = IE \Rightarrow V = \left[\frac{2IE}{m}\right]^{\frac{1}{2}} \qquad (2)$$

In this study, the limited impact energy was found to be IE=0.1J, thus the velocity of the machine parts, that subject the seed with the mass of m (kg) to the required impact energy, could be determined:

$$V = \left[\frac{0.2}{m}\right]^{\frac{1}{2}} \qquad (3)$$

For the sample seeds used in this study, the mean mass of the seeds, at optimum moisture content of 20%, found to be 0.000266 kg (data not shown). Thus, substituting the values of IE and m in to the equation 3, the velocity of impact gives about 27 m s^{-1}.

Based on above results, the best conditions for harvesting and other processing for corn seeds, in which seeds are subjected to impact loads, will be at moisture contents of about 17-20% with impact energy and velocity limited to about 0.1 J and 27 m s^{-1}, respectively. These features may be important in the case of selecting the time of harvesting and designing or adjusting the threshing and other mechanisms for handling or processing the seeds, to limit the impact energy and velocity of machine parts to 0.1 J and 27 m s^{-1}, from the viewpoint of minimizing yield losses due to the share of damaged seeds.

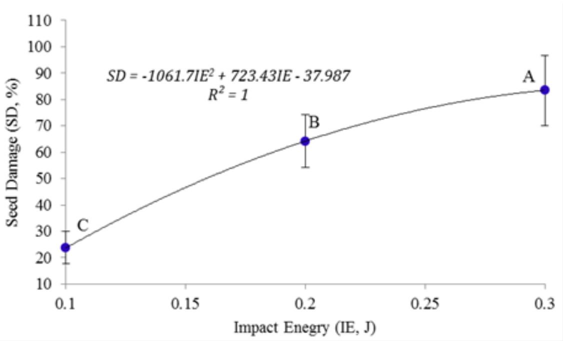

Figure 3: Effects of impact energy on percentage damage to corn seeds. Averages with the same letter have no significant difference at the 5% significance level.

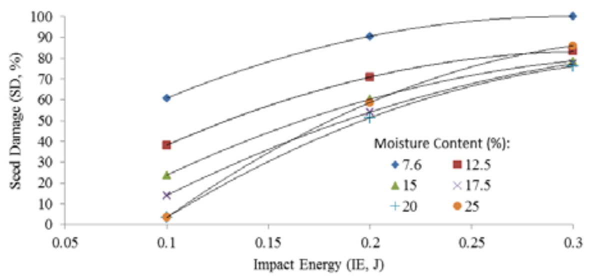

Figure 4: Corn seeds impact damage variation with impact energy for different seed moisture contents.

Table1. Equations representing the relationship between the percentage damage to corn seeds and impact energy for each moisture content.

Moisture content (%)	Equation	R2
7.60	$SD = -1006.8IE^2 + 598.75IE + 10.99$	0.999
12.5	$SD = -1016IE^2 + 631.63IE - 14.85$	0.992
15	$SD = -899.67IE^2 - 634IE - 30.63$	0.997
17.5	$SD = -833IE^2 + 649.43IE - 42.20$	0.999
20	$SD = -1166IE^2 + 829.53IE - 67.93$	0.998
25	$SD = -1448.5IE^2 + 997.22IE - 82.88$	0.997

All the indexes are significant at the level of 99.5%.
SD= seed damage (%), IE= impact velocity (J).

3.3. Modeling

An empirical relationship was developed utilizing the dependence of the corn seeds percentage damage (SD, %) on parameters such as seed moisture content (M, %), impact energy (IE, J), and $M \times IE$ as independent variables, with the help of regression techniques. The relationship is given as follows:

$$SD = 89.203 - 11.54M + 500.739IE + 13.69MIE + 0.205M^2 - 1061.667IE^2 \qquad R^2 = 0.986 \qquad (4)$$

The regression statistics for the model indicated that all terms were significant effects (at the 99.5% level) on the accuracy of the model. The p-value of predicting equation was <0.0001. The performance of the selected relationship for the prediction percentage of damage to corn seeds due to impact is shown in Fig 5. This figure shows the predicted percentage of damage data versus the same set of measured data. The scatter plot showed no tendency for the model to under- or over-estimate the predicted percentage of damage data. It is observed that the predictive capability was good and data points were well compressed about the ideal of unity-slope line selected. The linear adjustment between the observed and estimated values gives a slope practically equal to 1 (Y=0.9735X +1.4723). The resulting correlation coefficient and the p-value were 0.9732 and <0.0001, respectively, for the regression between observed and estimated values (Fig 5), indicating that the model provided satisfactory results over the whole set of values for the dependent variable.

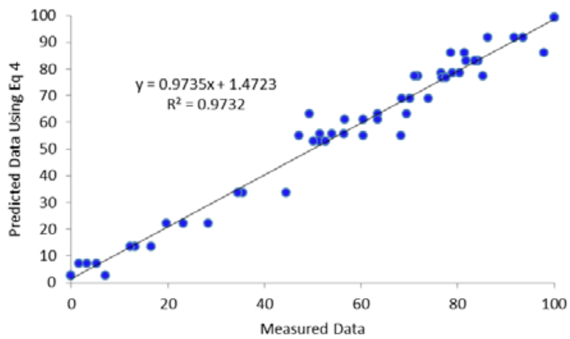

Figure 5: Correlation between the actual and the predicted data by the mathematical model (Eq. 4).

REFERENCES

ASAE, 1988. Moisture Measurement – Grain and Seeds. Agric. Eng. Yearbook, ASAE, Standard ASAE, 347-352.

Bartsch, J.A., Haugh, C.G., Athow, K.L. and Peart, R.M., 1979. Impact damage to soybean seed. ASAE Paper No. 79-3037. St. Joseph, MI: ASAE.

Baryeh E.A., 2002. A simple grain impact damage assessment device for developing countries. J. Food Eng., 56, 37-42.

Hoki M. and Pickett, L.K., 1973. Factors affecting mechanical damage of navy beans. *Transactions of the ASAE* 16(6):1154-1157.

Khazaei J., 2009. Influnce of impact velocity and moisture content on mechanical damage of white kindey beans under impact loadings. Cercetari agronomice in Moldova (Romania)., 1(137), 5-18.

Khazaei J., Shahbazi F., Massah J., Nikravesh M., and Kianmehr M. H., 2008. Evaluation and modeling of physical and physiological damage to wheat seeds under successive impact loadings: mathematical and neural networks modeling. *J. Crop Science*, 48,1532-1544.

Kim T.H., Opara L.U., Hampton J.G., Hardacre A.K., and MacKay B.R., 2002. The effects of grain temperature on breakage susceptibility in maize. Biosystems Eng., 82(4), 415–421.

Oluwole F.A., Aviara N.A., and Haque M.A., 2007. Effect of moisture content and impact energy on the crackability of sheanut. Agric. Eng. Int., CIGR Journal, 8:07- 002.

Parde S. R., Kausalb R. T., Jayasa D. S., and White, N. D. G., 2002. Mechanical damage to soybean seed during processing. J. Stored Product Res., 38,385–394.

Shahbazi F., Analooei M., and Saffar, A., 2011a. Mechanical damage to pinto bean seeds as affected by moisture content, impact velocity and seed orientation. Int. J. Food Eng., Vol. 7: Iss. 6, Article 1.

Shahbazi F., 2011. Impact Damage to Chickpea Seeds as Affected by Moisture Content and Impact Velocity. Appl. Eng. Agric., 25(7), 771-775.

Shahbazi F., 2014. Effects of Moisture Content and Impact Energy on the Cracking Characteristics of Walnuts. Int. J. Food Eng., 10(1),149–156.

Shahbazi F., Dolatshah A., and Valizadeh, S., 2014. Evaluation and modeling the mechanical damage to cowpea seeds under impact loading. Quality Assurance and Safety of Crops & Foods. *Article in Press*.

Shahbazi F., Saffar A., and Analloei M., 2011b. Mechanical damage to navy beans as affected by moisture content, impact velocity and seed orientation. Quality Assurance and Safety of Crops & Foods. 3, 205-211.

Shahbazi F., Valizadeh S., and Dolatshaie A., 2012. Breakage susceptibility of wheat and triticale seeds related to moisture content and impact energy. Cercetari agronomice in Moldova (Romania)., 3(151), 5-13.

Sosnowski S., 2006. Reasons of mechanical damage of bean seeds under dynamic loads. Act Agrophysica., 130, 1-65.

Sosnowski S., and Kuzniar P., 1999. Effect of dynamic loading on the quality of soybean. Int. Agrophysics., 13,125-132.

Szwed G., and Lukaszuk, J., 2007. Effect of rapeseed and wheat kernel moisture on impact damage. Int. Agrophysics., 21, 299-304.

A COMPLEX MODEL FOR FOREST ECOSYSTEM STATE ASSESSMENT BASED ON REMOTE SENSING DATA: CASE STUDY IN BAIKALSKY NATURE RESERVE

O. Grigorieva[(a)], O. Brovkina[(b)], V. Mochalov[(a)], Y. Akhtman[(c)], V. Zelentsov[(a)], S. Potryasaev[(a)], I. Kozyr[(d)], N. Belova[(d)]

[(a)]St.Petersburg Institute for Informatics and Automation of RAS, 14 line 39, 199178 St.Petersburg, Russia
[(b)]Global Change Research Institute, Bělidla 986/4a , 60300 Brno, Czech Republic
[(c)]GAMAYA company, CH-1015 Lausanne, Switzerland
[(d)]Baikalsky State Nature Biosphere Reserve, 34 Krasnogvardeyskaya Str., Tankhoy, Kabansky District, 671220 Buryatia Republic, Russia
[(a)]alenka12003@mail.ru, [(b)]brovkina.o@czechglobe.cz

ABSTRACT
This study describes a complex model for forest ecosystem state assessment in the Baikalsky Nature Reserve based on multispectral satellite and hyperspectral airborne data. The objective of the study is to estimate ecosystem stability, degree of anthropogenic load and the relative tension index of the environmental situation on the study territory. Results demonstrate the average sustainability of 0.8 (middle to high level) and an anthropogenic load of 0.3 (middle level). The ecological situation is estimated as satisfactory. The degradation of conifers indicates a decrease of protective functions of the ecosystem. Our proposed methodology for forest ecosystem state assessment is based on remote sensing data and can be potentially useful for regional and large-scale forest monitoring and management.

Keywords: forest ecosystem, satellite data, hyperspectral airborne data

1. INTRODUCTION

The application of modeling in ecology allows the prediction of the behavior of complex systems to which forest ecosystems belong (Scheller & Mladenoff 2007). Currently, forestry studies have demonstrated the beneficial approaches of modelling based on remote sensing (RS) data taking into account the growing condition, species composition, forest management arrangement, physical-geographical characteristics, and the size of the specific forest site. These models using RS data have been applied in variety of forest studies: terrestrial carbon cycling (Turner et al. 2004), forest decline (Lambert et al. 2013), biodiversity (Wang et al. 2010), forest structure (Gomez et al. 2012, Sokolov et al. 2014) and aboveground biomass (Lu et al. 2014; Brovkina et al. 2015).

A complex estimation of the functioning of a forest ecosystem has been less investigated using RS data-based modelling. Ravan et al. (1997) analysed the state of a forest ecosystem estimating the impacts of disturbance on forest structure using satellite RS in the Madhav National Park of India. Balenović et al. 2015 estimated and forecasted forest ecosystem productivity by integrating field measurements, RS, and modelling, on an oak forest (Quercus robur L.) site in Croatia. A number of complex forest biophysical parameters are considered to estimate the state of the forest ecosystem using RS data in Zawadzki et al. (2005). The application of solar radiation exergy is described as a tool for ecosystem health assessment in forest ecology, especially in the fields of ecological modelling (both mathematical and physical) in Jorgensen & Svirezhev 2004, and Silow & Mokry 2010. The ecosystem exergy represents the maximum energy capacity to perform useful work as the system proceeds to equilibrium, with irreversibility increasing its entropy at the expense of exergy. Taken by itself, the total exergy of an ecosystem is a measure of the change in entropy content from the equilibrium and the actual state. Differences in exergy for the past 20 years were estimated and compared with differences in biodiversity and biomass in Chinese eucalyptus plantations (Lu et al., 2011). Rosen (2002) confirmed that the biggest asset of forest ecosystem exergy analysis is that it can measure the disorder increase in ecosystems associated with human environmental impact.

The forest ecosystem of the Baikalsky Nature Reserve is a reference territory for assessing the impact of industrial air emissions of Southern Siberia. One of the most important missions of the Baikalsky Nature Reserve is to protect undisturbed cedar forests. Since 2007, a decline in forest processes has been observed in the Baikalsky Nature Reserve caused by global climate change, air pollution, insect pests and bacterial dropsy damage (annual report of Federal Forestry Agency of Russia, 2014; Belova, Morozova 2016). Nowadays, complex estimation of forest ecosystem state is a critical and relevant task. This study was initiated to develop a complex model for a forest ecosystem state assessment in the Baikalsky Nature Reserve based on RS data. Specifically, the objective of the study was to estimate ecosystem stability, the degree of anthropogenic load and a relative tension index of the environmental situation on the forest territory of the Baikalsky Nature Reserve.

2. METHODS

2.1. Study area

The study area is comprised of the Baikalsky Nature Reserve located along the southern coast of Lake Baikal in Russia (Fig. 1). Several forest species prevail in the study area: birch (Betula platyphylla Sukaczev), cedar (Pinus sibirica Du Tour), fir (Abies sibirica Ledeb.) and spruce (Picea obovata Ledeb.).

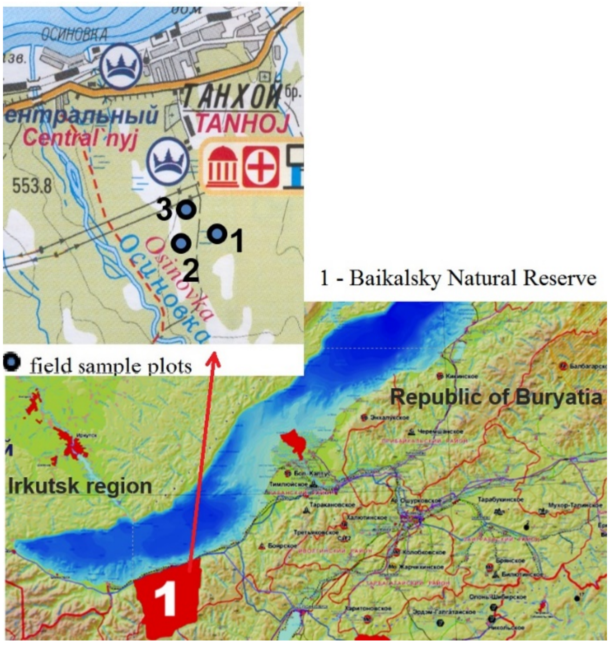

Figure 1: Location of the Baikalsky Natural Reserve and field sample plots

2.2. Data

Hyperspectral data in the spectral range of 400 – 900 nm with a spatial resolution of 0.4 m was acquired by an unmanned aerial vehicle (UAV) in June 2015. Pre-processing of hyperspectral data included radiometric, geometric and atmospheric corrections. Radiometrically corrected satellite scenes from Landsat 5 and Landsat 8 were downloaded from the U.S. Geological Survey data portal for the vegetation period of 2015 (http://earthexplorer.usgs.gov/). Atmospheric correction of satellite data was achieved with the FLAASH module of ENVI 5.1. Field data included sample cedar plots (3 plots) where the health status category of cedar was estimated (Table 1).

Table 1. Cedar health status of sample plots in 2015

Sample plot	Age class	DBH [sm]	N of trees	Health status category
1	IV	33	98	III
2	III	30	141	III
3	III	28	157	I - II

Health status category: III – highly weakened, IV – drying, V – deadwood. Age class: III – 120 years, IV – 160 years.

2.3. Complex model for assessment of forest ecosystem from RS data

The complex model for assessment of forest ecosystem was based on a separation of the study area to the degree of anthropogenic intensity (I) (Mochalov et al. 2015). Where I is an evaluation of the ecosystem's balance estimated from the degree of anthropogenic load, R, and potential sustainability, S: good (< 0.2), satisfactory (destruction of sensitive species) (0.2..0.5), tense (structural changes) (0.5..0.8), crisis (0.8..0.9), and catastrophic (destruction of the ecosystem) (> 0.9).

$$S = (AGB*NPP) / Ex, \quad (1)$$

$$I = R/ S, \quad (2)$$

where NPP is net primary productivity.

The degree of anthropogenic load was expressed as a sum of the ratio of the decline of the treed area, Sa, to the total forest area for each species, Sf.

The sustainability of forest ecosystems is an important indicator of the ecological state of the territory and characterizes the adaptive capacity of the ecosystem to identify and project anthropogenic load. This sustainability represents the fraction of absorbed solar radiance that can perform useful work, which is used for biomass accumulation in forest ecosystems and to ensure its productivity. S was determined based on the estimation of aboveground forest biomass, AGB, and solar radiation exergy, Ex, as indicators of the ecosystem state.

The technology of complex modelling included the classification of forest species, aboveground biomass estimation; detection of forest decline and the assessment of ecosystem state indicators (Fig. 2).

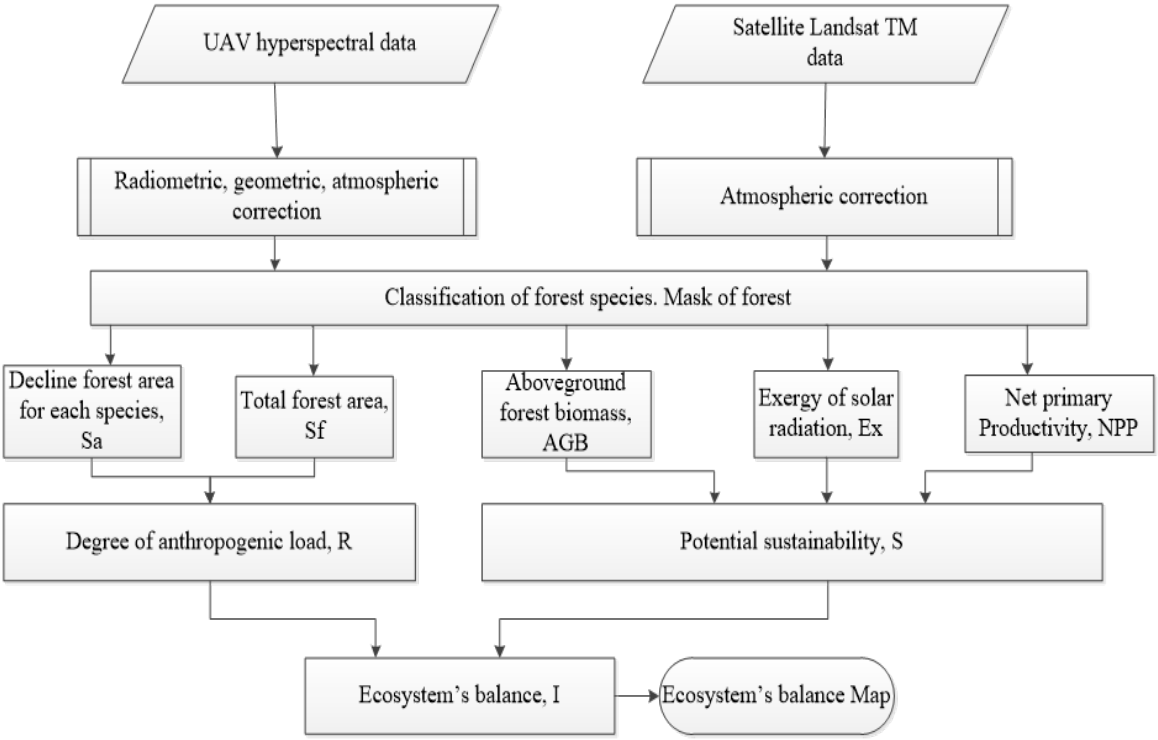

Figure 2: Framework of the technology of complex modeling for forest ecosystem state assessment

One of the main distinguishing features of the technology is the integrated processing of UAV hyperspectral data and satellite data while modelling (Sokolov et.al. 2012, 2014, 2015; Zelentsov et al. 2013, 2015).

2.3.1. Classification of forest species

The Spectral Angle Mapper method was used for the classification of forest species. The forest mask was obtained using the normalized difference vegetation index (NDVI) and near-infrared reflectance values. The accuracy of the classification result was estimated by the calculation of a confusion matrix. The results of classification were used for the AGB estimation.

2.3.2. Forest aboveground biomass estimation

AGB was estimated from local allometry (Shvidenko et al. 2008, Nikolaeva et al. 2008, Sevko 2014), where AGB is a function of the tree crown diameter for each species:

AGB = a*H+b (3)

for beech a = 7.8, b = -21.8 (r2=0.99), for cedar a = 13.1, b = -63.7 (r2=0.98);

H=a*CD+b (4)

for beech a = 3.9, b = 1.8 (r2=0.83), for cedar a = 4.5, b = 2.3 (r2=0.84);

where H – height of tree, CD – tree crown diameter. The average tree crown diameter algorithm was applied to derive crown diameter values from airborne hyperspectral data (Brovkina et al. 2015).

2.3.4. Assessment of solar radiation exergy

The exergy of the reflected solar radiation was calculated using the technique described by S. Yorgensen and Yu. Svirezhev using Landsat satellite data (Jorgensen & Svirezhev 2004) (5-7). This technique is based on multispectral images for a unit of surface which is performed by evaluating the “distance” between the real frequency distribution of the absorption spectrum of solar energy and the “equilibrium” frequency distribution. The degree of difference between the distributions is measured by the increment of Kullback entropy. The increment is zero when the frequency distribution of incoming radiation is equivalent to the frequency distribution of reflected radiation across the spectrum (meaning that the information receptor is equivalent to the information transmitter). If the Kullback entropy increment is positive, then there is an increment of information at the level of receptor and the reflective surface is in non-equilibrium state relative to the radiation spectrum.

$$E_x = E^{out}\left(K + \ln\frac{E^{out}}{E^{in}}\right) + B, \quad (5)$$

$$K = \sum_{v=1}^{n} p_v^{out} \ln\frac{p_v^{out}}{p_v^{int}}, \quad (6)$$

$$B = E^{int} - E^{out}, \quad (7)$$

where $E^{int} = \sum_{v=1}^{n} e_v^{int}$, incoming solar energy total; $E^{out} = \sum_{v=1}^{n} e_v^{out}$, reflected solar energy total; *n*-number of spectral bands; e_v^{int}, incoming energy in the range *v;* e_v^{out}, reflected energy in spectral range *v*; $p_v^{int} = \frac{e_v^{int}}{E^{int}}$, fraction of incoming energy in spectral range *v*; $p_v^{out} = \frac{e_v^{out}}{E^{out}}$, fraction of reflected energy in spectral range *v*. Spectral reflectance and surface temperature bands of satellite and airborne data will be inputs in (5 – 7).

2.3.5 Detection of forest decline

The algorithm to detect forest declination was based on Independent Component Analysis (Hyvarinen et al. 1997) that belongs to the methods for the detection of spectral anomalies and the automatic identification component of negative changes in the forest (Grigorieva 2014).

2.3.6 Validation of complex assessment of forest ecosystem

The official interior report "Dynamics of sanitary state of trees in the north part of the Baikalsky Nature Reserve" was used to validate the complex assessment of forest ecosystem from RS data.

3. RESULT AND DISCUSSION

Identification of tree decline from hyperspectral data (Fig. 3) successfully coincided with field reference data. An analysis of solar radiation exergy demonstrated significant variations of health and tree decline. These variations were interpreted as various exergy consumptions for the transpiration and the carbon deposition for trees of various healths. Results of complex modelling for assessment of the forest ecosystem in the Baikalsky Nature Reserve (Fig. 4) demonstrated that the average sustainability was 0.8 (medium to high level), and the anthropogenic load corresponded to 0.3 (medium level) in the study area (Table 2). Based on these indicators, the ecological situation was estimated as satisfactory. The forest ecosystem of the reserve has a margin of sustainability, but the degradation of conifers, the most sensitive to changes in the conditions of species' growth, indicates a decrease of the protective functions of ecosystems. The forest ecosystem state assessment from RS data corresponds to conclusions about the ecological situation in the official annual report of the Baikalsky Nature Reserve for 2015, where forest decline and drying of 10% of the cedar population was detected in the study area.

The usage of the proposed complex model allowed us to present a detailed map of the main forest-forming species and to identify forest stands with negative changes in health in the study area. This complex model for forest ecosystem state assessment seems promising for regional and large-scale forest monitoring and management.

Figure 3: Map of tree decline from hyperspectral data processing (red color represents tree decline)

Table 2. Indicators of ecological state

Indicator / year	2015
I, ecosystem's balance	0.4
R, degree of anthropogenic load	0.3
S, ecosystem sustainability	0.8
Assessment of ecological situation	satisfactory

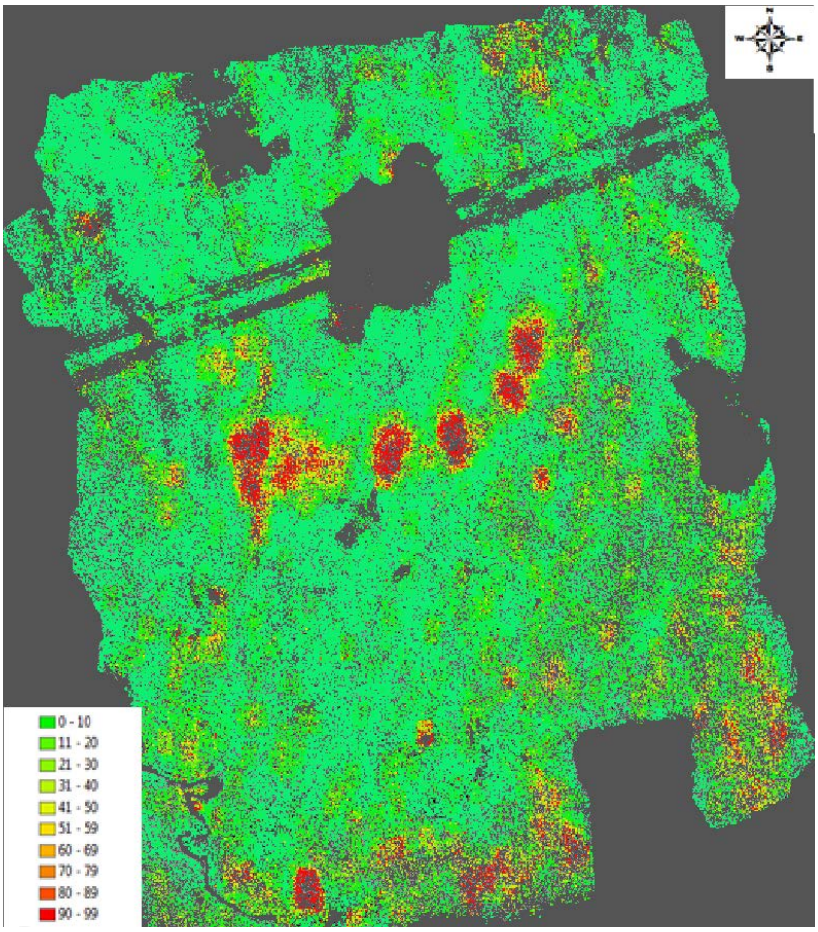

Figure 4: Map of ecosystem's balance (I) distribution on study area (I values are in %)

ACKNOWLEDGMENTS

This research is supported by the Ministry of Education, Youth and Sports of the Czech Republic within the National Sustainability Program I (NPU I) (grant number LO1415), partially supported by the Russian Foundation for Basic Research (grants 16-07-00779, 16-07-00925, 16-08-00510), grant 074-U01 (ITMO University), Program STC of Union State "Monitoring-SG" (project 1.4.1-1), State researches 0073–2014–0009, 0073–2015–0007.

REFERENCES

Evans W.A., 1994. Approaches to intelligent information retrieval. Information Processing and Management, 7 (2), 147–168.

Balenović, I., Jazbec, A., Marjanović, H., Paladinić, E., Vuletić, D. 2015. Modeling tree characteristics of individual black pine (Pinus nigra arn.) trees for use in remote sensing-based inventory. Forests. 6 (2).

Belova, N.A, Morozova, T.I. 2016. Dynamics o stone pine stands health at Baikal Reserve and adjacent territories // Monitoring and biological control methods of woody plant pests and pathogens: Proceedings of International conference. Moscow. Krasnoyarsk: SIF SB RAS, 27-28.

Brovkina, O., Latypov, I., Cienciala, E. 2015. Estimating average tree crown size using high resolution airborne data. J. Appl. Remote Sens. 9.

Brovkina, O., Zemek, F., Fabianek, T. 2015. Aboveground biomass estimation with airborne hyperspectral and LiDAR data in TesinskeBeskydy Mountains. Beskydy 8 (1).

Grigorieva, O.V. 2014. Observation of forest degradation using airborne and satellite hyperspectral data. Earth from space, 1.

Gómez, C., Wulder, M.A., Montes, F., Delgado, J.A. 2012. Modeling forest structural Parameters in the Mediterranean pines of Central Spain using QuickBird-2 imagery and classification and regression tree analysis (CART). Remote Sensing, 4.

Hyvarinen A., Oja E. 1997. A fast fixed-point algorithm for Independent Component Analysis. NeuralComputation, 9.

Jorgensen J.S. and Svirezhev Yu. M. 2004. Towards a thermodynamic theory for ecological systems," Elsever, Oxford.

Lambert, J., Drenou, C.,Denux, J.-P., Balent, G.,Cheret, V. 2013. Monitoring forest decline through remote sensing time series analysis. GIScience& Remote Sensing, 50 (4).

Lu, D., Chen, Q., Wang, G., Liu, L., Li, G., Moran, E. 2014. A survey of remote sensing-based aboveground biomass estimation methods in forest ecosystems. International Journal of Digital Earth.

Lu, H., Wang, Z., Campbell, D., Ren, H., Wang, J. 2011. Emergy and eco-exergy evaluation of four forest restoration modes in southeast China. Ecological Engineering, 37.

Mochalov, V.F., Grigorieva, O., Brovkina, O., Potrjasaev, S. 2015. A system for environmental monitoring of the Russian spaceport “Vostochny”. Proceeding of the conference “Global change: A complex challenge”, Brno, Czech Republic.

Nikolaeva, S.A., Velisevich, S.N., Savchuk, D.A. 2008. Ontogenesis of Siberian cedar in a Ket-Chulym interfluve. Bulletin of the Tomsk State University. Biology, 3 (in Russian).

Ravan, Sh., Roy, P. 1997. Satellite remote sensing for ecological analysis of forested landscape. Plant Ecology 131 (2).

Rosen, M. 2002. Can exergy help us understand and address environmental concerns. Exergy 2, 214–217.

Scheller R.M., Mladenoff D.J. 2007. An ecological classification of forest landscape simulation models: Tools and strategies for understanding broad-scale forested ecosystems. Landscape Ecology, 22.

Sevko O.A. 2014. Influence of birch admixture on radial growth of pine in mixed pine-birch stands. Proceedings of BSTU Forestry, 1.

Shirish A. Ravan, P.S. Roy. 1997. Satellite remote sensing for ecological analysis of forested landscape. Plant Ecology. 131 (2).

Shvidenko, A.Z., Schepaschenko, D.G., Nilsson S. and BuluyYu.I. 2008. Tables and models of growth and productivity of forest species forNorthern Eurasia. Second edition, Moscow.

Silow, E., Mokry, A. 2010. Exergy as tool for ecosystem health assessment. Entropy, 12.

Sokolov, V., Zelentsov, V., Brovkina, O., Mochalov, V., Potryasaev, S. 2014. Complex Objects Remote Sensing Forest Monitoring and Modeling. - Modern Trends and Techniques in Computer Science. Advances in Intelligent Systems and Computing, Volume 285, 2014, 445-453.

Sokolov, B.V., Zelentsov, V.A., Brovkina, O., Victor F. Mochalov, V.F., Potryasaev. S.A. 2015. Models adaptation of complex objects structure dynamics control – Intelligent Integrated Decision Support Systems for Territory Management. - Intelligent Systems in Cybernetics and Automation Theory. Proceedings of the 4th Computer Science On-line Conference (CSOC2015), Advances in Intelligent Systems and Computing, 348, 21-34.

Sokolov, B.V., Okhtilev, M.Yu, Zelentsov, V.A., Maslova, M.A. 2012. The intelligent monitoring technology based on integrated ground and aerospace data. - Proc. of the Int. Conf. on Harbor Maritime and Multimodal Logistics M&S. 112–117.

Sokolov, B.V., Zelentsov, V.A., Yusupov, R.M., Merkuryev. Yu.A. 2014. Multiple models of information fusion processes: Quality definition and estimation. J. Comput. Sci. **5**, 380.

Turner, D.P., Scott V. Ollinger, S.V., Kimball, J.S. 2004. Integrating Remote Sensing and Ecosystem Process Models for Landscape- to Regional-Scale Analysis of the Carbon Cycle. BioScience 54 (6).

Wang, K., Franklin, S.E., Guo, X.,Cattet, M. 2010. Remote sensing of ecology, biodiversity and conservation: areview from the perspective of remote sensing specialists. Sensors, 10 (11).

Zawadski, J., Cieszewski, Ch., Zasada, M., Lowe, R. 2005. Applying geostatistics for investigations of forest ecosystem using remote sensing imagery. Silva Fennica 39 (4).

Zelentsov, V.A., Kovalev, A.P., Okhtilev, M.Yu, et al. 2013. Methodology of creating and implementing intelligent information technologies for ground and space monitoring of complex objects. - SPIIRAS Proceedings, 5, 7–81.

Zelentsov, V.A., Krylenko, I.N., Pimanov, I.Yu, Potryasaev, S.A., Sokolov, B.V., Akhtman, Y. 2015. Bases of Construction of the Remote Sensing Data Processing, Storage and Visualization System Based on Service-Oriented Architectureт - Izv. Vuzov Pribiristroenie. 58 (3), 241—243.

ANALYSIS AND EVALUATION A WEEE MANAGEMENT SYSTEM IN ITALY: A SIMULATION STUDY

Roberto Montanari[(a)], Marta Rinaldi[(b)], Teresa Murino[(c)], Liberatina C. Santillo[(d)], Eleonora Bottani[(e)]

[(a),(b),(e)] Department of Industrial Engineering, University of Parma – viale G.P.Usberti 181/A, 43124 Parma (Italy)
[(c),(d)] Dipartimento di Ingegneria Chimica, dei Materiali e della Produzione Industriale, University of Naples Federico II – Piazzale Tecchio 80, 80125 Napoli (Italy)

[(a)]roberto.montanari@unipr.it, [(b)]marta.rinaldi@unipr.it, [(c)]murino@unina.it, [(d)]santillo@unina.it, [(e)]eleonora.bottani@unipr.it

ABSTRACT
This paper presents a simulation study to evaluate the current performance of a waste of electrical and electronic equipment (WEEE) management system in the north of Italy.
The model takes into account several actors of the real WEEE supply network and allows to analyze different alternative scenarios for the functioning of the same network. The behavior of a real treatment plant has been simulated considering the incoming flow of waste material and all the outflows of recycled goods. The analysis is focused on two specific WEEE categories treated in the plant, which have been chosen as the most dangerous categories for the human health and the environment.
Some key performance indicators (KPIs) have been defined and used to assess the performance of the current WEEE network and compare it with some alternative configurations.
As it grounds on a real scenario, the model is expected to provide interesting proposals for future actions about the WEEE management in Italy.

1. INTRODUCTION
In the last years, the European governments have increasingly focused on the theme of the end-of-life management and recovery because of the lack of resources and the problem of waste management (Directive 2002/96/EC). In such context, reverse logistic activities become crucial to manage the reverse flow of materials from the final costumer to the manufacturer (Achillas et al., 2010).
As a consequence, the topic of the performance of closed-loop supply chains is becoming more and more studied in the current literature (Nukala & Gupta, 2007, Georgiadis & Besiou, 2010, Phuc et al. 2013; Bottani et al., 2015).
The interest in recycling electronic goods has recently increased, with the purpose of obtaining raw and secondary materials that can be put again in the production system and consequently sold on the market. Consequently, several case studies on the return flow of waste of electric and electronic equipment (WEEE) were published in recent years (e.g., Krikke et al., 2003, Gomes et al., 2011, Alavi et al., 2015).
WEEE include big and small electrical equipment such as computers, TV-sets, fridges and cell phones that don't work anymore. WEEE are grouped into 5 different categories depending on the kind of equipment. To be more precise, the categories are:

- R1 - refrigerating equipment (e.g. refrigerators, freezers, for conditioning equipment);
- R2 – "Big white" equipment (e.g. washing machines, dishwashers, microwave ovens, cookers, etc.);
- R3 - TV and monitor (e.g. televisions or computer monitors);
- R4 – ICT equipment, lighting equipment and others (e.g. vacuum cleaners, sewing machines, irons, fryers, blenders, computers components, printers, fax machines, mobile phones, video recorders, radios…);
- R5 - Light sources (e.g. neon, energy saving lamps, mercury vapor, sodium, iodide).

The main problems of the WEEE disposal is the presence of hazardous substances and the constant growth of their production volumes (Sthiannopkao & Wong, 2013). Also, WEEE recycling should ensure economic profitability of recovering the related raw materials (such as steel, aluminum, plastic…) and making them reusable. To this end, it is self-evident that a good recycling system is needed to maximize the recovery of components, as well as to dispose the non-recyclable material.
In Italy, the WEEE management systems are defined by the Decreto Legislativo 151/2005. Such a decree describes the organization of the global WEEE management system in terms of actors, manufacturers, local authorities, distributors and treatment plants, as shown in Figure 1.
The logistic network plays a crucial role in managing the reverse flow of WEEE. In particular, the location and capacity of both the collection points and the treatment plants are among the main leverages that affect the performance of the whole system.
This study focuses on the performance evaluation of a real WEEE management system, i.e. that of the area of

Parma in the north of Italy. We investigate, in particular, the flow of materials from the collection points to the treatment plant. All the data on the material flows have been provided from the local group that manages the garbage collection in the area of Parma and of the neighbor districts.

The remainder of the paper is organized as follows: section 2 analyses the context, section 3 exposes the logic of the simulation model. Then, the main results are shown in section 4 and some general conclusions are presented in section 5.

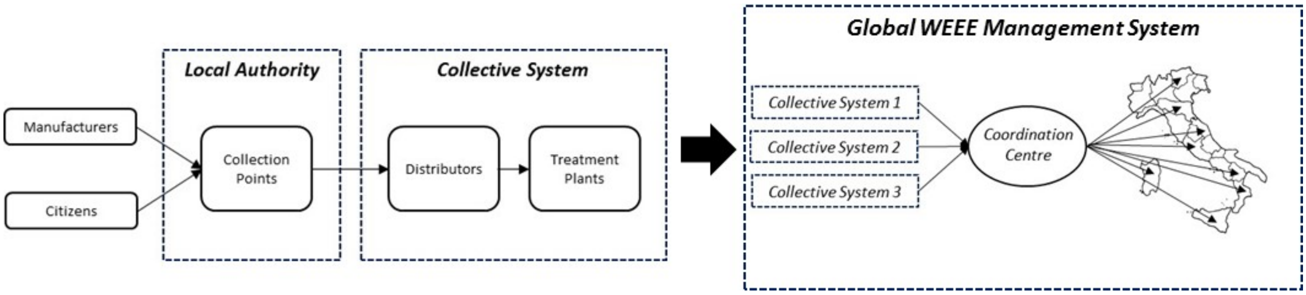

Figure 1: Italian WEEE management system

2. THE WEEE MANAGEMENT SYSTEM

In Italy, the total amount of WEEE recovered in 2014 accounts for about 230,000,000 kg/year in the whole country, with 136,386 pickups in a year.

In this study, we analyze the situation of a specific region, i.e. Emilia Romagna, which in 2014 achieved the second place in terms of WEEE total collection, with the 10% of the total amount of WEEE of Italy collected in that region. In such region, 11 different institution operate with the aim of managing the collection of the urban waste. Iren, the company that was involved in this study, manages the WEEE collection in the municipality area of Parma and controls 153 collection points. The total amount of material recovered in such area is about 1,650,000 kg/year, of which 19% R1, 30% R2, 27% R3, 23% R4 and 1% R5.

A detailed analysis of the WEEE collection system shows that Iren manages only the first part of the supply chain, i.e. from the end-users to the collection points, while the collective system handles the flow of WEEE from the collection points to the treatment plants. The collection system also makes decisions about the number and location of the plants involved in the recovery system, as well as on the amount of WEEE material that will be shipped to each of them. Finally, a coordination center should supervise the work of the collective systems, in order to guarantee a good service in each area of the country.

3. THE MODEL

A simulation model has been created using MS Excel^{TM} with the purpose of reproducing the flow of WEEE in the targeted area, as well as to simulate the treatment process of WEEE at the processing plant.

A specific plant, belonging to the consortium, has been visited with, with the purpose of collecting the necessary data to simulate its daily work. Example of these data are the production capacity and the possible constraints (e.g. the warehouse capacity). The targeted processing plant treats only 2 WEEE categories, i.e. R1 (refrigerators) and R3 (TVs and monitors). Indeed, each treatment plant is usually specialized in (and authorized for) the processing of a limited number of WEEE categories, because of the complexity of the processes required for the different WEEE. The categories treated by the targeted plant are considered as the most dangerous ones for the human health and the environment. The plant works 5 days/week for 8 hours/day in a one-shift situation, although the capacity of the plant could be doubled working on two shifts per day.

Overall, the network considered in the model consists of the treatment plant that receives the materials from (1) some collection points managed by Iren by means of external distributors, (2) other collection points located out of the Parma area but sufficiently close to the plant. Finally, the plant delivers the recovered materials to different markets and it disposes the waste in specific disposal plants. The supply chain examined is shown in Figure 2.

The simulation model developed is able to reproduce the behavior of the whole system by the treatment plant perspective. To this end, it is composed of 4 spreadsheets, one for each main process of the plant: the first one organizes the input data collected for the two categories, the second and the third ones reproduce the two treatment processes and the last one manages the stock of the output and provides the results of the whole simulation.

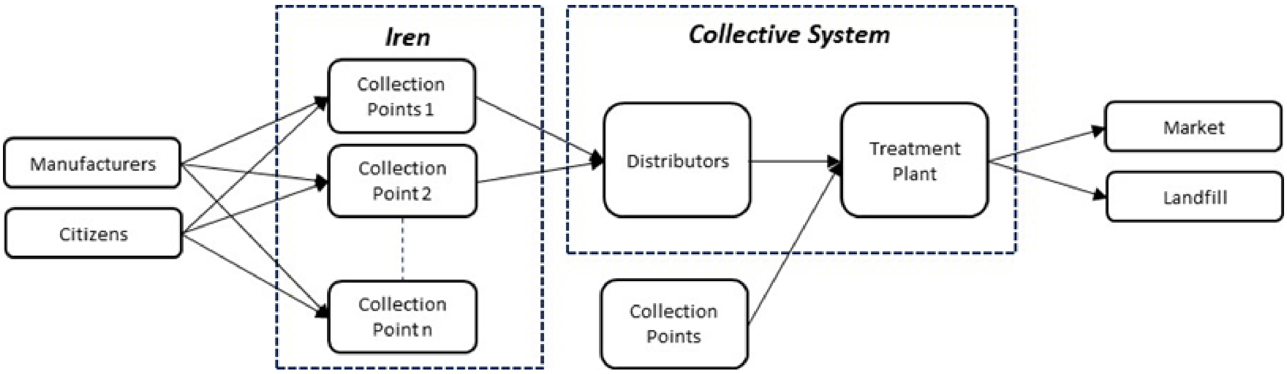

Figure 2: the supply chain modeled

In order to evaluate the performance of the collection and treatment system, as well as its response to the increasing needs of the WEEE management system, two different scenarios have been reproduced. We launched 10 replicates of each scenario simulated, to provide suitable results from the statistical point of view.

The first scenario aims to reproducing the current system (AS IS analysis), to evaluate its current performance and to identify its critical points. To this extent, the amount of the WEEE material processed by the plant (and set as input in the simulation model) reflects the real quantity treated by the plant in 2014. In the simulation, after a statistical analysis of the available data carried out with SPSS software package, the daily amount of WEEE treated was modelled with a uniform distribution. Some key performance indicators (KPIs) have been defined to compare the current situation and the future proposals; in particular, the plant aims at stocking the input material not more than one day.

For each replicate $r = 1,..10$, the average time in stock G_r is calculated as follows:

$$G_r = \frac{T}{I_r} \text{ [day]} \tag{1}$$

where $T = 260$ days/year represents the number of working days per year of and I_r is the inventory turnover rate, calculated as:

$$I_r = \frac{Kg\ treated_r}{Kg\ not\ treated_r} \tag{2}$$

Thus, the average time in stock G_r has to respect that constraint:

$$G_r \text{ (R1)} \leq 1 \text{ day; } G_r \text{ (R3)} \leq 1 \text{ day} \tag{3}$$

Moreover, a cost/benefit evaluation has been included in the study to compare the different scenarios.

In particular, the total cost of each scenario has been calculated as the sum of different cost elements:

- cost of transport from the collection point to the plant;
- cost of stock, considering both the incoming WEEE and the final products at the treatment plant;
- cost of labor at the treatment plant;
- cost of disposal of the non-recycled materials.

As saving, the economic income is due to the sale of the recovered material and to a gate fee levied upon a given quantity of waste received.

The second scenario (TO BE evaluation) takes into account the possible situation where the treatment plant receives the materials from all the collection points of Parma, with the purpose of minimizing the total distance covered for collection.

The same simulation model has been used to reproduce the TO BE situation. The only main modification refers to the input data related to the incoming quantities. In this scenario, the quantity of R1 and R3 collected by Iren in 2014 have been added to the quantity treated by the plant in the same period; then, again after a statistical analysis carried out with SPSS software package, a uniform distribution has been hypothesized to reproduce the input data of the model.

4. RESULTS AND DISCUSSION

The first analysis brings out that in the current situation the plant is able to respect the main constraint, as shown in Table 1.

Replicate	G_r (R1) [day]	G_r (R3) [day]
1	0.79	0.002
2	0.43	0.002
3	0.75	0.003
4	0.06	0.000
5	0.33	0.002
6	0.45	0.003
7	0.58	0.004
8	0.37	0.001
9	0.38	0.003
10	0.40	0.003

Table 1: AS IS average time in stock for the two categories.

In particular, the results show that the capacity of the plant to treat R3 is highly oversized; indeed, the plant is able to process the WEEE material with a very low time in stock.

A specific analysis of the input data underlines that the whole system does not operate by minimizing the distance between the collection points and treatment plants. The main reason concerns the fact that the consortium probably sorts the WEEE among all of the plants, regardless of distance considerations. Such results motivated us to verify the feasibility of having the targeted plant treating the whole amount of WEEE materials collected in the area of Parma. The results of the simulation are shown in Table 2.

Replicate	G_r (R1) [day]	G_r (R3) [day]
1	1.217	24.46
2	0.592	78.71
3	1.061	133.76
4	0.076	27.38
5	0.398	248.30
6	0.560	303.86
7	0.727	361.78
8	0.469	209.08
9	0.466	473.43
10	0.490	530.19

Table 2: TO BE #1 average time in stock for the two categories.

The analysis of the TO BE scenario shows that the treatment plant considered would be able to work all the R1 quantities accumulated in the area of Parma, but the average time in stock exceeds the limit defined by the company two out of ten times (replication 1 and 3). Such constraint is the most relevant one because of the lack of space to stock the incoming WEEE.

Moreover, Table 2 shows as the plant is not able to process the incoming amount of R3, with a resulting increase of G_r (R3) for all the replications.

As a solution, in order to manage the new R3 volume the plant should duplicate the working shift; this last situation would minimize the distance and the cost of the transport of the whole system but the R1 line would not need it.

After all the considerations above, a second TO BE scenario has been modeled (TO BE #2): in this case, the scenario considers the constrain of the average level of stock and hypothesizes a one-shift situation for the treatment of R1 (the same of the previous TO BE #1 scenario) and a two-shift situation for R3, with the purpose of optimizing the total cost of the whole system. In this latter case, the plant would be able to process all the incoming WEEE with G_r (R3)<1 day, but the total capacity of the plant would work under its production capacity. In fact, the incoming amount of R3 doesn't justify the second working shift.

Scenario	Average Incomes [€]	Average total cost [€]	Net Profit [€]
AS IS	19676	9868	9808
TO BE #1	28421	15156	13265
TO BE #2	28432	14216	14216

Table 3: Economic results of the simulation model.

Also, from an economic point of view, Table 3 shows that the new scenario TO BE #2 is better than the current situation. The total cost growths because of the increase of the amount of material treated, but for the same reason also the sale of the material recovered bring to a high income.

5. CONCLUSIONS

This study focuses on the performance evaluation of the WEEE management system in the area of Parma in the north of Italy. In particular, the waste flow of 2 specific categories, i.e. R1 and R3, have been analyzed. A detailed analysis, carried out exploiting a simulation model, has showed that the system could be improved by minimizing the distance covered to ship the WEEE from the collection points to the treatment plants. A particular solution has also been defined considering the capacity of a real plant and its constraints.

The simulation model has proved to be very useful from a practical point of view; in fact, it allows to compare different scenarios, with the purpose of optimizing the efficiency of the plant and minimizing the distance covered by the distributors. Moreover, the topic of the waste management is very relevant around the world, as it involves a lot of actors and public institutions; for this reason, more and more researchers are working on it.

Future research activities could include in the study all the treatment plants served by Iren in order to analyze the efficiency of the whole system in the area of Parma.

REFERENCES

Achillas, C., Vlachokostas, C., Aidonis, D., Moussiopoulos, Iakovou, E., Banias, G., 2010. Optimising reverse logistics network to support policy-making in the case of electrical and electronic equipment. Waste Management, 30(12), 2592–2600.

Alavi N., Shirmardi M., Babaei A., Takdastan A., Bagheri N., 2015. Waste electrical and electronic equipment (WEEE) estimation: A case study of Ahvaz City, Iran. Journal of the Air & Waste Management Association, 65(3), 298-305.

Bottani, E., Montanari, R., Rinaldi, M., Vignali, G., 2015. Modelling and multi-objective optimization of closed loop supply chains: a case study. Computers & Industrial Engineering, 87, 328-342.

Directive 2002/96/EC of the European Parliament and of the Council, of 27 January 2003, on Waste Electrical and Electronic Equipment (WEEE).

Decreto Legislativo 25 luglio 2005, n.151 "Attuazione delle direttive 2002/95/CE, 2002/96/CE e 2003/108/CE, relative alla riduzione dell'uso di sostanze pericolose nelle apparecchiature elettriche ed elettroniche, nonché allo smaltimento dei rifiuti", Gazzetta Ufficiale n. 175 del 29 luglio 2005.

Georgiadis P. & Besiou M., 2010. Environmental and economical sustainability of WEEE closed-loop supply chains with recycling: a system dynamics analysis. International Journal of Advanced Manufacturing Technology, 47, 475–493.

Gomes, M.I., Barbosa-Povoa, A.P., Novais A.Q., 2011. Modelling a recovery network for WEEE: A case study in Portugal. Manufacturing & Service. Waste Management, 31, 1645–1660.

Krikke, H., Bloemhof-Ruwaard, J., Van Wassenhove, L.N., 2003. Concurrent product and closed-loop supply chain design with an application to refrigerators. International Journal of Production Research, 41(16), 3689–3719.

Nukala, S. & Gupta, S.M., 2007. Performance measurement in a closed-loop supply chain network. Proceedings of the 2007 Northeast Decision Sciences Institute Conference, Baltimore, Maryland, pp. 474-479, March 28-March 30.

Phuc P.N., Yu V.F., Chou S., 2013. Optimizing the fuzzy closed-loop supply chain for electrical and electronic equipments. International Journal of Fuzzy Systems, Vol. 15, N.1.

Sthiannopkao S., Wong M.H., 2013. Handling e-waste in developed and developing countries: Initiatives, practices, and consequences. Science of the Total Environment, 463–464, 1147–1153.

AUTHORS BIOGRAPHY

Roberto MONTANARI is Full professor of Mechanical Plants at the University of Parma. He graduated (with distinction) in 1999 in Mechanical Engineering at the University of Parma. His research activities mainly concern equipment maintenance, power plants, food plants, logistics, supply chain management, supply chain modelling and simulation, inventory management. He has published his research in approx. 70 papers, which appear in qualified international journals and conferences. He acts as a referee for several scientific journals, is editorial board member of 2 international scientific journals and editor of a scientific journal.

Marta RINALDI is research fellow of the University of Parma. She graduated (with distinction) in Industrial Engineering and Management in 2011, and got her Ph.D. in Industrial Engineering in 2015, both at the University of Parma. She currently works on discrete event simulation and its application to industrial plants, logistics, supply chain management, supply chain modelling and simulation, inventory management, manufacturing systems and business processes. She is author (or co-author) of more than 10 papers published in international journals.

Eleonora BOTTANI is Associate professor of Industrial Logistics at the Department of Industrial Engineering of the University of Parma. She graduated (with distinction) in Industrial Engineering and Management in 2002, and got her PhD in Industrial Engineering in 2006, both at the University of Parma. Her research interests are in the field of logistics and supply chain management. She is the coordinator of a national project, called ESCALATE (Economic and environmental Sustainability of Supply Chain and Logistics with Advanced Technologies) related to supply chain sustainability. She is author (or co-author) of approx. 120 scientific papers, referee for more than 60 international scientific journals, editorial board member of five scientific journals, an Associate Editor for one of those journals, and editor-in-chief of a scientific journal.

Teresa MURINO graduated in Mechanical Engineering and is assistant professor in the ING-IND 17 “Industrial Mechanical System Engineering” disciplinary group, at the University of Naples Federico II. She teaches Manufacturing System Management, Goods and Services Production System, and Industrial Logistics at Engineering Faculty. She is also Professor at “Consorzio Nettuno”. She is also reviewer for Elsevier Editorials, and other journal ISI indexed. The research activities is mainly concerned about the following topics: Simulation modelling; Maintenance strategies; Supply Chain Management models; Quick Response Manufacturing; Sustainable production processes; Location-Routing and vehicle routing Problem, Lean Service and Lean production implementation.

Liberatina C. SANTILLO graduated in Mechanical Engineering in 1986 and, since 2004, she is Full professor at the Department of Chemical Engineering, Materials and Industrial Production of the University of Naples Federico II. She teaches Safety of Industrial plants at the Master degree course in Mechanical Engineering and Production systems at the Degree course in Engineering Management. She is coordinator of the Master in “Safety at the workplace”. She has been lecturer at numerous courses on safety at work and fire prevention. She is author (or coauthor) of numerous international publications on manufacturing.

INCLUDING RELIABILITY IN THE ANALYSIS OF MARKET DRIVEN RENEWABLE ENERGY SYSTEMS WITH STORAGE

Pedro Mateo[(a)], Cristina Azcárate[(b)], Fermín Mallor[(c)]

[(a)] University of Zaragoza
[(b) (c)] Public University of Navarre

[(a)]mateo@unizar.es, [(b)]cazcarate@unavarra.es, [(c)]mallor@unavarra.es

ABSTRACT
The possibility of renewable energy systems to store energy facilitates their participation in the electricity market as well as to control the forecast errors in the renewable source and then to increase the reliability of the system as provider of energy. This paper optimizes the management of this energy system considering simultaneously both goals, an economic goal and a reliability goal. Policies to provide the electricity dispatch schedule for the day ahead (tactical decisions) and to control the energy storage each hour (operational decisions) are obtained from a sequence of mathematical problems. A simulation model is developed to assess the performance of these policies in a stochastic framework that considers the variability and uncertainty in the renewable source.

Keywords: Energy Storage System (ESS), Renewable Energy Management, Tactical and Operational Decisions, Simulation and Optimization

1. INTRODUCTION

The aim of electricity companies is to get as much profit as they can by selling the product they commercialize: the electricity. However, as any other company in every economic sector, they are also obliged to provide a service of quality (by contractual enforcement or simply because it is a strategic requirement to survive in a competitive environment). An important part of the service quality provided by a company in the energy sector is to supply energy whenever it is demanded. However, a handicap for renewable energy companies is that the sun does not always shine and the wind does not always blow when they are required. Cost-effective energy storage technologies help to overcome this problem enabling the management of the generated renewable energy.

The stored energy can be used to improve achievements in the two above mentioned objectives: the economic one by storing the energy when prices are low and selling it when prices are higher, and the reliability one by supplying the demanded energy when the renewable sources are not available. Furthermore, the storage facilitates the participation of the electricity companies in the day-ahead electricity market. The grid operator receives the electricity dispatch schedule from the wind farm managers in advance. When the power output of the wind farm differs from the schedule submitted the wind farm owner is financially punished.

This paper simultaneously deals with the problem of determining the number of kWh that should be committed by an electricity company in the day-ahead electricity market and the operational management of the energy storage system (ESS), with the aim of simultaneously achieving a maximum economic return as well as a maximum reliability. Thus this bi-objective optimization problem is simultaneously of tactical and operational nature. Furthermore, decisions about how much electricity to commit each hour of the day-ahead is based on available forecasts for the renewable energy resource. That is, our analysis incorporates both forecasting and uncertainty in resource availability into the analysis which allows a more realistic assessment of the reliability of the energy system. However, the inclusion of the stochastic environment in which the energy system evolves also leads to the formulation of more complex mathematical models.

Many papers have studied the management of renewable energy systems with ESS, (see Connolly et al., 2010, the reviews Luo et al., 2015, and Zhao et al., 2015, and the references therein) some focused on the tactical problem and optimizing the economic problem as for example Aguado et al. (2009), where a mixed integer linear programming model was used embedded in a simulation model. This model was improved in Azcarate et al (2012) to incorporate a probabilistic wind speed forecast (PWSF). Operational decisions were not optimized in either of these two articles, which consider only simple strategies oriented towards fitting the committed energy as much as possible. A type of parametric operational strategies for the ESS was studied in Mallor et al (2015), but the commitments were obtained independently of the implemented operational management. In Kou, Gao, and (2015) an operational strategy for the management of a set of batteries connected to a wind-farm is proposed to control the deviations from a dispatch curve, and then paying more attention to the reliability goal.

In this paper we propose a bi-objective stochastic linear problem to model the operational and tactical problems which incorporate a PWSF. They are solved by using a rolling horizon strategy, which allows the assessment of the reliability of the ESS achieved in the recent past for building the subsequent optimization problems that drive the tactical and operational policies. The sequence of stochastic linear problems is solved by a method inspired by the Stochastic Approximation Average (SAA) technique (see Kim, Pasupathy, and Henderson, 2015, for an explanation of this mathematical method to solve stochastic optimization problems). We particularize the mathematical model to a wind energy system with ESS based on hydrogen (H2) technologies. A discrete event simulation model is developed to mimic the operation of such wind energy system with storage. Using this simulation model we can assess, under different stochastic scenarios, the performance of the management policies obtained from the solution of the optimization problems. Nevertheless, the models can be easily adapted to other intermittent renewable energies and ways of energy storage.

The paper is organized as follows. In Section 2, the management problem of an energy system with storage, regarding economic and reliability goals, is defined. In section 3 we present the two stochastic mathematical linear problems that model the tactical and operational problems, respectively. In Section 4 a simulation framework is built to assess and to calibrate the management policies obtained as outcome of the optimization problems. Simulation results are included in Section 5 to illustrate the capability of our mathematical approach to get optimal operational and tactical management policies. The paper ends with some remarks and conclusions.

2. PROBLEM DEFINITION

In this Section the economic and stochastic environment context of the wind farm with ESS is described, particularly, the economic rules that govern the grid connected electricity market, the variability and uncertainty of the wind resource and related reliability issues. All these factors strongly influence the performance of the adopted operation and control strategies for the ESS. Next subsections describe their mathematical modelling.

2.1. Electricity Market and Economic Assessment

We consider an electricity company owning a wind energy system grid-connected with ESS based on the production of H2. The electricity dispatch schedule of the wind farm has to be submitted in advance to the grid operator. In this way, the company participates in the electricity market through committing energy to be sold for the day ahead. These commitments are made once per day by declaring the amount of energy that they are selling in each one of the 24 hours of the following day. Specifically, let Y_i be the amount of kWh committed for selling at hour i. The revenue obtained from the selling of Y_i kWh at hour i is $C_{c_i}Y_i$, where C_{c_i} is the unit price of a committed kWh at hour i. Let Z_i be the amount of kWh ultimately sold at hour i. Deviations of the dumped energy Z_i from the committed energy Y_i have a penalty: when the sold energy Z_i is less than Y_i, an amount C_{p_i} should be paid for each kWh committed and not supplied (furthermore, the renewable energy system becomes a non-reliable energy supplier). For the case in which the dispatched energy Z_i exceeds the committed energy Y_i, the selling price of each kWh in excess, C_{s_i}, is less than the committed kWh price, C_{c_i}. Thus, the total economic revenue at hour i with Y_i committed KWh and Z_i kWh sold is:

$$C_{c_i}Y_i + C_{s_i}d_i^+ - \left(C_{c_i} + C_{p_i}\right)d_i^- \qquad (1)$$

where

$$Z_i + d_i^- - d_i^+ = Y_i, \quad \text{with} \quad d_i^-, d_i^+ \geq 0$$

Here, the deviational variables d_i^- and d_i^+ express the negative and positive deviations of the supplied energy with regard to the commitments. Clearly, from an economic point of view the greatest revenue are obtained when variables Y_i take values as highest as possible and the deviation variables take value zero. The quotient d_i^-/Y_i measures the lack of reliability of the system at time i.

The dispatched energy Z_i is the result of adding the X_i^O kWh obtained from the ESS to the G_i kWh generated from the renewable source at hour i and subtracting the amount X_i^I of kWh stored in the ESS.

That is,

$$Z_i = G_i - X_i^I + X_i^O$$

Determining the values for X_i^O and X_i^I are the decisions that constitute the operational decision making. Determining the values of Y_i (once per day, in the day-ahead electricity market), for each one of the 24 hours of the day ahead are the decisions that constitute the tactical decision making.

2.2. Variability and uncertainty

The decision-making is performed in a stochastic environment, which has to be taken into account to obtain meaningful results. The value G_i is not known with certainty in advance. Decisions are made based on a forecast of the renewable resource, which is subject to errors. Specifically, we assume that a Probabilistic Wind Speed Forecast (PWSF) at each time t is available: a set of *m* predicted wind speed trajectories for the near future. These *m* different forecasts for the wind speed are used as inputs of the power curve, which converts wind speed to power generation. After this transformation, we obtain a probabilistic forecast of the amount of electricity produced for each of the next *n* hours: $G_m = \{G_{ij},\ i = 1, \dots, n\}_{j=1}^{m}$, where G_{ij} is the KWh generated at hour i associated with the j-th predicted wind speed curve.

2.3. Reliability Assessment

In regions with high penetration of renewable energy it is necessary to measure the capacity of the generation system to cover the load without unexpected imports.

In the literature two main measures are used to assess the reliability of any energy generator system (see Callaway, 2010): the expected time that the system does not supply the demanded energy (the Loss of Load Probability - LOLP) and the expected amount of demanded energy not supplied by the energy system (the Loss of Load Expectation - LOLE). Both are used to assess the performance of the system in the long term. In our analysis we need to adapt these measures to get a local measure of the energy system reliability performance in order to drive tactical and operational decisions to meet reliability goals at every moment over time.

We propose the following index R_t^E to measure the local reliability at time t:

$$R_t^E = 1 - \frac{\sum_{k=0}^{t-1} \lambda^k (Y_{t-k} - Z_{t-k})^+}{\sum_{k=0}^{t-1} \lambda^k Y_{t-k}}$$

where,

$0 < \lambda \leq 1$, and $(Y_{t-k} - Z_{t-k})^+ = \max\{Y_{t-k} - Z_{t-k}, 0\}$

When λ is 1, this index calculates the ratio of committed energy not supplied by the energy system, and then it corresponds with an estimation of the long term reliability measure LOLE. When $\lambda < 1$, a geometric moving average is defined where the reliability behavior of the system in the far away past contributes to the index result less than its reliability behavior in the recent past and present. The greater the value of λ the greater the influence of the reliability in the past in the present value of the reliability index. That is, λ represents a memory-size parameter.

Similarly, we define a local version R_t^P of the LOLP

$$R_t^P = 1 - \frac{\sum_{k=0}^{t-1} \lambda^k 1_{\{Y_{t-k} > Z_{t-k}\}}}{\sum_{k=0}^{t-1} \lambda^k}$$

If R^E denotes the reliability goal for the amount of committed energy supplied by the renewable system (that is, for the LOLE value) then,

$$\varphi_t^E = \begin{cases} \dfrac{R_t^E}{R^E} & \text{when } R_t^E < R^E \\ 1 & \text{when } R_t^E \geq R^E \end{cases}$$

is a reliability ratio that measures at time t the deviation of the system from the general reliability goal. This index can be calculated at every time t, and it is introduced in the mathematical optimization problem to induce outcomes providing management policies supporting the increase of the reliability goal.

3. MATHEMATICAL OPTIMIZATION PROBLEM

In this section we propose a mathematical optimization problem whose solution provides the tactical (Y_i values) and operational (X_i^I, X_i^O values) management of the energy system. The mathematical model deals with the uncertainty in the wind speed forecast by considering that a PWSF is available, and includes both objectives the economic and the reliability one.

3.1. Formulation of the Optimization Problem for the Energy System Operational Management

Let suppose, without loss of generality, that the present time is denoted by t, that the commitments of energy Y_i are known (they are determined by a similar problem described in next section concerning the tactical problem). A reliability goal R^E is fixed and it is know the reliability ratio φ_t^E. The operation of the ESS in the next hour (denoted by index 1) is determined by the values of the decision variables X_1^I, X_1^O obtained as solution of the following mathematical problem.

Problem [OP]:

$$\begin{aligned} Maximize \sum_{i=1}^{n} C_{c_i} Y_i + C_{s_1} \frac{1}{m} \sum_{j=1}^{m} d_{1j}^+ - (C_{c_1} + C_{p_1}) \frac{1}{m} \sum_{j=1}^{m} d_{1j}^- \\ + \sum_{i=2}^{n} \left(C_{s_i} d_i^+ - (C_{c_i} + C_{p_i}) d_i^- \right) \\ - (1 - \varphi_t^E) C_R \left(\frac{1}{m} \sum_{j=1}^{m} d_{1j}^- + \sum_{i=2}^{n} d_i^- \right) \end{aligned}$$

Subject to

$$G_{1j} - X_1^I + X_1^O + d_{1j}^- - d_{1j}^+ = Y_1 \quad j = 1, \dots, m \qquad (1)$$

$$T_1 + efI\ X_1^I - efO^{-1}\ X_1^O = T_2 \quad j = 1, \dots, m \qquad (2)$$

$$G_{ij} - X_{ij}^I + X_{ij}^O = Z_{ij} \quad i = 2, \dots, n, \ j = 1 \dots, m \qquad (3)$$

$$T_{ij} + efI\ X_{ij}^I - efO^{-1}\ X_{ij}^O = T_{i+1\, j} \quad i = 2, \dots, n \quad j = 1 \dots, m \qquad (4)$$

$$Z_i = \frac{\sum_{j=1}^m Z_{ij}}{m} \quad i = 2, \dots, n, \qquad (5)$$

$$Z_i + d_i^- - d_i^+ = Y_i \quad i = 2, \dots, n \qquad (6)$$

$$X_1^I, X_{ij}^I \leq Cap_{transf}/efI \quad i = 2, \dots, n, j = 1 \dots, m \qquad (7)$$

$$X_1^O,\ X_{ij}^O \leq Cap_{Recovery} * efO \quad i = 2, \dots, n, j = 1 \dots, m \qquad (8)$$

$$T_{ij} \leq Cap_{Tank} \quad i = 2, \dots, n, j = 1 \dots, m \qquad (9)$$

$$Z_i, Z_{ij},\ d_{1j}^+,\ d_{1j}^-, d_i^-, d_i^+, X_1^O, X_1^I, X_{ij}^I, X_{ij}^O, T_{ij} \geq 0$$

Observe that constraints (1) determine the deviation variables associated to the operational decision variables X_1^I, X_1^O which will be the only ones that will be implemented in practice. The other decision variables, X_{ij}^I, X_{ij}^O, are only used to evolve the system in the future to evaluate the consequences of the present decisions. Constraints (2) update the state of the energy storage system. Constraints (3) define the amount of kWh to be released in the future according to each wind trajectory, (4) assures that the employed policies are feasible, (5) estimates the expected kWh released into the grid and (6) evaluates the deviations of this average with respect to the committed kWh. The remaining constraints, (7), (8) and (9), are the capacity constraints.

3.2. Formulation of the Optimization Problem for the Energy System Tactical Management

Once per day, the managers should decide how much energy to commit for each of the 24 hours of the day ahead. Suppose that the decision is made every day at 12 a.m., then i=1 corresponds to the hour from 12 a.m. to 1 p.m., i=2 to the hour from 1 p.m. to 2 p.m., and so on. The commitments for the 12 hours ranging from 12 a.m. to 12 p.m. are known because they were fixed the day before. This problem is solved by formulating a problem similar to the previous one, where the decision variables of interest to determine the electricity dispatch schedule are $\mathrm{Y_i}, i = 13, \dots, 36$. These values define the tactical decisions because they are considered as the electricity selling commitments. There are two differences respect to the problem [OP]:

- the $\mathrm{Y_i}$ are known parameters for the indices i corresponding to hours of the current day, $i = 1, \dots, 12$, but they are decision variables for each of the 24 hours of the day ahead, that is, indices $i = 13, \dots, 36$.
- the reliability influence on the tactical decisions is modeled by modifying the constraint (5) in the following way:

$$Z_i = (\varphi_{\mathrm{t}}^{\mathrm{E}})^{W_t} \frac{\sum_{j=1}^{m} Z_{ij}}{m} \quad \mathrm{i} = 2, \dots, \mathrm{n}$$

where $W_t = \sum_{k=0}^{t-1} \lambda^{\mathrm{k}} 1_{\{\mathrm{Y_{t-k}} > \mathrm{Z_{t-k}}\}}$.

When the reliability goal is not being achieved then the factor $(\varphi_{\mathrm{t}}^{\mathrm{E}})^{W_t}$ induce a reduction in the amount of released electricity and then also in the value of the scheduled energy, favoring in this way the ultimate supply of the scheduled energy.

Then the mathematical problem to obtain the tactical management of the renewable system is:

Problem [TP]:

$$Maximize \sum_{i=1}^{n} C_{c_i} Y_i + C_{s_1} \frac{1}{m} \sum_{j=1}^{m} d_{1j}^{+} - (C_{c_1} + C_{p_1}) \frac{1}{m} \sum_{j=1}^{m} d_{1j}^{-} + \sum_{i=2}^{n} \left(C_{s_i} d_i^{+} - (C_{c_i} + C_{p_i}) d_i^{-} \right)$$

Subject to

$$G_{1j} - X_1^I + X_1^O + d_{1j}^{-} - d_{1j}^{+} = Y_1 \quad \mathrm{j} = 1, \dots, \mathrm{m} \quad (1)$$
$$T_1 + efI\ X_1^I - efO^{-1} X_1^O = T_2 \quad \mathrm{j} = 1, \dots, \mathrm{m} \quad (2)$$
$$G_{ij} - X_{ij}^I + X_{ij}^O = Z_{ij} \quad \mathrm{i} = 2, \dots, \mathrm{n},\ \mathrm{j} = 1 \dots, \mathrm{m} \quad (3)$$
$$T_{ij} + efI\ X_{ij}^I - efO^{-1} X_{ij}^O = T_{i+1\,j} \quad \mathrm{i} = 2, \dots, \mathrm{n},\ \mathrm{j} = 1 \dots, \mathrm{m} \quad (4)$$

$$Z_i = (\varphi_t^E)^{W_t} \frac{\sum_{j=1}^{m} z_{ij}}{m} \quad i = 2, \dots, n, \quad (5)$$
$$Z_i + d_i^{-} - d_i^{+} = Y_i \quad \mathrm{i} = 2, \dots, \mathrm{n} \quad (6)$$
$$X_1^I, X_{ij}^I \le Cap_{transf}/efI \quad \mathrm{i} = 2, \dots, \mathrm{n}, \mathrm{j} = 1 \dots, \mathrm{m} \quad (7)$$
$$X_1^O,\ X_{ij}^O \le Cap_{Recovery} * efO \quad \mathrm{i} = 2, \dots, \mathrm{n}, \mathrm{j} = 1 \dots, \mathrm{m} \quad (8)$$
$$T_{ij} \le Cap_{Tank} \quad \mathrm{i} = 2, \dots, \mathrm{n}, \mathrm{j} = 1 \dots, \mathrm{m} \quad (9)$$
$$Z_i, Z_{ij},\ d_{1j}^{+},\ d_{1j}^{-}, d_i^{-}, d_i^{+}, X_1^O, X_1^I, X_{ij}^I, X_{ij}^O, T_{ij} \ge 0$$

4. SIMULATION FRAMEWORK

We develop a discrete time simulation model to test the management policies in different environments defined by the electricity prices, by the accuracy of the PWSF and by different reliability goals.

The simulation model includes all of the important equipment that comprises the wind-H2 energy system (wind generators, electrolisers, compressors, H2-tank, fuel cells,...).

The logic of the simulation is described in Figure 1. Before beginning the simulation the energy system is defined by providing value to the parameters that dimension it (transformation curves, efficiencies, capacities,…), a goal of reliability is fixed and the length of the simulation set. Time is initialized at zero.

The clock of the simulation is advanced in steps of one hour. First, the PWSF is generated by simulation by using the method proposed in Mallor et al. (2009): an autoregressive time series model generates autocorrelated errors that modify the true wind speed series. The method uses maximum relative errors that vary in the forecast horizon from an initial value to a final value following different functional patterns. All these parameters can be modified. Following this method *m* wind speed trajectories are generated. From them the probabilistic electricity generation forecast for the next *n* hours are obtained.

First it is check if the current hour is an hour to send the electricity dispatch schedule for the day ahead to the grid regulator. If it is, then the problem OP is solved to get the operational policy, that is, the amount of electricity that either has to be stored in the next hour or has to be released from the storage. Then, the energy system is updated taking into account the electricity production simulated at that hour: level of energy in the storage, economic profit from the selling of electricity and reliability of the energy systems regarding the commitments.

If it is the hour to send the grid operator the electricity dispatch schedule then the problem TP is solved to obtain the commitments for the 24 hours of the day ahead. Then, the OP problem is solved for that hour.

After updating the statistical counters, the clock of the simulation is advanced one hour and the previous procedure is repeated again. This simulation framework is useful to test different values for the memory parameter λ used in the definition of the local indices of reliability and the extra penalty parameter $\mathrm{C_R}$ used to favor the reliability goal in the objective function.

The simulation model has been implemented in Java and the optimization problems are solved by using the CPLEX solver. The size of the optimization problems allows to obtaining the optimal solution very quickly and as a consequence the simulation of one year of this energy system only takes less than one minute with a computer with an i7 processor.

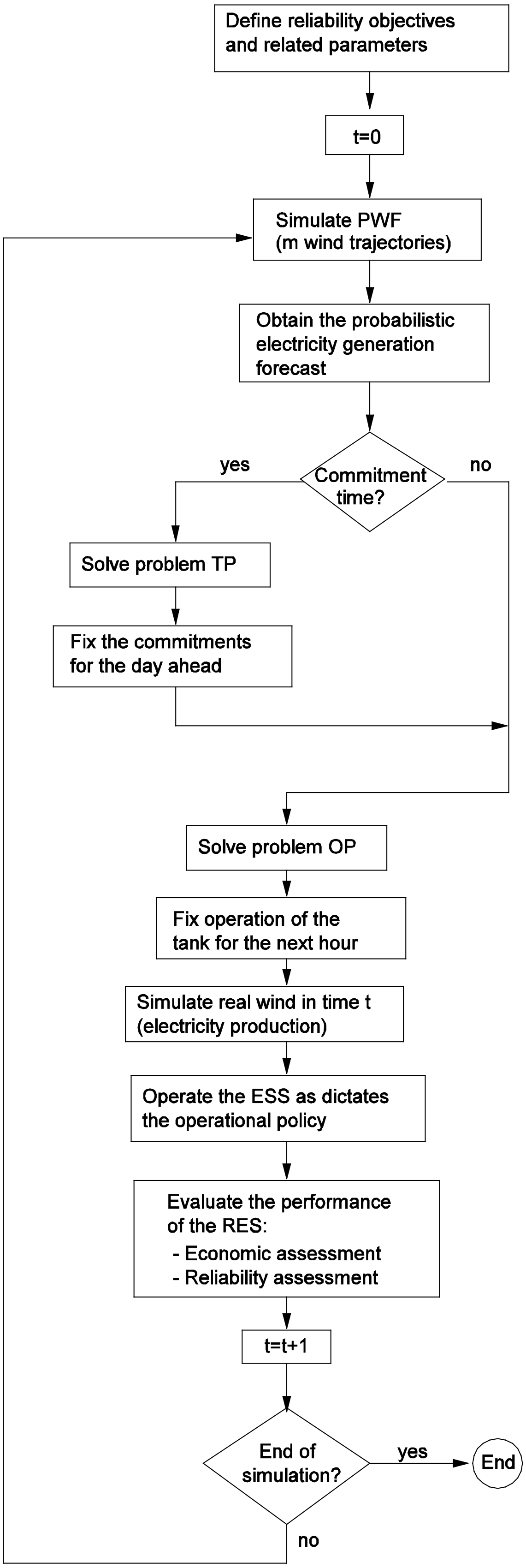

Figure 1: Organigram of the simulation framework.

5. RESULTS AND CONCLUSIONS

In this section in order to illustrate the methodology proposed in this research work to obtain both tactical and operational management policies of an energy system with ESS, we consider a renewable wind-farm system with H2-based storage inspired by a real system that the authors studied in a previous paper (see Aguado et al. (2009)). We present graphically (Figures 2 and 3) ten days of simulation results, although the system has been simulated for a whole year. Figure 2 shows the electricity production during these ten days. We use real wind speed data as the true wind speed data during the simulation, and from it we simulate the PWSF and its associated electricity production.

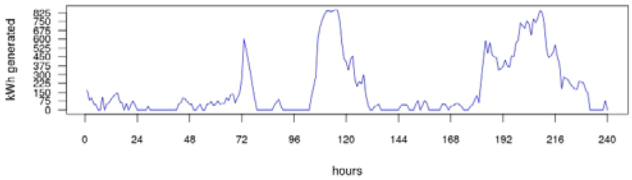

Figure 2: Electricity production of the wind farm.

The simulation experiments are designed to show the effect of introducing the reliability goal in the management of the system, in terms of both economic cost and reliability improvement. Figure 3 shows these results when the objective for the reliability is set to 0,98. In the top graphic of Figure 3 we see that the management including the reliability goal is able to improve it when the local reliability measure decays below the fixed threshold. Furthermore, the biggest differences in the reliability achieved by the two management policies are observed at short periods of maximum electricity production. The reliability of the energy system during the whole year is 92.7% without reliability goal, but if this reliability goal is considered then the reliability increases over 97%. However this improvement has a counterpart in economic terms. The down graphic of Figure 3 shows the revenue obtained from the electricity selling in both cases, and their difference. This difference is not always in favor of one of the management policies but in the long term it is necessary to pay a price for the reliability improvement. Our simulation results provide a decrement of the revenue over 7,5%. The improvement of 4,3% in reliability and 7,5% of worsening in revenue depend on the goal set for the reliability but also of the memory and extra-penalty parameters used to model the reliability in the optimization problems. These parameters could be optimized for a specific application (specific energy system in a specific site) by combining simulation with optimization. As result a Pareto frontier reliability/revenue would be obtained to select from it the best management policy according to the wishes of the energy system manager.

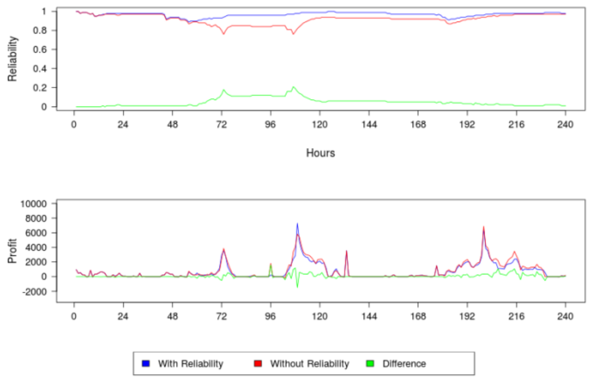

Figure 3: Comparison in terms of reliability and economic revenue of managing the energy system with and without reliability goal.

ACKNOWLEDGMENTS
The authors are grateful to the research staff of the National Renewable Energy Centre in Spain (CENER) for technical support and advice in understanding energy storage systems. This paper has been supported by grant MTM2012-36025.

APPENDIX A. List of Symbols, Abbreviations, Parameters and Variables

C_{c_i}: unit price of committed energy at hour i

C_{p_i}: unit penalty cost of not supplying committed energy at hour i

C_{s_i}: unit price of surplus energy at hour i

C_R: additional unit penalty cost of not supplying committed energy to achieve reliability goal

$Cap_{Recovery}$: maximum capacity of the recovery process (H2 → kWh)

Cap_{Tank} : maximum storage capacity of the tank

Cap_{transf}: maximum capacity of the transformation process (kWh → H2)

d_i^-: negative deviation of the supplied energy with regard to the commitments

d_i^+: positive deviation of the supplied energy with regard to the commitments

d_{ij}^-: negative deviation of the supplied energy with regard to the commitments associated with the j-th predicted wind speed curve

d_{ij}^+: positive deviation of the supplied energy with regard to the commitments associated with the j-th predicted wind speed curve

EfI : efficiency rates of the transformation process

EfO : efficiency rates of the recovery process

G_i : kWh generated at hour i

G_{ij} : kWh generated at hour i associated with the j-th predicted wind speed curve

m: number of wind speed trajectories in the PWSF

n: planning horizon, measured in hours

PWSF : probabilistic wind speed forecast

T_i : kWh stored in the tank at hour i

T_{ij} : kWh stored in the tank at hour i associated with the j-th predicted curve

X_i^I : kWh transformed into H2 and stored in the tank

X_i^I : kWh transformed into H2 and stored in the tank, at time i, associated with the j-th predicted wind speed curve

X_i^O : kWh obtained transforming H2 from the tank, at time i, into electricity (recovery process)

X_i^O : kWh recovered from the tank, at time i, associated with the j-th predicted wind speed curve

Y_i : kWh committed for selling at hour i

Z_i : kWh sold at hour i

Z_{ij} : kWh sold at hour i associated with the j-th wind speed predicted curve

φ_t^E : reliability ratio at time t

REFERENCES

Aguado M., Ayerbe E., Azcárate C., Blanco R., Garde R., Mallor F., Rivas D., 2009. Economical assessment of a wind-hydrogen energy system usingWindHyGen® software. International Journal of Hydrogen Energy, 34, 2845–54. Doi:10.1016/j.ijhydene.2008.12.098

Azcárate C., Blanco R., Mallor F., Garde R., Aguado M., 2012. Peaking strategies for the management of wind-H2 energy systems. Renew Energy 47, 103–11. Doi:10.1016/j.renene.2012.04.016

Callaway, D. S., 2010. Sequential Reliability Forecasting for Wind Energy: Temperature Dependence and Probability Distributions. IEEE Transactions on Energy Conversion, 25 (2), 577-585. Doi: 10.1109/TEC.2009.2039219

Connolly D., Lund H., Mathiesen B. V., Leahy M., 2010. A review of computer tools for analysing the integration of renewable energy into various energy systems. Appl Energy, 87, 1059–82. Doi:10.1016/j.renene.2015.02.001

Kim S., Pasupathy R., Henderson S. G., 2015. A Guide to Sample Average Approximation. In Handbook of Simulation Optimization, International Series in Operations Research & Management Science, 16, M. C. Fu (Ed.) Springer New York. Doi: 10.1007/978-1-4939-1384-8_8

Kou P., Gao F., Guan X., 2015. Stochastic predictive control of battery energy storage for wind farm dispatching: Using probabilistic wind power forecasts. Renew Energy, 80, 286-300.

Luo X., Wang J., Dooner M., Clarke J., 2015. Overview of current development in electrical energy storage technologies and the application potential in power system operation. Appl Energy, 137, 511–36.

Mallor et al. (2009) Mallor F, Azcárate C and Blanco R (2009). Including risk in management models for the simulation of energy production systems. In Proceedings of the 39th International Conference on Computers & Industrial Engineering. Computers and Industrial Engineering. 1821-1826, IEEE CNF.

Mallor F., Azcárate C., Blanco R., Mateo P., 2015. Operational management of renewable energy systems with storage using an optimisation-based

simulation methodology, Journal of Simulation, 9, 263-78. Doi: 10.1057/jos.2015.16
Zhao H, Wu Q, Hu S, Xu H, Rasmussen CN., 2015. Review of energy storage system for wind power integration support. Appl Energy, 137, 545–53.

AUTHORS BIOGRAPHY

Fermin Mallor studied mathematics at the University of Zaragoza, Spain. He received the Doctorate degree in mathematics from the Public University of Navarre, Spain, in 1994. He is currently a Professor in the Department of Statistics and Operations Research, Public University of Navarra. In addition to having taught for more than 25 years university courses in simulation, operations research, and statistics, he has successfully applied his knowledge in simulation and statistical modeling to the analysis of complex real-world problems arising in several industrial companies and institutions. He is particularly interested in applications in the fields of health and energy. His research interests include simulation modeling, optimization with simulation, functional data analysis, and reliability.

Cristina Azcarate studied mathematics at the University of Zaragoza, Spain. She received his doctorate in mathematics from the Public University of Navarre, in 1995. Currently she is an Associated Professor in statistics and operations research. She teaches optimization and simulation to civil engineers. Her research interests are simulation modeling and optimization with simulation, applied to healthcare and energy.

Pedro M. Mateo received his Ph.D. degree in Sciences from the University of Zaragoza, Spain, in 1995. Since 1998 he is an Associate Professor in the Department of Statistical Methods of the University of Zaragoza, Spain. His current research interests include machine learning, multi-objective evolutionary algorithms and simulation modeling.

ECO-MODEL FOR DC ELECTRICAL SYSTEMS IN STANDALONE BUILDINGS

Tony C. Castillo [a], Ana M. Macarulla[b], Oihane Kamara[c] and Cruz E. Borges[d]

[(a),(b),(c),(d)]Faculty of Engineering, University of Deusto, Avda. Universidades 24, 48007, Bilbao, Spain
[(a),(b),(c),(d)]DeustoTech - Deusto Foundation, Avda Universidades, 24, 48007, Bilbao, Spain
[(a)]University of Oriente, N. of Anzoátegui, Technological Institute, Avda. Universidad-Vía Alterna, Barcelona,Venezuela

[(a)]tony.castillo@opendeusto.es, [(b)]ana.macarulla@deusto.es, [(c)]oihane.esteban@deusto.es, [(d)]cruz.borges@deusto.es

ABSTRACT
Global contribution from buildings towards energy consumption is becoming a serious and pressing matter in terms of sustainability and world economies. In addition, the continuous population growth influences the demand for building services and comfort levels significantly, ensuring that the trend in energy demand will continue to increase in the future. For this reason, energy efficiency in buildings is a primary objective for energy policy at regional, national and international levels. Standalone buildings using Photovoltaic modules on Direct Current can represent a good solution to stop climate change and a decisive input for the new production models of low carbon electricity. This article presents a model to help on the design of these installations able to keep current levels of comfort without any cutoff or interruption.

Keywords: photovoltaic energy, standalone buildings, DC

1. INTRODUCTION
Everything suggests that, far from diminishing, the global consumption of energy will continue to increase in the future years. Only in 2012, the total amount of consumption was around $560 \cdot 10^{18}$ Joules ($2016 \cdot 10^{21}$ Wh) (Blok et al. 2015). This significant increase in energy consumption is directly influenced by several variables such as population growth, increased quality of life, weak awareness about energy saving, extreme temperatures, insufficient energy policies, international energy context, and volatility of fuel prices. The impact of these variables may vary from one region to another in the world, and their evolution over time determines the variation on the degree of growth of energy consumption. (Díaz 2014).
Within this scope, the high amount of energy consumption in buildings represents a worrying matter. There is far too much energy being used whether for heating rooms, production of hot water, cooling, lighting, etc. In fact, 40% of the overall energy consumption in cities occur within residential buildings with only 31% coming from heating and domestic appliances (Blok et al. 2015). This represents an important problem for the distribution networks when balancing the high energy demand: when the amount of energy consumption increases, so does the ecological footprint (Ghita et al. 2016), as well as the unavailability of the conventional energy resources needed to meet the power demand. The main overcome to this problem is being led by the introduction of the renewable sources of energy generation. Out of the amount of renewable sources existent, solar energy is one the most used for powering cars, homes, electric devices, even serving as support for energy generation in some industries.
This work presents the use of solar photovoltaic (PV) energy for supply electricity in systems off grid with the purpose of avoiding the overcharge of the distribution networks and minimize the carbon footprint. According to Eurostat, 27.19% of the total energy produced in the Europe Union (Eurostat 2013) in 2013 had its origin in renewable resources with only 2.4% coming from solar PV. The use of a DC-microgrid (Ingale et al. 2016) benefits in the sense that it can be controlled locally and the energy can be provided to a local grid or can be consumed in a stand-alone manner. Microgrids are very useful during natural disasters since they improve the performance and overall efficiency of both the transmission and distribution networks, and they are also helpful for electrifying faraway towns.
In addition to the high consumption, we have to consider the low efficiency presented in all the current technology deployed worldwide. According to (Blok et al. 2015) we still squander more than 98% of all of the energy we produce through inefficient use and wasteful means of transport and production. It is possible to make a more efficient use of the energy with straightforward changes in the actual model consumption. For instance, (Sanjeev et al. 2015) conclude that this “comparison between AC and DC home shows that even though the cost of DC equipment is high, a significant reduction in losses and power consumption gives more importance to DC grid.”
There are two main models of PV generation, the most known are based on I nstallations connected to the network and the second one is off-grid, but both systems make use of inverters to convert direct current (DC) into alternating current (AC) that is injected into the grid or installation. Note that most home appliances have an AC rectifier to convert the AC obtained from the grid to DC to be used. Therefore, the conversion process DC-AC-DC is redundant. Moreover, the inverter is a high frequency switching device: when turned on, it increases

switching losses and heating dissipation which in turn cause power loses, therefore reducing the efficiency of the photovoltaic system. In addition, this component is one of the most expensive in a PV installation (Encinas et al. 2014)

The model developed in this work presents an enhanced standalone installation (a facility prepared for generating all the energy necessary for keeping on all the home appliances without retrieving energy from the commercial network) where conversion to AC has been eliminated, and include a storage system based on chemical ion-lithium batteries. The main advantages of this alternative are:

- It is **more efficient**, because the inverter generates the greatest losses in the entire photovoltaic system (Aguirre et al. 2014).
- It is **cheaper**, because the inverter is the second most expensive component of the PV installation (Encinas et al. 2014).
- It is **more robust**, because it is supported by batteries and has fewer components that can fail (IRENA-a 2015).

Energy generation from renewable sources is one of the most recognized solutions to stand up against climate change due to its social, environmental, and economic benefits. Any increment in the levels of contribution to global energy generation is a contribution to the sustainability of the planet itself. In this context, we propose the use of a DC model for energy generation and consumption as a way to reduce the impact derived from the use of fossil fuels, copper mining and the overall cost of the installation, increasing energy efficiency in domestic systems.

The main purpose of this investigation is to prove that Eco-Model for DC Electrical Systems in Standalone Buildings (PVDCB) is technically, economically, socially and environmentally has more advantages than the use of photovoltaic systems powered by AC photovoltaic generation for residential current networks in standalone buildings.

2. RELATED WORK

There are various models of PV generation and most of them use the inverter in the facility for the reasons given previously. This section presents some projects that have deployed PV systems using DC.

(Williamson et al. 2011) found motivation in the analysis of power losses due to the inefficiencies of the power supply unit (PSU) where significant amounts of the energy supplied are turned into heat. In addition to this, switch-mode power supplies (SMPS) often have a poor power factor and introduce significant harmonic distortions into the grid. Project Edison SMART-DC, introduced some changes in the energy consumption behaviour at the PC room of the University of Bath's Library and Learning Centre (LLC). The existing array of 50 computers was replaced with 50 new DC powered units with a centralized AC/DC converter and an integral energy storage facility. They achieved an important number of benefits with their DC powered network. The output heat was reduced and shifted away from the user to the converter, thus reducing fan noise and air conditioning use while a reduction in energy consumption was achieved as consequence of the use of both efficient components and demand response strategies. The magnitude of the 3rd – 9th current harmonics was also significantly reduced by a factor of approximately 2-4 times, and finally there was an increase in the security of supply to the network due to the use of storage in the system. Test over 18 months shows that the new DC network and its associated PCs consumed about 30% less electrical power than the AC-powered PCs they replaced (Aggarwal et al. 2015). They manage the local DC network so, during times of high energy tariff, they isolated it from the grid, with the batteries powering all 50 PCs and monitors for 8+ hours. Once the energy tariff falls, the rectifier can be switched back on, recharging the batteries, and powering the PCs. As consequence, the benefits and flexibility of the SMART-DC network lends itself ideally to the integration of intermittent renewables especially to the micro-wind turbines and photovoltaic panels (PV). The energy generated by PV is natively DC and through a simple charge controller, the inefficiencies normally associated with converting it to AC are all avoided.

(Pandey et al. 2015) show a cluster of buildings in stand-alone mode, these were a couple of small houses joined together to the DC bus, connected to a community battery bank for avoiding sudden charging/discharging of home cluster battery packs. This distributed grid (DG) is implemented from a hybrid solar and wind renewable energy generators. They studied his facility in two sceneries: one with a fixed wind generation (12 m/s) and variable solar irradiance until it reached 1000 W/m^2, and the second scenario studied the stochastic behavior of wind and solar power production to analyze the battery pack viability during over-generation and under-generation conditions. For the effective current sharing, a droop control loop is used and it gives further voltage reference to outer voltage loop control, which suffices the buck and boost mode for charging and discharging. To avoid instability issues of peak current mode control, the slope technique is used. The proposed control compensation technique is able to manage the power balance while extracting the maximum power from the wind and solar DG.

The research DC grid initiative in India (Sanjeev et al. 2015) make a comparison between AC and DC in home. The results of this project show that even though the cost of DC equipment is high a significant reduction in losses and power consumption gives more importance to DC grid. The DC micro grids can save up to 78.65% of energy make than AC grid. They studied two types of DC grids: the first one has a power sharing done by the power vs. voltage droop characteristics (John et al. 2013) and voltage is common control element for all the three homes and actual DC link voltage is always compared with reference for closed loop operation (Kakigano et al.

2010). This type of configuration provides more flexibility in power sharing among the homes and less fluctuations in DC voltage since they are all interconnected. In this case every home is having individual storage and its associated converters, this increases individual expenditure and maintenance cost.
The second type consists of three homes powered by DC that are not interconnected. Every home has a single AC-DC converter that is used to balance individual DC link voltage. Every home has an array of PV panels to meet the demand. When generation is greater than the load then it charges a battery otherwise the battery discharges to meet the demand. If battery is at minimum state of charge (SOC) then the power from the utility (AC grid) is used to compensate the power loss.

3. MODEL DESCRIPTION

The PVDCB is the model defined for the hall of residences (SR) belonging to the University of Deusto situated in Bilbao, a region in the north of Spain. The building is composed by 3 towers full of bedrooms with all the necessary services needed to provide comfort to 304 students: Wi-Fi, dining room, reception, laundry room, industrial kitchen, elevators, PC's room, hot water, central heating, medical and psychology attention, etc. during the whole year. The model, is composed of 6 subsystems: 4 of them represent the production and consumption of energy (generation, storage, control, consumption), and the other 2 involve the complementary measurement and protection subsystems. It has been implemented in SimPowerSystems (SPS) (Mathworks 2015), The block diagram in Figure 1 shows the conceptual diagram of the interaction between the different subsystems with the input being solar irradiance and temperature, and the output being the total current and power consumption. The subsystems are classified as follows:

1. **Consumption:** this subsystem simulates the energy consumption of the building.
2. **Generation:** this block is used to model the solar photovoltaic cells disposed for the solar energy harvesting.
3. **Storage:** this subsystem corresponds to the battery bank that acts as energy backup when there is not enough solar irradiation to feed the system.
4. **Control:** this subsystem models the DC-DC converter of the installation.
5. **Protection (complementary):** the purpose of this subsystem is to protect the whole installation against short circuits, voltage fluctuations, etc.
6. **Measuring (complementary):** subsystem which gathers all the instrumentation needed to monitor the system from the process of solar harvesting to the deployment of energy consumption.

3.1. Consumption Subsystem

This subsystem simulates the energy consumption of the building by reproducing the load effects to the PVDCB. The load of SR had been simulated as a variable electrical load, as shown in Figure 2.

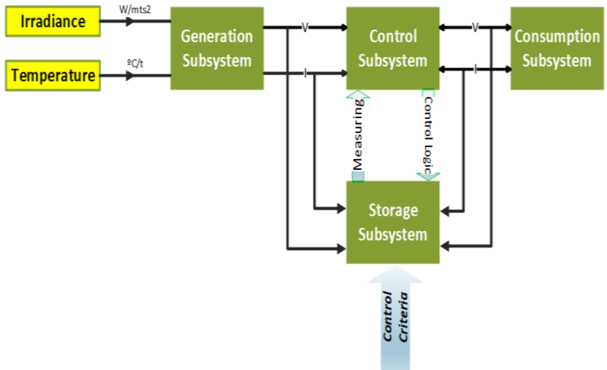

Figure 1. Block diagram of PVDCB.

The consumption data comes from the real reading of the electric meter, taken every 15 minutes for three years (2012, 2013 and 2014). These data have been collected into a spreadsheet and are loaded by the simulator in form of power (W) or energy (Wh). Moreover, this subsystem is fed by the battery bank, by voltage (V) and current (A).

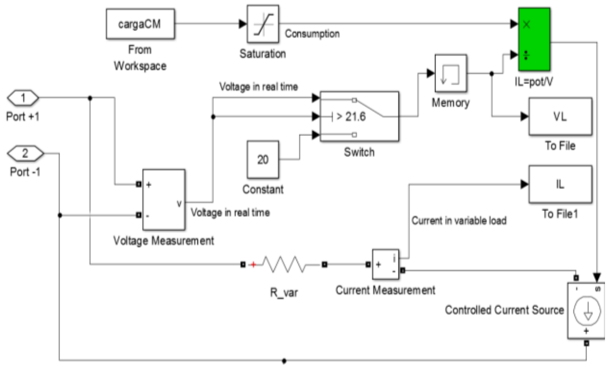

Figure 2. Consumption subsystem (variable load representation of the SR).

Figure 2 shows a diagram of the consumption subsystem. The current is calculated through dividing the power by the voltage ($I = \mathrm{P} \cdot V^{-1}$). According to the Ohm's Law ($I = V \cdot R^{-1}$), the SR is represented by a variable resistance.

3.2. Generation Subsystem

This subsystem reproduces the behavior of the solar array modules, which convert sunlight (direct, indirect and/or diffuse) into renewable DC energy. Figure 3 shows the inputs and PV panels that are part of the generation subsystem.
The generation subsystem is fed with real values of irradiance and temperature obtained from the analysis of the energy load of the SR. Figure 4 shows the physical model of the solar cell used.

Out of all the solar panel available, the Top Sun-TS 420TA1 solar panel was chosen for its good performance. Its principal characteristics are presented in Table 1 and the conceptual model is available in the SimPowersystem library.

Table 1. Electrical characteristics of the Top Sun-TS 420TA1 solar panel.

Model	Monocrystalline 3 busbar [96 cells]
	TS-S420
Power Output (Wp)	420
Max Voltage (V)	49.70
Max Current (A)	8.45
Open Circuit Voltage (V)	60.77
Short Circuit Current (A)	9.00
Efficiency (%)	16.38
Tolerance (%)	0~+3

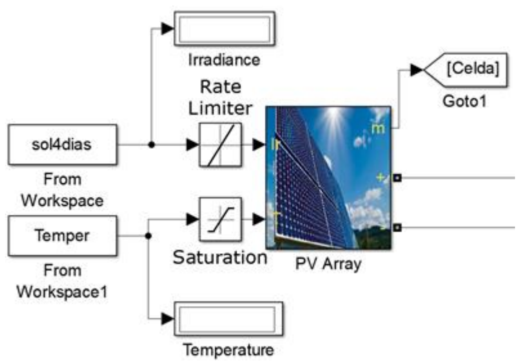

Figure 3. Generation Subsystem of PVDCB.

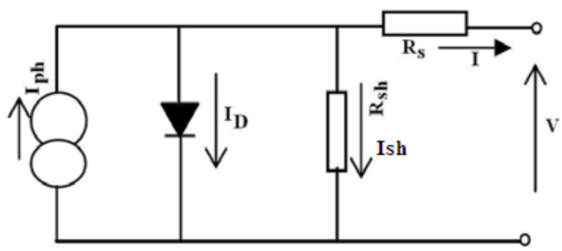

Figure 4. Approximate physical model for the solar cell (approximate).

The Equations 1 and 2 define the characteristics of I-V solar photovoltaic module plate:

$$I = I_{ph} - I_0 \cdot \left[exp^{\left(\frac{V+Rs\cdot I}{Vt\cdot a}\right)} - 1\right] - \frac{V+Rs\cdot I}{Rsh} \quad (1)$$

$$V_T = \frac{k\cdot T}{q} \cdot Ncell \quad (2)$$

where:
I_{ph}: photo current
V: open circuit voltage
V_T: Thermal voltage from the PV cell
I_o: saturation current of the diode
a: idealization factor diode, a number close to 1.0
Rs: series resistance ≈0Ω
Rp: parallel resistor (high value)
k: Boltzmann constant = $1.3806488\cdot10^{-23}$ J/K
q: electron charge = $1.6022\cdot10^{-19}$ C
T: cell temperature (K)
Ncell: number of cells connected in series to a module.

In order to ensure the energy supply for the SR, a review and analysis of the energy demand load was necessary in order to keep the operability of all the systems that constitute the SR. The analysis of the SR data determines the size of generation and storage subsystems based on values like the average consumption and the peak consumption of the facility. Table 2 shows the most important values that summarize the analysis of the energy consumption. Those data are important for the correct sizing of panels and batteries.

Table 2. SR study of behavior in energy consumption.

Energy average (kWh)	Energy Peak (kWh)	Minimum Consumption (times)	Mode value (kWh)	Median value (kWh)
13.96	37.25	43	9.75	11.75

The data in Table 2 make possible to define the conditions under which the facility should be prepared to meet energy peaks. Note that the value of the energy peaks is close to three times the average energy consumption. The implantation of PVDCB at SR expects to help decrease significantly the amount of energy consumption due to the fact that DC grids are much more efficient than AC powered buildings. For these reasons, the facility was sized to deliver twice the average energy consumption during the month with the highest consumption (June), and with the worst solar photovoltaic generation month being (December). The average consumption in June is 16.81 kWh, so the security value established is 33.61 kWh. Knowing that the panels are capable of delivering 420 Wh, setting 75 V voltage and 600 A of current. Therefore, we estimated that 2 arrays of 77 panels are needed in order to meet the energy consumption at the SR.

3.3. Storage Subsystem

The storage energy subsystem is composed of a set of batteries operating as a complementary energy source to the PVDCB system in order to ensure power supply to the building at night or when the weather conditions affect solar radiation. Batteries are now a standard component in photovoltaic installations, allowing the creation of standalone systems disconnected from the distribution network. Batteries are the only equipment used in this model to disconnect the installation of the commercial power grid, therefore, they are of great interest since they serve as main support and turn as PVDCB backup system (IRENA-b 2015)
The batteries selected for this research are the lithium-iron phosphate (LiFePO4), due to the fact that this type of batteries do not contain toxic elements, have an efficiency of 98%, and are lighter and have less volume

than lead acid batteries. Besides that, they can be discharged at least up to 20% of their capacity while reaching a life of over 10,000 cycles. The current big disadvantage is the high initial price (about three times that of a lead battery), however it is decreasing continuously, and soon will be competitive enough to be considered as lead option (Energía Renovable Peru Con Deltavolt 2016). Therefore, we estimated that 2 arrays of 77 panels are needed in order to meet the energy consumption at the SR.
In this stage of the research, PVDCB uses batteries 6V 25 S Model 3 MIL from Australian manufacturer Raylite, specially made for solar applications. This battery is modelled in Simulink/SPS.
Another important point to measure the feasibility of the proposal factor is the size of the installation. In a first step to optimize the storage capacity (Mascarós 2015) was consulted in order to define the amount of batteries needed for the same work without interruption and without solar generation between three to eight days according to consumption of the installation. The Equations 3 and 4 defines the average daily consumption.

$$L_{MD,CC} = \sum\left(P_{CC,i} \cdot t_i\right) \quad (3)$$

Where:
$L_{MD,CC}$: is the average daily energy Wh consumed at the facility, current continues to the rated voltage of 24 V
$P_{CC,i}$: the power DC consumed in W into load
t_i: is the time of daily operation of the load in h

$$L_{MD,CC2} = \sum\left(P_{CC2,i} \cdot t_i\right) \quad (4)$$

Where:
$L_{(MD,\ CC2)}$: is the daily average energy Wh consumed at the facility in a different DC voltage at rated
$P_{(CC,\ i)}$: is the power DC consumed in W into load
t_i: is the time of daily operation of the load in hours

Note that we give two equations for the determination of the energy consumption for the SR. The first is focused at the rated voltage while the second focused on one different voltage to the rated voltage. At this first stage of the modelization we have used a voltage of 24 V for solar PV.
Usually, storage systems are sized to operate under a minimum of 3 and a maximum of 8 days of autonomy (Aparicio 2010; Mascarós 2015; Sumathi et al. 2015; and Vallina 2010) with a depth of seasonal discharge of 70% for days without solar generation. For this specific model, the autonomy of the system is established for a period of 3 days with its current consumption without compromising any the comforts of the SR. Equation 5 shows the amount of the energy necessary to be storaged.

$$C_D = \frac{L_{MD,Total}}{PD_D \cdot V_N} = \frac{1451.5 kW \cdot h}{0.2 \cdot 24} = 302400 A \cdot h \quad (5)$$

Where:
$L_{MD,Total}$: is the average daily energy given in Wh consumed at the facility, current continues at rated voltage
P_{DD}: is the depth of discharge allowed daily
V_N: is the nominal battery voltage

The algorithm for designing the size of the storage subsystem takes into account the following aspects to calculate the appropriate configuration:

- Total daily energy to be supplied by the battery without discharge totally equal to 1451.5 kWh on a winter day (January 2, 2012).
- Depth of discharge daily equal to 20%. This level has been arbitrarily set after displaying what would be achieved with the same guarantee the life of the cells at approximately 5000 cycles.
- Depth of discharge seasonal (sunless days) maximum equals to 70%. This discharge is for cases than include the existence of sunless days.
- Short circuit current of the PV panels equal to 9.12 A. This value is given by the manufacturer of the panels PV.
- Number of branches of PV solar cells in parallel equal to 77. This value is the product of the previous step sizing of solar installation.
- Rated voltage cells used is equal to 6V batteries. This value is referred to the tension that handles each battery cell.
- Discharge capacity in C100 hours equals to 900 A. This value is the amount of current that can be extract from the battery in a period of 100 hours of continuous use.

In the case of a day with an energy consumption of 1451.5 kWh, as on January 2, 2012, the model implemented is shown in Figure 5, and results are as follows:

- Minimum Nominal Capacity (Ah): 302395.83
- Maximum Rated Capacity of the batteries (Ah): 17556
- Number of cells connected in series 6V: 4
- Number of parallel battery branches: 335.99
- DOD Allowable (%): 70%

For the success of this research, we need to analyze the optimal sizing of energy storage system so that the proposal of the present model can be economically viable. This could help to power small villages in developing countries because the process of energy harvesting is similar in worldwide. Any country could even receive economic benefits by pouring the excess of energy power into the grid in the energy market. This action can improve the power generation through the form of decentralization of energy generation.

3.4. Charge/Discharge Control Subsystem

Usually, a set of DC-DC buck converters are included in order to keep the panels operating at their point of maximum power (MPP) and to maintain the charging voltage of the batteries at optimum levels. This subsystem could recover between 10-30% of the energy losses of photovoltaic solar installations per year (Ghaffari et al. 2012). At the current level of development of this model, the converter is able to keep steady output of 24 V, so that it can be used either in the battery charging and/or to supply the SR (Figure 6).

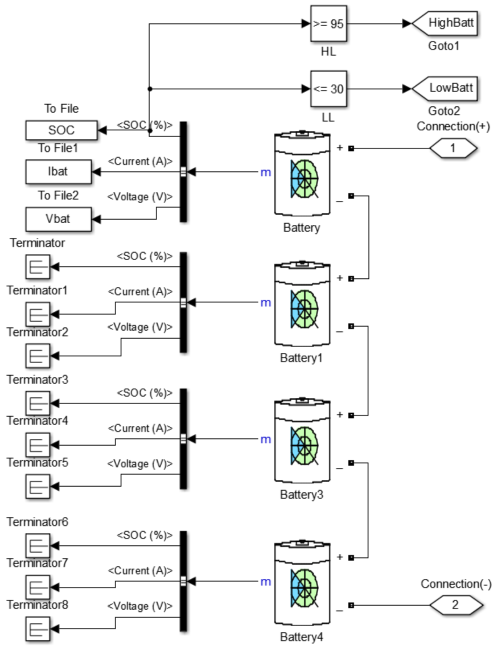

Figure 5. The association of the energy storage system conformed by 4 batteries of 6 V cells.

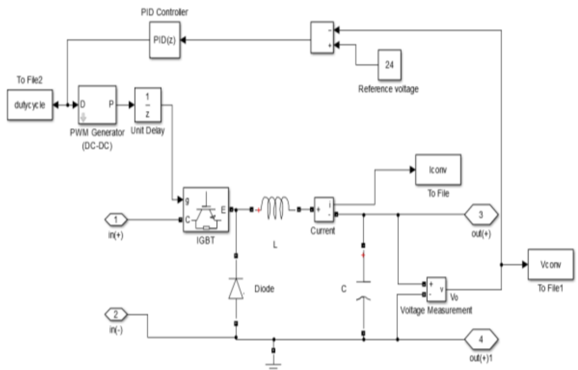

Figure 6. Buck converter SimPowerSystems diagram.

The 24V buck converter is managed by an IGBT an electronic solid state switch that is able to handle high levels of currents and high speed voltages.

The data used to design and implement the buck converter are as follows:

- The input voltage to the buck converter is the output received by the solar panels, which in turn becomes the system input.
- Rated output voltage equal to 24 V is the value to keep for battery charging.
- Load resistance is of 0.015 Ohm. The maximum value for the RL is obtained with the maximum consumption of current according to the
- This value is the minimum taking relationship $P = V^2 \cdot R^{-1} = R = V^2 \cdot P^{-1}$ at the time when the power consumed at SR takes its maximum value.
- Ripple maximum level is 5% (this level was arbitrarily set based on experience)
- Switching frequency equal to 10000 Hz, (this frequency is half the optimum frequency for this system but it was decided to reduce some simulation time).

After entering the above data at MATLAB script the following results were obtained:

- The duty cycle is: 0.21
- The inductor L is: $0.73 \cdot 10^{-6}$ H
- The capacitor "C" of the converter is: $26.667 \cdot 10^{-3}$ F

The value of the variable load is obtained at the time at which the SR reaches its peak consumption 37.25 kWh. The fixed input voltage of 110V, comes from the associated solar panels because, according to the manufacturer of the modules, the maximum output voltage of each one is 49.7 V, so output of two associated panels is 99.4 V. The voltage measured during the simulation was close to 110 V, because the plates were well irradiated.

The duty cycle is given by the PWM block which in turn receives the value of PI controller fed by the error with a set point of 24 V. A PI controller has been adjusted experimentally (P=0.15, I=0.5).

3.5. Protection Subsystem

This subsystem looks after the correct operation of the PVDCB and thus avoid deep discharge, overload, reverse currents and inverse voltages, that make unsteady the functioning of the PVDCB. It is noteworthy that, unlike the previous four subsystems, this and the monitoring subsystem are not located in a single place at the model, but are scattered throughout the whole facility.

Figure 7 shows the two elements of the protection subsystem. One is the voltage stabilization capacitor that works as a memory that stores the output voltage from the PV panels. This is required to maintain a steady input voltage to the DC-DC buck converter at all times and avoid sudden voltage fluctuations, thus minimizing the presence of noise at the input of the DC-DC converter than could create a miscalculation of the duty cycle.

A semiconductor power diode is placed exactly between the capacitor and the buck to prevent reverse currents toward the array of solar panels that could generate short circuit currents. In order to choose the correct diode, it is necessary to take into account the maximum current that will flow from the panels, and choose a power diode

capable of supporting at least the double of the value of current in reverse and the reverse peak voltage that could appear into the terminals from buck converter.
The subsystem has been designed to limit batteries discharges up to 20% daily, only if process of solar photovoltaic harvest does not occur. In addition, the subsystem is prepared to supply energy during 72 continuous hours, and in those cases, the storage subsystem could be discharged more that 20%. The facility is sized to allow discharges up to 70% of the energy stored in the batteries. Note that this condition should not be very recurrent because it can generate unexpected power outages, making necessary to make an appropriate sizing of the system of accumulation. In addition, Also a protection logic for the high or low level of the batteries has been designed. If the batteries reach 30% of its DOD, the low-level logic comparison block (LowBatt) issues a "true" value equivalent to a logic 1. That value is then transferred to the FROM LowBatt block. A value of 1 closes the switch, which means that current stops its flow.

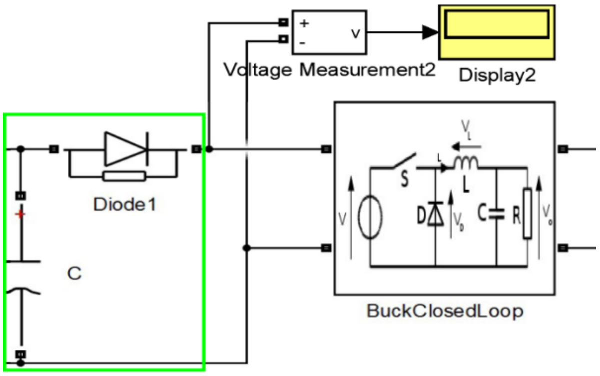

Figure 7. Components of protection subsystem.

3.6. Measurement subsystem

This subsystem comprises all the instruments that collect information regarding the behavior of the PVDCB and that make possible the management and monitoring of all the signals generated by the system. Some of these signals, recorded and saved in SimPowerSystems blocks “To File”, refer to inputs for the model, but the majority relate to data necessary to analyze the performance of the PVDCB and propose improvements.

4. COMPONENTS AND DATA FOR SIMULATION

Currently, the environment and simulation time is fixed. As mentioned in Section 3, the facility used for study is the hall of residence of the University of Deusto, mainly because of the possibility to access historical data related to the energy consumption of the building. The simulation time was set to 48 hours due to the computational time required to execute a simulation. The software used was Matlab/Simulink 2015b, specifically the SimPowerSystem library. The PC used was a DELL laptop Inspiron 5559, with Intel Core i5-6200U processor, 2.3 GHz, 8GB of RAM, running on 64 bits Windows 10 operating system.

The efficiency of the solar panel is mainly affected by two variables (assuming that the orientation of the panels is optimal and that shading over does not exist). In order to build a realistic model, we used the actual temperature and irradiance values referring to the coordinates of the SR: Bilbao latitude 43.3º North, longitude 2.9º West, and height 24 meters. These values were obtained by the collaboration of the European Commision through its Photovoltaic Geographical Information System PVGIS (“PV Potential Estimation Utility” 2015). The simulation data from a repository of official meteorological data from the European Union (http://re.jrc.ec.europa.eu/pvgis/apps4/pvest.php) are used, as is the Geographic Information System with Photovoltaics. Thus it is possible to emulate the process of measuring and recording data of a real solar system.
The energy consumption data was directly obtained from the energy manager at the SR. The data comprises three years of data consumption and helps emulate the behavior between the energy generation at the coordinates indicated above and he consumption in the building studied every day for the different seasons of the year.

5. RESULTS AND DISCUSSION

As preliminary results, the evolution of several parameters from a 48 hours simulation are presented. Figure 8 shows the DC current demanded by the load based on energy real data consumption. It shows that current peaks are close to 1000 A, but, in average, the current consumption is lower in the morning hours and bigger in evening hours.

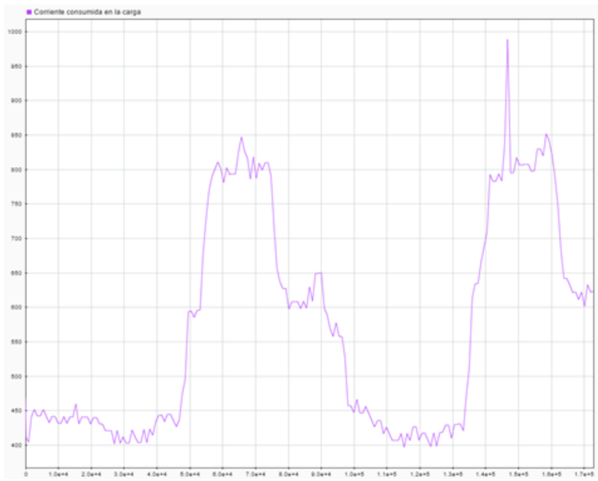

Figure 8. DC current consumption SR during 48 hours.

Figure 9 shows the output voltage of the energy storage system. Its behavior is the expected: an inverse voltage peak is produced at the same time than occurs the biggest current consumption, but in average the voltage is kept into the output expected value.

Figure 10 shows all outputs measured in the photovoltaic modules during 12 hours, this is the order:

1. The power caught from solar irradiance

2. The current I_PV
3. The irradiance peak at this day
4. The output voltage of the modules
5. The output current than flow across the panel diode
6. The maximum value of temperature for the day simulated

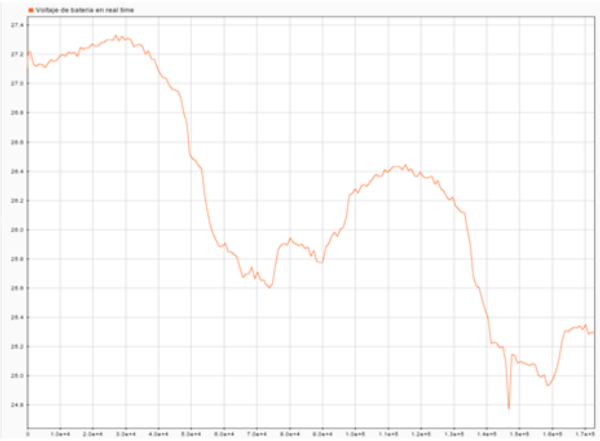

Figure 9. Performance of DC voltage SR for 48 hours.

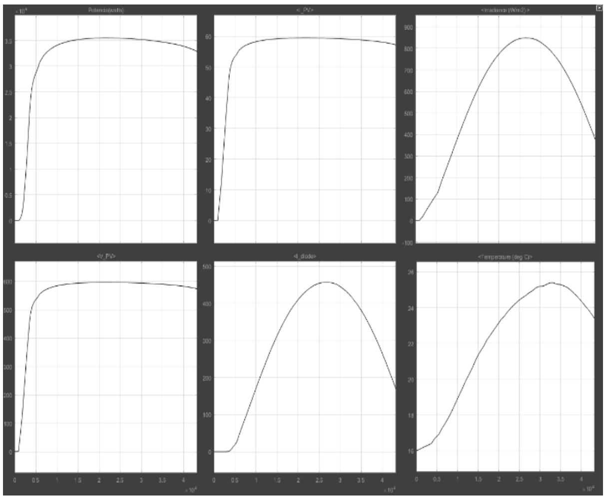

Figure 10. Oscilloscope screens.

The behavior of one of the batteries is represented in Figure 11. As the simulation is carried out without solar energy supply, charge level decreases continuously. Charge level goes to 65% and voltage, from its maximum value, 7 V, goes to 6.6 V.

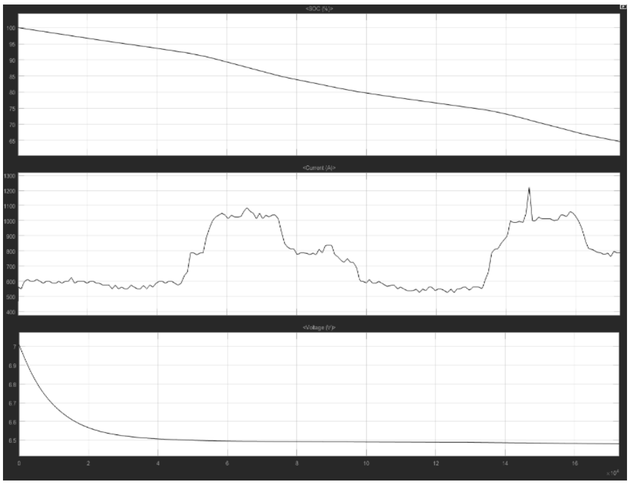

Figure 11. Battery behavior after 48 hours.

The behavior of the converter buck DC-DC is shown in Figure 12. It shows that the system is working into the desired values of control, avoiding too high fluctuations in DC output voltage.

After the several simulations preliminaries of the SR buildings, we can observe that a distributed generation is a feasible way to overcome the climate change, because it is technically viable, and the graphs shows that it is possible support power systems as kitchen, elevator, heat commodities, etc. This is very interesting because the DC energy is being used in applications that does not demand too much power for the system.

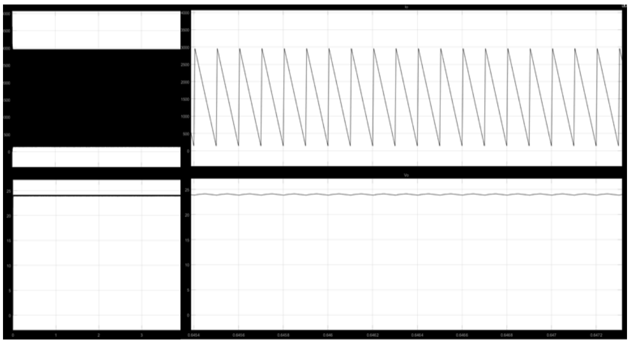

Figure 12. Output for the buck of the subsystem of control.

6. CONCLUSIONS AND FUTURE WORK

The model presented in this paper is a first approximation of a real future DC installation which intends to show that the use of a distributed generation system is a feasible option for the generation of energy from renewable resources. The system modelled is strong enough to meet the energy demand of a service building such as a student's residence. The greatest contribution of this work is the development of a comprehensive DC model for a standalone building based on real data consumption and photovoltaic solar energy generation, using the MATLAB and Simulink libraries. So far, in the state of the art, there is a great amount of research directed towards developing models for energy generation and supply in microgrids powered by AC. Currently, there are applications that use DC power such as street lighting, intelligent traffic lights or telecommunication antennas. However, there is no model generation and supply DC developed to maintain security systems and comfort of standalone buildings exclusively with DC electricity, since all the models developed to date make use of the DC-AC conversion to power domestic installations.

The future developments considered as a follow up of the work presented in this paper are detailed as follows:

- **Design of an intelligent control** to balance and manage the charge and discharge of the batteries that give support to the standalone PV installation. Batteries experience a wide range of operational conditions in PV applications, including varying rates of charge and discharge, frequency and depth of discharges, temperature fluctuations, and the methods and limits of charge regulation. These variables make it very difficult to accurately predict battery performance and lifetime in PV systems.
- **Design of a control of Maximum Power Point Tracker (MPPT)** for keep photovoltaic modules operating at its optimal level. The MPPT algorithm is a method for maintaining the modules at its maximum power point. Currently, is the only method available for extracting the maximum energy possible and, in consequence, avoid losing efficiency in the solar panel.
- **Develop of a sizing optimization model** in order to make economical, technician, and environmentally feasible this purpose.

ACKNOWLEDGMENTS

This work was partially supported by the Erasmus Mundus SUD-UE 1301256 given by European Commission and the PRE_2015_2_0003 grant given by the Basque Government. The authors would also like to thank Gorka Sorrosal and J.I. García-Quintanilla for their helpful support during the execution of this work. Special thanks to Ana Gracia Amillo from the Joint Research Centre of the European Commission for her valuable support during the execution of this research.

REFERENCES

Aggarwal R., Miles R., Ben W., Surendra K., Jacob A., Clive J., Chris H., and Philip B. 2015. Project Edison SmartDC – DC Local Network in the University Library. University of Bath. http://www.bath.ac.uk/ris/kta/projects/smartdc.html. [Accessed March 11]

Aguirre G., Marteniuk J., and Botterón F., 2014. Implementación de Estrategias de MPPT para Sistemas de Generación Fotovoltaicos en un Convertidor Boost CC-CC. In Biennial Congress of Argentina (ARGENCON), 352–57. 11-13 June 2014, Bariloche, Argentina.

Aparicio M. P. 2010. Energía Solar Fotovoltáica : Cálculo de una Instalación Aislada. Barcelona, Spain: Marcombo.

Blok K., Hofheinz P., and Kerkhoven J. 2015. The 2015 Energy Productivity and Economic Prosperity Index. How Efficiency Will Drive Growth, Create Jobs and Spread Wellbeing throughout Society.

Díaz T. D. F. 2014. Escenarios Energéticos a 2050 Para Las Smart Grids en Colombia Basados en los Estudios Wec Energy Scenarios 2050, Energy Trilemma 2013 y Issues Map Monitor 2013. Universidad Pontificia Bolivariana.

Encinas D. Lopez F., Segador C., Cosme J. M., and Cuadros L., 2014. Instalaciones Fotovoltaicas Para Autoconsumo. Análisis de Viabilidad y Determinación de Parámetros Óptimos de Diseño para el Proyecto. In 18th International Congress on Project Management and Engineering, 15-25. 16–18 July 2014, Teruel, Spain.

Energía Renovable Peru Con Deltavolt. 2016. http://deltavolt.pe/energia-renovable/baterias [Accessed February 2].

Ghaffari A., Sridhar S., and Miroslav K., 2012. Power Optimization for Photovoltaic Micro-Converters Using Multivariable Gradient-Based Extremum-Seeking. In American Control Conference, 3383–88. 27-29 June 2012, Montréal, Canada.

Ghita B., Karim M., Lagrioui A., and Zinelaabidine N., 2016. Optimization and Modeling of a given PV System Has a Single Load. Journal of Theoretical and Applied Information Technology 86 (1): 112–19.

Ingale G. B., Subhransu P., and Umesh C. P., 2016. Design of Stand Alone PV System for DC-Micro Grid. In Proc. IEEE Int. Conf. Energy Efficient Technologies for Sustainability, 13-19. 7 and 8 April 2016, India.

IRENA. 2015. Off-Grid Renewable Energy Systems: Status and Methodological Issues. (a). [Accessed January 11]

IRENA. 2015. Battery Storage for Renewables: Market Status and Technology Outlook. (b). [Accessed January 11]

Mascarós M. V., 2015. Instalaciones Generadoras Fotovoltaicas. Un Cambio Hacia La Sostenibilidad. M Madrid, Spain: Editorial Paraninfo.

Mathworks. 2015. “Matlab/Simulink.” http://es.mathworks.com/products/matlab/.

Pandey G., Sri N. S., Bharat S. R., and Gonzalez-Longatt F. M., 2015. Smart DC Grid for Autonomous Zero Net Electric Energy of Cluster of Buildings. IFAC-PapersOnLine 48 (30). Elsevier B.V.: 108–13.

Photovoltaic Geographical Information System. PV Potential Estimation Utility. 2015. http://re.jrc.ec.europa.eu/pvgis/apps4/pvest.php?lang=es&map=europe. [Accessed March 16]

Sanjeev P., Narayana P. P., and Pramod A., 2015. DC Grid Initiative in India. 9th IFAC Symposium on Control of Power and Energy Systems (CPES) 48 (30). Elsevier B.V.: 1–6. 09-11 December 2015, New Delhi, India.

Sumathi S. L., Ashok K., and Surekha P., 2015. Solar PV and Wind Energy Conversion Systems. Edited by Springer. Switzerland.
Eurostat. Statics Explained. 2013. T1Gross_electricity_generation_by_fuel,_GWh,_EU-28,_1990-2013.png (755×907). 2016. http://ec.europa.eu/eurostat/statistics-explained/images/0/04/T1Gross_electricity_generation_by_fuel%2C_GWh%2C_EU-28%2C_1990-2013.png. [Accessed February 23]
Vallina M. M., 2010. Instalaciones Solares Fotovoltaicas. Madrid, Spain: Editorial Paraninfo.
Williamson B. J., Redfern Ma., Aggarwal R. K., Allinson J., Harris C., Bowley P., and Hotchkiss R., 2011. Project Edison: SMART-DC. IEEE PES Innovative Smart Grid Technologies Conference Europe, 1–10. 5-7 Dec. 2011, Manchester, UK.

AUTHORS BIOGRAPHY

Tony Castillo C., Chemistry's Technician (U.E.N. Technical School "Eugenio Mendoza", 1993), Technologist in Electronics (University of Orient, Venezuela, 2001), Graduate in Education, Industrial Technical Mention (University of Orient, Venezuela, 2005), Master in maintenance management (institutional agreement between University of the Armed Forces and University of Orient, Venezuela, 2008). His teaching activity has been focused especially in the field of analogue electronics, especially in the area of power electronics. His research work is related to the maintenance system in the industrial sector. He is actually PhD student in Deusto University, Spain developing studies in energy Solar Photovoltaic.

Ana M. Macarulla, Industrial Engineer specialized in Electricity (University of Navarra, 1990) and Dr. in Automatic Control (University of Navarra, 1996). Researcher at CEIT-IK4 from 1990-1997, lecturer in the University of the Basque Country (1997-1999). Since 1999 she is lecturer in the Department of Industrial Technology at the Faculty of Engineering of the University of Deusto and researcher at Energy Unit of DeustoTech. His teaching activity has been focused especially in the field of automatic control, especially in the area of nonlinear, multivariable, adaptive and predictive control. His research work is related to the modelling and development of control algorithms. She is collaborating in activities related to climate change, energy policy and environmental sustainability.

Oihane Kamara, Engineering in Computer Science (2010) and Master's Degree in Development and Integration of Software Solutions (2012) by the University of Deusto. In 2010, she started working at the DeustoTech-Energy Unit focusing on the analysis and development of digital applications for the calculus of the ecological footprint within the construction sector, and the energy optimization of industrial processes within the foundry industry. Ever since, her lines of research have broadened including geospatial technologies (GIS) and intelligent agent systems (MAS) for supply networks and Smart Buildings, the development of databases, visualization tools and Artificial Intelligence-based techniques for the calculus of pollutant emissions in vehicles and metering data from different sources. She is currently developing her Ph.D on the application of Artificial Intelligence algorithms on the optimization of energy efficiency in buildings considering several sources of generation.

Cruz E. Borges, received his diploma degree in Mathematics from University of La Laguna (Spain) and his Ph.D from University of Cantabria where he solve Symbolic Regression Problems using Genetic Programming and Numerical Methods. He has made a postdoc at DeustoTech where he develops forecasting techniques to predict the energy consumption of buildings (CENIT ENERGOS, ITEA2 IMPONET and ITEA2 NEMO&CODED) and have also developed Decision Support Systems for the evaluation of energy efficiency measures (MANUNET ENEPRO and HEFICAL). Currently, he leads the smart grid group of the Energy Unit of DeustoTech.

AN APPROACH TO ESTIMATE THE WATER FOOTPRINT OF THE BIOETHANOL SUPPLY CHAIN AND ITS DYNAMIC SIMULATION

Armin Trujillo-Mata[(a)], Guillermo Cortés-Robles[(b)], Cuauhtémoc Sánchez-Ramírez[(c)], Julio Blanco-Fernández[(d)], Emilio Jiménez-Macías[(e)]

[(a),(b),(c)] Graduate Studies and Research Division, Orizaba Institute of Technology, Av. Oriente 9 Num. 852 Col. Emiliano Zapata, 94320. Orizaba, Veracruz, Mexico; Telephone: +52 (272) 7257056.
[(d)(e)] High Technical School of Industrial Engineering, University of La Rioja, Edificio Departamental, C/San José Calasanz 31, 26004, Logroño, La Rioja, Spain

[(a)] atrujillom@ito-depi.edu.mx , [(b)] gcortes@itorizaba.edu.mx, [(c)] csanchez@itorizaba.edu.mx,
[(d)] julio.blanco@unirioja.es, [(e)] emilio.jimenez@unirioja.es

ABSTRACT
The Supply Chain Management as a source of competitiveness evolves continually. In the last decade, the sustainability of the supply chain represents a key success factor. The energy industry is not an exception. The global pressure to reduce emissions combined with the negative tendency in the world oil reserves is impelling the improvement and development of renewable sources of energy. The bioethanol industry is one of the most active sectors. Under this environment, the market is facing a conflict: to increase productivity (more resources consumed), without compromising the future natural resources. As the bioethanol industry accelerates its productivity and market share, another renewable resource suffers for this expansion: the water reserves. This work proposes to integrate the Bioethanol Supply Chain Analysis with the Water Footprint Assessment. Since water changes in time under the influence of several factors, the System Dynamics approach is very useful to deal with variables that change continually over time. Consequently, a model to evaluate the water footprint of the bioethanol supply chain through the system dynamics approach enables the capacity to simulate the impact of bioethanol production on water resources over time. This work presents a Causal-Loops Diagram useful to observe and analyze the complex relationship that the components of the bioethanol supply chain have.

Keywords: bioethanol supply chain, system dynamics modeling, water footprint assessment, causal loops diagram

1. INTRODUCTION

In recent years, industries have shown a growing interest in managing water consumption effectively. Water availability for domestic, agricultural and industrial use has become an increasingly important topic of international and interdisciplinary research (Susnik et al., 2012). Moreover, there is also a growing awareness on diverse environmental issues such as global warming and climate change that encourage research to explore the best practices for efficient water consumption. Under such restrictive conditions, it is clear that as the population of the world increases and water availability decreases, companies must redesign their supply chains (Carter & Jennings, 2002). Consequently, there are still big opportunities to define the best practices and methodologies to help managers to design policies and strategies to improve the supply chain management. The objective of this effort is to ensure the sustainability of supply chains by reducing the environmental impact that they have. The biofuels supply chain is one of the more dynamic fields looking for better practices for sustainability (Akgul et al., 2012; Bernardi et al., 2012; Dumanli et al., 2007; Eksioglu et al., 2009). It is also crucial to notice that water is not a fundamental element analyzed in the biofuels supply chain. However, local sources supply the water used in biofuel production, a condition that frequently has an impact, not only on domestic sectors but also in the community. In consequence, water plays a vital role in supply chains, especially in biofuels supply chains due to the nature of their raw materials. Therefore, it would be useful in any supply chain, and particularly in the biofuel supply chain, to determine the amount of water consumed in the production of biofuels. The Water Footprint Assessment is a useful approach to reach this objective. However, like any other systems, the bioethanol supply chain is in constant evolution. The System Dynamics Simulation is useful to model and test different scenarios and hypothesis over time. Consequently, this work proposes an integration between the Water Footprint Assessment and the System Dynamics Simulation.

2. SUSTAINABLE SUPPLY CHAINS

In recent years, the supply chain management has gained interest as an essential element to increase the efficiency of the decision-making process in diverse sectors. According to Mentzer et al. (2001), the Supply Chain (SC) is “a set of three or more entities (organizations or individuals) directly involved in the upstream and downstream flows of products, services, finances, and/or information from a source to a customer". Another useful definition for the Supply Chain Management (SCM), is "Supply Chain Management is the systemic and strategic coordination of the traditional business functions and the tactics across these business functions within a particular company and across businesses within the supply chain". Mentzer et al. (2001), Gold & Seuring (2011), and Martínez-Jurado & Moyano-Fuentes (2014), offer a more detailed description of the supply chain foundations and the supply chain management. According to Winter & Knemeyer (2013), the field of SCM has an inherent connection to sustainability.

In the past decade, the implementation of several initiatives to improve the environmental performance of firms has been tested. Among these initiatives, which also aim to accelerate the implementation of cleaner production approaches, are environmental clubs, waste exchange programs, eco-industrial parks, and sustainable supply chain initiatives (Hoof & Thiell, 2014). There is an increasing interest in the sustainability of supply chains, essentially motivated for the incorporation of environmental and social issues in the daily work of middle and top managers (Seuring & Müller, 2008).

It is important to mention that most of the articles reviewed do not focus specifically on modeling a sustainable supply chain considering water as a relevant resource for sustainability, nor its required practices.

2.1. Biofuels and the supply chain analysis

The biofuel industry is growing explosively due to environmental regulations, and renewable or sustainable energy needs. Thus, it is imperative to analyze the biofuels supply chain. An et al. (2011) propose a generalized structure based on the agricultural biomass feedstock to examine what currently is known about biofuels supply chains. This structure was developed trying to show, in a general way, how a biofuel supply chain structure is formed. Authors identify various elements such as farms, biomass storage sites, pre-processing facilities, refineries, distribution centers, and service stations that supply customers.

It is important to consider the impact that the analysis of the biofuel supply chain has over the decision-making process, particularly on logistics activities. Dumanli et al (2007) examine the changes that must be planned for transforming the traditional fossil supply chain to a more sustainable chain. The main topic of this article is the production and exploitation of biomass. Authors then analyze the characteristics, logistics and environmental aspects of this supply chain without neglecting the economic, legal and technical issues. Finally, the conclusion shows that it is possible to implement a sustainable and environmentally friendly energy system that creates economic value for a country. Even if the authors explain the basic relations among several important variables in this supply chain, all relationships are evaluated from a static and deterministic point of view.

Eksioglu et al. (2009) carried out a work where they developed a mixed integer programming (MIP) model. The model searches the minimization of the total cost of a biomass supply chain, accounting for deterioration, seasonality and availability of biomass materials. The proposed model identifies the optimal number, size and location of collection facilities, bio-refineries, as well as the amount of biomass shipped, biomass processed and held as inventory. Sustainability is not a central topic in this article.

In the work of Zhang et al. (2013), authors explore this relation through a mixed and integer linear programming (MILP) model. This model minimizes the total annualized costs of switchgrass-based supply chains (SBSC) by optimizing the diverse individual logistic aspects of this SC. However, the study does not consider the dynamic behavior of the supply chain. A dynamic analysis is useful because biofuel supply chains are complex and have a dynamic performance over time (Barisa et al., 2015).

Another approach for sustainability in biofuel supply chains has to do with optimization. Akgul et al. (2012) developed a model that addresses sustainability issues, such as the use of food crops, land use requirements of second-generation crops, and competition for biomass with other sectors. However, issues related to water behavior, their impact, its performance over time on the lands, and the most efficient use for these crops is not considered.

Mafakheri & Nasiri (2014) classify the different models that best deal with decision problems in the various states of a biomass supply chain in five categories, which are the following: i) Biomass harvesting and collection, ii) Biomass pre-treatment, iii) Biomass storage, iv) Biomass transport, and v) Biomass energy conversion. They also identify as the most influencing challenges, diverse issues such as technical and technological, financial, social, environmental, policy/regulatory and institutional/organizational. In this research, it should have been interesting to analyze the relationship between all these issues from the dynamic point of view. In other work, Månsson et al. (2014) use the supply chain approach for analyzing the existing biofuel supply chains in Sweden, in terms of security of supply. Then, authors explain the possibilities to achieve synergies between the implementation of practices to mitigate climate change through an increased production and use of biofuels. None of these works focuses on the analysis of the water consumption in the case of the bioethanol production.

Avinash et al. (2014) describe the biodiesel supply chain. Authors examine the development of biofuel as a substitute for fossil fuels to explore several possible benefits such as: 1) to relieve the world energy and economic crisis; 2) to analyze the environmental impacts that biofuels have on the road transportation and 3) the possible large-scale impacts of biofuel crops on food-based agricultural lands. However, the study

does not take into account the effect that the biofuel production has on water consumption.
Recently, some researchers have recognized that water availability is a severe agriculture constraint to the production of energy crops (Tan et al., 2009). As a partial conclusion, this literature review showed that none of the revised articles analyzes water availability and its impact on supply chains from a dynamic point of view.

3. THE WATER FOOTPRINT IN SUPPLY CHAINS

In general, the renewable forms of energy are considered “green” because they cause little depletion of the Earth's resources (Hall & Scrase, 1998). However, there is still enough effort to specify and analyze in detail, why water plays a crucial role in sustainable biofuels supply chains; mainly to assess the impact that water consumption has in the environment where biofuel is produced. Awareness regarding this issue is growing. According to (Ruini et al., 2013), in the last decade there has been a bigger interest in the evaluation of the water footprint in parallel with the carbon footprint. The Water Footprint Assessment (WFA) opens the door to the analysis of complex water relationships. This analysis also produces vital information for policy actors, business leaders, regulators and managers about their responsibilities on this increasingly scarce resource (Chapagain & Orr, 2009).

3.1. The concept of water footprint

The water footprint of a product is the volume of freshwater used to produce it, measured over the full supply chain (Hoekstra et al., 2011; Kongboon & Sampattagul, 2012). In other words, the water footprint is the water utilized in diverse processes; such as industrial and power generation, as well as the water pollute it through these same processes. The water footprint concept considers the source where the water comes from. The water origin defines its class: blue, green and gray water. According to Hoekstra et al. (2011), blue water refers to the consumption of blue water resources (surface and groundwater such as rivers, lakes, etc.) along the supply chain of a product. Green water is the rainwater stored in soil as moisture, and it refers to the consumption of green water resources (rainwater insofar as it does not become run-off). It concentrates on the use of rainwater, specifically in the flow of soil evapotranspiration used in agriculture and forestry. Finally, gray water refers to the water that has been polluted by a process. It is defined as the volume of freshwater that is required to assimilate a load of pollutants given natural background concentrations and existing ambient water quality standards. The sum of green water, blue water, and gray water that requires a product or service within its whole development process is the water footprint.

3.2. The water footprint assessment methodology

Hoekstra et al. (2011) defined the general methodology as follows: i) Setting goals and scope, ii) Water footprint accounting, iii)Water footprint sustainability assessment, iv)Water footprint response formulation.
Figure 1 shows the minimal phases that every water footprint assessment must have.

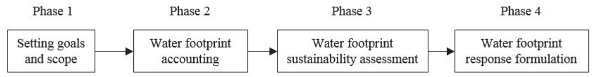

Figure 1. Four distinct phases in water footprint assessment (Hoekstra et al., 2011).

Since the approach of water footprint assessment has been used to evaluate the impacts of specific consumption and production practices on freshwater quality and sustainability, it becomes very important in diverse production processes, particularly for the biofuels process. A more detailed insight about the water footprint components and its assessment, is offered also by Galan-del-Castillo & Velazquez (2010).

3.3. The importance of water footprint assessment in biofuels production process

Until the recent past, there have been few thoughts in the science and practice of water management about water consumption and pollution along the whole production process and supply chains (Hoekstra et al., 2011). As a result, there is not enough awareness regarding the fact that the organizations and characteristics of a production process and supply chain strongly influence the volumes of water consumption that can be associated with a final consumer product. Therefore, it becomes of great importance to be aware of the amount of water used or consumed in any process or supply chains. The water footprint is an indicator of this consumption.
According to Gerbens-Leenes et al. (2009), in the coming decades human beings will face critical challenges, not only to meet the basic needs for water, but also to ensure that the water from rivers, streams, lakes, and aquifers does not affect freshwater ecosystems performing ecological functions. Authors also point out that higher demand for food, in combination with a shift from fossil energy towards bioenergy, puts additional pressure on freshwater resources. This pressure increases the urgency to propose a process of sustainable intensification by increasing the efficiency of water use. Dominguez-Faus, et al. (2009) analyze the management of land and water explaining that as biofuel production increases, a growing need exists to understand and mitigate potential impacts to water resources. Authors discuss that the most significant effects, are related to the agricultural stages of the biofuel life cycle known as the water footprint. Hence, it is necessary to consider that a continuous growth in biofuel production could have far-reaching environmental repercussions.
According to Hoekstra et al. (2011), freshwater is increasingly becoming a global resource, driven by growing international trade in water-intensive commodities. Because of this phenomenon, water resources have become spatially disconnected from the

consumers. One example is the case of cotton. From field to the end product, the cotton passes through diverse production steps with different impacts on water resources. Additionally, these stages of production are often located in different places and final consumption yet in another location. Hence, the impact that a final cotton product has on the globe's water resources can only be estimated through the analysis of its supply chain, and tracing the origins of the product.

The water footprint of biofuel energy depends on the crop being cultivated, the yield selected for this purpose, climatic conditions at the location for production, and agricultural practices (Gerbens-Leenes et al., 2009). Jeswani & Azapagic (2011) review some of the approaches and methodologies for the assessment of the impacts that the consumption of freshwater has in the production of ethanol in 12 different countries but they do not do it dynamically. Thus, only a few studies have examined the relationship between biofuel consumption and pressure on water resources.

4. SYSTEM DYNAMICS ANALYSIS FOR RENEWABLE ENERGY AND BIOFUELS SUPPLY CHAINS

Systems thinking is the process of understanding how things, like parts of a set, influence each other. According to Aslani et al. (2014), System Dynamics (SD) is a methodology based on system thinking to understand and model the behavior and activities of complex systems over time. Therefore, this robust and powerful methodology is used as a decision support tool that helps to identify the interaction of the different components of any complex system (Jimenez et al., 2001). System dynamics models use causal loops diagrams (CLD), which help analyze feedback loops, variables, levels, and delays that can affect the behavior of a system over a specific time. A SD model can depict the interaction and relation that have the different variables of a biofuel supply chain, such as water use and water availability. For a more detailed description about SD, the work of Forrester, (1958), Rehan et al. (2013) and Chen & Wei (2014) is highly recommended.

The research on the application of system dynamics methodology for different aspects of the biofuel supply chain has evolved in the last decade (Barisa et al., 2014). Despite this effort, there are just a few works in the area of biofuels supply chain using the System Dynamics approach. Rendon-Sagardi et al. (2014) carried one of these studies. Authors developed a System Dynamics Model to evaluate whether the production of ethanol in Mexico could meet the potential demand for this substance as a biofuel additive. Even if this work is relevant, water is not analyzed as an important element of the supply chain of ethanol, nor is it evaluated from a dynamic point of view.

Next section explores the relationship between system dynamics and the water footprint.

4.1. System Dynamics modeling for the Water Footprint in biofuels supply chain

Water plays a crucial role in biofuels supply chain, and it is a valuable resource, which has a dynamic behavior. The water consumption and usage also have a potential impact on socio-economics policies; hence diverse research has been supported by system dynamics to visualize the action and effect that hydrologic resources could have in different sectors. Susnik et al. (2012) developed a system dynamics model to analyze the current and future behavior of a catchment to assess water scarcity in Tunisia. The work of Jin et al. (2009) incorporates the system dynamics approach into the ecological footprint for forecasting the ecological footprint. Rehan et al. (2013) developed causal loop diagrams and a system dynamics model to support the financially sustainable management of urban water distribution networks. Thus, it is outlined that the system dynamics is a useful tool to model water management and water security systems. Thus, it becomes very important to develop and apply a methodology that helps to get an insight into the impact that water could have in any region by simulating its dynamic behavior through time.

After a careful analysis of several works, it is possible to propose a general model to integrate system dynamic simulation and water footprint assessment. This basic model contains two stages: (1) theoretical foundations: state-of-the-art and (2) methodological approach. Next section describes both stages.

4.2. Application of the SD-WFA approach

A basic process to deploy the SD-WFA synergy has four stages: 1) Conceptualization: this stage collects basic information about the supply chain under analysis. In this step the construction of the causal loops diagram (CLD) is useful to represent the relationship among variables, 2) Formulation: in this step, it is necessary to define the parameters of the variables influencing the system under study. The model of the system is another product of this stage. 3) Evaluation: in this step, the verification and validation of the simulation model is carried out, and finally, 4) Implementation: in this step the model is able to generate results and works as a support for the decision making process.

It is worth mentioning that in this research, the application of SD modeling remains with the preparation of a causal loops diagram (CLD), which is the final output of the conceptualization stage. Conceptualization is the first stage in the System Dynamics methodology. Figure 2 represents a general scheme for the sugarcane-based ethanol supply chain in the stage of production.

The CLD in Figure 2 is an approximation model that was developed considering the conceptualization for bioethanol production in Mexico. Next points describe the feedback loops defining the dynamics of the system under study.

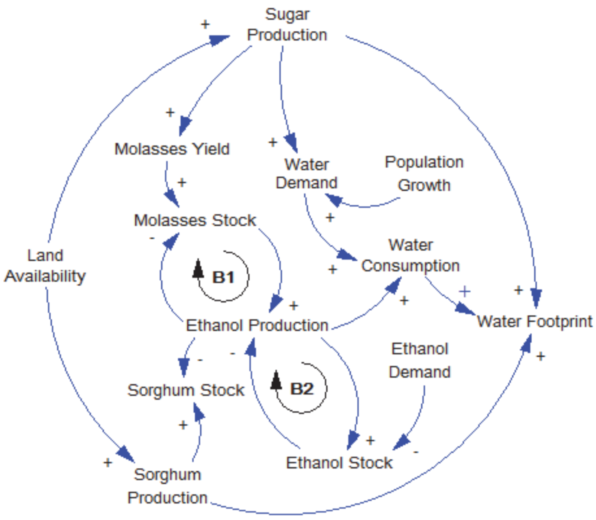

Figure 2. CLD for the analysis of the ethanol production and its water footprint.

- In Loop B1: if the molasses stock increases, the volume of ethanol that can be produced also increases. In the other way, if the production of ethanol increases, the molasses stock decreases.
- Loop B2 represents the ethanol stock in regards to the ethanol production volume. When the production volume of ethanol increases, the ethanol stock also increases. But if the ethanol stock increases, the production volume of ethanol decreases.

The other relations depicted in the CLD can be interpreted as follows. The variable ethanol stock for example, depends on the variable ethanol demand. The variable water consumption depends on the variable ethanol production. This relation is positive because if the ethanol production volume increases, the water consumption also increases. Water consumption in turn, depends on the variable water demand, which has a positive relation with the variable population growth. This is because as population rate increases, the water demand also increases.

Finally, the variable water consumption has a direct impact on the variable water footprint. This is because water footprint is an indicator of the water consumed in the process. The relationship is positive because if the consumption of water increases, the water footprint indicator will be greater.

5. CONCLUSIONS

This work proposes a model able to incorporate the water footprint assessment of ethanol in the production stage of its supply chain. The model has a particularity: it is possible to evaluate the performance dynamically. The System Dynamics approach and its modeling technique could help the ethanol industry to develop policies and strategies that contribute to fulfilling the sustainability requirements of its supply chain. This goal is reachable because the model correlates the water consumption associated with the main crop and production processes from a dynamic point of view.

With this preliminary model is possible to observe the usefulness of the System Dynamics approach to model and integrate both concepts: the supply chain analysis and the water footprint assessment. Integration of System Dynamics Modeling to the Water Footprint Assessment of Bioethanol Supply Chains promises to help managers in the biofuels industry get a more in depth comprehension of consumption of water along the process, and therefore, develop strategies and policies that give better management practices of water resources.

As a future work and improvement of the proposed model, it is necessary to consider the analysis and assessment of the water footprint in all the stages of the supply chain, including the distribution stage of biofuel. More knowledge and insight about the ethanol industry will be available if the oil production system and market fluctuations are take into account in the present analysis. However, the complexity and effort to model this integration will also increase.

ACKNOWLEDGMENTS

This work was sponsored by the National Council of Science and Technology (CONACYT) and the Public Education Secretary (SEP) through PROMEP. Additionally, the ROPRIN working group (Network of Optimization in Industrial Processes) supported this work.

REFERENCES

Akgul, O., Shah, N., & Papageorgiou, L. G. (2012). Economic optimisation of a UK advanced biofuel supply chain. Biomass and Bioenergy, 41, 57–72. http://doi.org/10.1016/j.biombioe.2012.01.040

An, H., Wilhelm, W. E., & Searcy, S. W. (2011). Biofuel and petroleum-based fuel supply chain research: A literature review. Biomass and Bioenergy, 35(9), 3763–3774. http://doi.org/10.1016/j.biombioe.2011.06.021

Aslani, A., Helo, P., & Naaranoja, M. (2014). Role of renewable energy policies in energy dependency in Finland: System dynamics approach. Applied Energy, 113, 758–765. http://doi.org/10.1016/j.apenergy.2013.08.015

Barisa, A., Romagnoli, F., Blumberga, A., & Blumberga, D. (2015). Future biodiesel policy designs and consumption patterns in Latvia: a system dynamics model. Journal of Cleaner Production, 88, 71–82. http://doi.org/10.1016/j.jclepro.2014.05.067

Bernardi, A., Giarola, S., Bezzo, F., Padova, U., & April, R. (2012). Optimizing the economics and the carbon and water footprints of bioethanol supply chains. Biofuels Bioproducts and Biorefining. http://doi.org/10.1002/bbb

Carter, C. R., & Jennings, M. M. (2002). Logistics social responsibility: an integrative framework. Journal of Business Logistics, 23(1), 145–180.

Chapagain, A. K., & Orr, S. (2009). An improved water footprint methodology linking global consumption

to local water resources: A case of Spanish tomatoes. Journal of Environmental Management, 90(2), 1219–1228. http://doi.org/10.1016/j.jenvman.2008.06.006
Chen, Z., & Wei, S. (2014). Application of System Dynamics to Water Security Research. Water Resources Management, 28(2), 287–300. http://doi.org/10.1007/s11269-013-0496-8
Dominguez-Faus, R., Powers, S. E., Burken, J. G., & Alvarez, P. J. (2009). The Water Footprint of Biofuels: A Drink or Drive Issue? Environmental Science and Technology, 43(9), 3005–3010. http://doi.org/10.1021/es802162x
Dumanli, A. G., Gulyurtlu, I., & Yürüm, Y. (2007). Fuel supply chain analysis of Turkey. Renewable and Sustainable Energy Reviews, 11, 2058–2082. http://doi.org/10.1016/j.rser.2006.03.011
Eksioglu, S. D., Acharya, A., Leightley, L. E., & Arora, S. (2009). Analyzing the design and management of biomass-to-biorefinery supply chain. Computers and Industrial Engineering, 57, 1342–1352. http://doi.org/10.1016/j.cie.2009.07.003
Forrester, J. W. (1958). Industrial dynamics: a major breakthrough for decision makers. Harvard Business Review, (August), 37–66.
Galan-del-Castillo, E., & Velazquez, E. (2010). From water to energy : The virtual water content and water footprint of biofuel consumption in Spain. Energy Policy, 38(3), 1345–1352. http://doi.org/10.1016/j.enpol.2009.11.015
Gerbens-Leenes, W., Hoekstra, A. Y., & Meer, T. H. Van Der. (2009). The water footprint of bioenergy. Proceedings of the National Academy of Sciences, 106(25), 10219–10223. http://doi.org/10.1073/pnas.0812619106
Gold, S., & Seuring, S. (2011). Supply chain and logistics issues of bio-energy production. Journal of Cleaner Production, 19(1), 32–42. http://doi.org/10.1016/j.jclepro.2010.08.009
Hall, D. O., & Scrase, J. I. (1998). Will biomass be the environmentally friendly fuel of the future? Biomass and Bioenergy, 15(4), 357–367.
Hoekstra, A. Y., Chapagain, A. K., Aldaya, M. M., & Mekonnen, M. M. (2011). The Water Footprint Assessment Manual. Setting the Global Standard (1st ed.). London: Earthscan.
Hoof, B. Van, & Thiell, M. (2014). Collaboration capacity for sustainable supply chain management: small and medium-sized enterprises in Mexico. Journal of Cleaner Production, 67, 239–248. http://doi.org/10.1016/j.jclepro.2013.12.030
Jeswani, H. K., & Azapagic, A. (2011). Water footprint: Methodologies and a case study for assessing the impacts of water use. Journal of Cleaner Production, 19(12), 1288–1299. http://doi.org/10.1016/j.jclepro.2011.04.003
Jimenez, E., Recalde, L., & Silva, M. (2001). Forrester diagrams and continuous Petri nets: A comparative view. Proceedings of the Emerging Technologies and Factory Automation 2001 8th IEEE International Conference on, Volume: 2 http://doi.org/10.1109/ETFA.2001.997674
Jin, W. J., Xu, L., & Yang, Z. (2009). Modeling a policy making framework for urban sustainability: Incorporating system dynamics into the ecological footprint. Ecological Economics, 68, 2938–2949. http://doi.org/10.1016/j.ecolecon.2009.06.010
Kongboon, R., & Sampattagul, S. (2012). The water footprint of sugarcane and cassava in northern Thailand. Procedia - Social and Behavioral Sciences, 40, 451–460. http://doi.org/10.1016/j.sbspro.2012.03.215
Mafakheri, F., & Nasiri, F. (2014). Modeling of biomass-to-energy supply chain operations : Applications , challenges and research directions. Energy Policy, 67, 116–126. http://doi.org/10.1016/j.enpol.2013.11.071
Månsson, A., Sanches-Pereira, A., & Hermann, S. (2014). Biofuels for road transport : Analysing evolving supply chains in Sweden from an energy security perspective. Applied Energy, 123, 349–357. http://doi.org/10.1016/j.apenergy.2014.01.098
Martínez-Jurado, P. J., & Moyano-Fuentes, J. (2014). Lean Management , Supply Chain Management and Sustainability : A Literature Review. Journal of Cleaner Production, 85, 134–150. http://doi.org/10.1016/j.jclepro.2013.09.042
Mentzer, J. T., DeWitt, W., Keebler, J. S., Min, S., Nix, N. W., Smith, C. D., & Zacharia, Z. G. (2001). Defining Supply Chain Management. Journal of Business Logistics, 22(2), 1–25.
Rehan, R., Knight, M. A., Unger, A. J. A., & Haas, C. T. (2013). Development of a system dynamics model for financially sustainable management of municipal watermain networks. Water Research, 47(20), 7184–7205. http://doi.org/10.1016/j.watres.2013.09.061
Rendon-Sagardi, M. A., Sanchez-Ramirez, C., Cortes-Robles, G., Alor-Hernandez, G., & Cedillo-Campos, M. G. (2014). Dynamic analysis of feasibility in ethanol supply chain for biofuel production in Mexico. Applied Energy, 123, 358–367. http://doi.org/10.1016/j.apenergy.2014.01.023
Ruini, L., Marino, M., Pignatelli, S., Laio, F., & Ridolfi, L. (2013). Water footprint of a large-sized food company: The case of Barilla pasta production. Water Resources and Industry, 2, 7–24. http://doi.org/10.1016/j.wri.2013.04.002
Seuring, S., & Müller, M. (2008). From a literature review to a conceptual framework for sustainable supply chain management. Journal of Cleaner Production, 16, 1699–1710. http://doi.org/10.1016/j.jclepro.2008.04.020
Susnik, J., Vamvakeridou-Lyroudia, L. S., Savic, D. A., & Kapelan, Z. (2012). Integrated System Dynamics Modelling for water scarcity assessment: Case study of the Kairouan region.

Science of the Total Environment, 440, 290–306. http://doi.org/10.1016/j.scitotenv.2012.05.085
Tan, R. R., Chwan, D., Aviso, K. B., & Kok Sum, D. (2009). The use of graphical pinch analysis for visualizing water footprint constraints in biofuel production. Applied Energy, 86(5), 605–609. http://doi.org/10.1016/j.apenergy.2008.10.004
Winter, M., & Knemeyer, A. M. (2013). Exploring the integration of sustainability and supply chain management. Current state and opportunities for future inquiry. International Journal of Physical Distribution and Logistics Management, 43(1), 18–38. http://doi.org/10.1108/09600031311293237
Zhang, J., Osmani, A., Awudu, I., & Gonela, V. (2013). An integrated optimization model for switchgrass-based bioethanol supply chain. Applied Energy, 102, 1205–1217. http://doi.org/10.1016/j.apenergy.2012.06.054

COMPARISON OF TRADITIONAL AND CLIMATE-CONTROLLED MUSHROOM CULTIVATION PROCESSES

Leiva-Lázaro, F.J.[(a)], Blanco-Fernández, J.[(b)], Martínez-Cámara, E.[(c)], Latorre-Biel, JI[(d)], Jiménez-Macías, E.[(e)]

[(a,b,c)] Department of Mechanical Engineering. University of La Rioja. Logroño. Spain.
[(d)] Department of Mechanical, Energy and Materials Engineering,
Public University of Navarre, Tudela, Spain.
[(e)] Department of Electrical Engineering. University of La Rioja. Logroño. Spain.

[(a)] francisco.leiva@unirioja.es, [(b)] julio.blanco@unirioja.es, [(c)] e.camara@eolicas.com,
[(d)] juanignacio.latorre@unavarra.es, [(e)] emilio.jimenez@unirioja.es

ABSTRACT
Originally mushroom cultivation was carried out in caves that have gradually been replaced by climate controlled chambers, to control climatic conditions, requiring only energy consumption and cooling systems. The climate controlled chambers allow higher control over the weather conditions inside the growing chambers, temperature, and humidity, compared to the traditional cultivation process.
However, this advantage implies an increase in energy consumption, much higher than the traditional cultivation process, due to the demand of the Heating, Ventilating and Air Conditioning system (HVAC). As a result, the climate controlled cultivation process requires higher investments that the traditional cultivation process. The results of this study indicate that traditional cultivation systems have higher average production than climate controlled systems. Furthermore, higher investments are needed in climate controlled cultivation systems. However, traditional cultivation systems are totally dependent on weather conditions, as a result, cold and hot seasons are not favourable for these cultivation systems.

Keywords: Mushroom cultivation, Agaricus Bisporus, Economic analysis, production analysis

1. INTRODUCTION
Agaricus bisporus is a specie of basidiomycota fungus from the Agaricaceae family native to Europe and North America (Leiva et al., 2016). The Agaricus Bisporus is the most cultivated fungus worldwide (Foulongne-Oriol et al., 2014; Tautorus, 1985; Ma et al., 2014; Saravanan et al., 2013) over 70 countries (Ma et al., 2014; Saravanan et al., 2013). It is one of the most consumed vegetable crops worldwide (Wani et al., 2010).
The cultivated edible fungus Agaricus bisporus accounts for 70% of the world annual output of edible mushrooms (Durrant et al., 1991). It accounts for nearly 40% of the world's mushroom supply (Sanchez et al., 2009).
The fungus mainly grows on partially decomposed substrate (Donini et al., 2006) in regions with mid temperature and high humidity (Akinyele et al., 2012). In intensive cultivation, Agaricus bisporus is produced on a composted substrate consisting of mixtures of hay, corncobs, wheat straw, horse and poultry manures, cottonseed hulls, corn stover, gypsum and other raw materials (Royse et al., 2009: Burton et al., 1997; González-Matute et al., 2006; Straatsma et al., 2000). The development of fruit bodies of A. bisporus requires a non-nutritional layer of casing soil on top of the nutritious compost (Straatsma et al., 2013). Casing soil has an important role in the cultivation of Agaricus bisporus (Gülser et al., 2003).
Parameters, such as temperature and humidity, must be constantly controlled. Usually, the fungus is cultivated in caves (traditional cultivation) as temperature and humidity are ideal for the cultivation process. However, the traditional cultivation has been replaced by climate controlled chambers, because critical parameters are totally under control.
The research presented, allows to obtain tools for planning environmental and economic strategies in the mushroom production process. Furthermore, the study is a proper tool to identify economic and environmental impact assessment of resources consumption. In addition, the research also allows the selection of alternatives for waste management and comparison between different options within a new process with the objective of minimizing environmental impacts, reduce energy consumption and costs.
As a continuation of Leiva-Lázaro et al. (2015), which was devoted to a general comparison between traditional and climate controlled cultivation of mushroom Agaricus Bisporus variety by the identification of environmental impacts of the production processes, this paper analyses the difference between traditional cultivation and climate controlled cultivation processes throughout an economic analysis, considering expenses and production quantity of both cultivation processes.

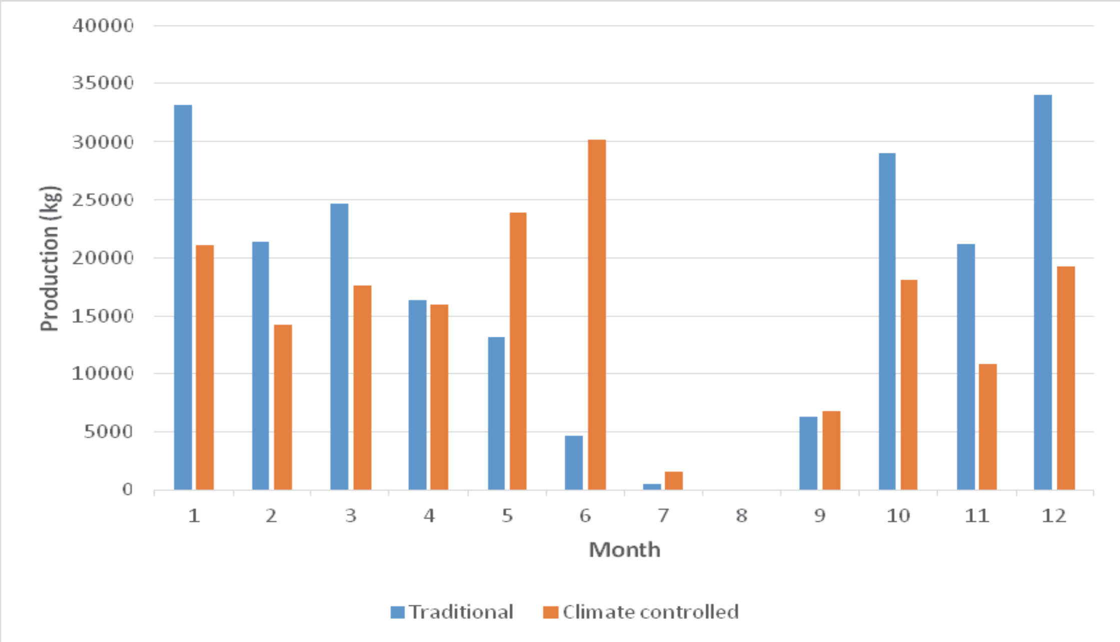

Figure 1: Production in a year for both cultivation processes

2. TRADITIONAL AND CLIMATE CONTROLLED PROCESS

A brief summary of both processes, traditional cultivation and climate controlled cultivation, is presented in this section so that readers can understand the differences which will be analysed without necessity of reviewing the references, although a deeper description can be found in Leiva-Lázaro et al. (2015) , Leiva et al. (2015), and Leiva et al. (2016).
The traditional cultivation process is carried out in cellars formerly used for wine production, which helps to maintain ideal temperature conditions for the mushroom cultivation. These wineries have only a ventilation system that renews the indoor air with fresh air, without control of temperature or humidity inside the room. The cellars are used rectangular 35 meters long, 4.5 meters wide and 2.4 meters high with a front door for input loading and unloading. The ventilation system is placed at the front and rear of the cellar, as a result the air flow inside the warehouse is adequate.
The climate controlled cultivation process takes place in rooms climatically controlled (relative humidity and temperature). These rooms have an air conditioning system and numerous air intakes for a homogeneous distribution in the room. The cellars are used rectangular 32 meters long, 7 meters wide and 4 meters high with a back door for loading and unloading packages of compost and casing material, and a front for staff access. All parameters are constantly controlled and monitored.
The production process includes the following stages:

2.1. Climatization.

The cultivation process conducted in climate controlled rooms, has a constant control of the temperature and a heating system supplied by biomass.

2.2. Ventilation.

The growing process in ventilated chambers features just a ventilation system to keep clean air constantly recirculating through the interior of the chambers

2.3. Preparation of the covering soil.

The first phase of the growing process is to prepare the soil used to cover the compost packages.
The process begins with the disinfection of the area where the covering soil is prepared, in order to prevent the appearance of diseases during the growing process. Peat is deposited in the disinfected area. This peat does not contain sufficient moisture, so water is added to bring the moisture content up to the level required for covering soil. Finally, fungicides are also added to prevent pests and diseases during the cultivation process.

2.4. Preparation of the growing chambers.

The next phase of the process is the preparation of the growing chambers to place the compost packages. The process begins with the disinfection of the growing chambers to prevent the appearance of diseases during the cultivation process. Once disinfection is complete, the chambers are prepared by setting out the cages where the compost packages will be placed. The compost packages are then placed on the cages so that the cultivation process can begin

2.5. Cultivation process.

The next phase is the cultivation process, which culminates with the harvesting of the end product. This process begins once all the compost packages have been placed on the cages in the chambers with the covering soil previously prepared. Then water is added to start the growing phase. Continual fumigation by adding fungicides and insecticides is required to prevent the appearance of pests during the process. During the cultivation process homogenisation (activation of the mycelium) and fruiting (development of the fruiting bodies) begin. When the fruiting process is completed the fruiting bodies are harvested.

2.6. Waste management.

The final phase is the management of the waste produced during the process. The waste produced is placed in a separate container for collection and treatment at a specific plant.

With the differences presented in the previous description, the temperature and the relative humidity are also different, as shown in Figure2 (Leiva el al. 2015) what will drive the different productions and also to different economic cost, which is the main point of the analysis of this work.

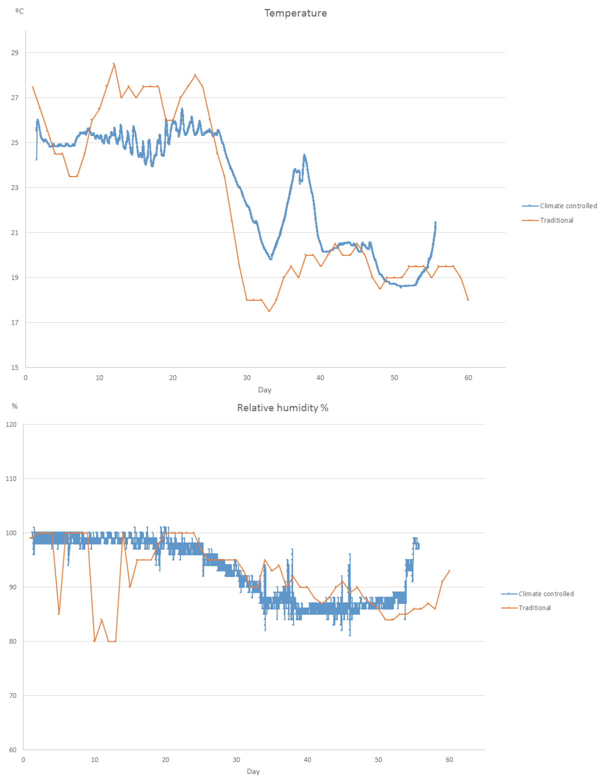

Figure 2: Differences in temperature and relative humidity with traditional and climate controlled cultivation processes (Leiva et al., 2015)

3. METHODOLOGY

This paper focuses on the comparison of existing cultivation processes in the study area from the economic and productive point of view. For the analysis, prices of the inputs used in the production process of both crops have been considered to present an economic comparison of both cultivation processes. Data and energy consumption were measured for the final study.

3.1. Ventilated growing chambers

The growing process in ventilated chambers features just a ventilation system to keep clean air constantly recirculating through the interior of the chambers (Leiva et al., 2015). As a result, the weather conditions inside the growing chambers are not under control, especially in winter and summer, when temperature and humidity levels are extreme for the fungus cultivation.

3.2. Climate controlled growing chambers

The cultivation process conducted in climate controlled rooms, has a constant control of the temperature and humidity (Pardo-Giménez et al., 2014). A computerized environmental control system is an invaluable tool for mushroom culture monitoring environmental parameters such as temperature, humidity, airflow, pressure, and carbon dioxide and oxygen content (Sánchez, 2010). A climate controlled system supplied by biomass and electricity, keeps the temperature at the desired level for an optimal production thorough the year.

4. RESULTS

Data gathered during the study is presented in this part. All data was collected during a year for both cultivation processes, traditional and climate controlled cultivation process. Expenses and production for both processes were collected for the study presented.

4.1. Mushroom production

Both cultivation processes under study were analyzed under the productive point of view through a year. Inputs and outputs by both crops, have been collected to make a comparison between the two cultivation processes. The amounts produced by each cultivation process is collected in Figure 1.

Figure 1 shows the production comparison for both cultivation processes thorough a year. In summer, mainly the climate controlled cultivation process is used because the temperature is very high and the humidity very low for the cultivation process. Using the traditional system in hot conditions will result in a poor production because the climate conditions are not proper for mushroom cultivation. However, using the climate controlled with high temperatures will result in high expenses for the amount of electricity used by the climate system to cool down the temperature of the outer air.

Time required for both processes are slightly different. The traditional cultivation process requires an average of 63 days. Oppositely, the climate controlled cultivation process requires less time, 58 days. Compared data is shown in Figure 3.

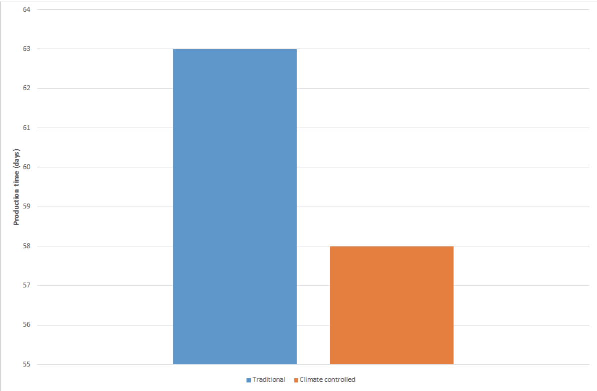

Figure 3: Time required for the cultivation process

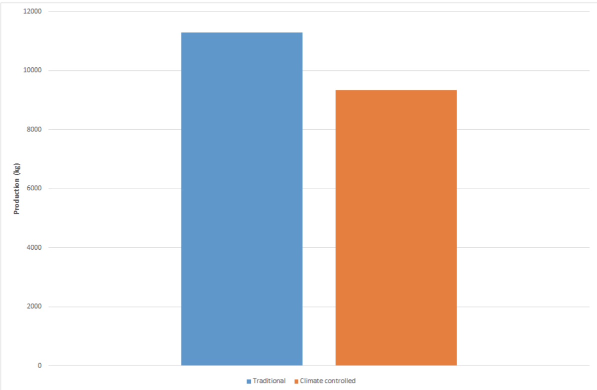

Figure 4: Quantity produced per chamber

The time required for the cultivation process is a bit lower in the climate controlled process. However, the amount produced per chamber is higher in the traditional system (Figure 4).

Figure 4 shows that the quantity produced per chamber, is slightly higher in the traditional rather than in the climate controlled process. The average quantity in the traditional process is 6.82 kg/cultivation package, and in the climate controlled process is 5.65 kg/ cultivation package.

Despite the fact that the climate controlled process guarantees a great control over the climatic conditions inside the chambers, the production is lower than the traditional process

4.2. Economic analysis

Both cultivation processes under study were also analysed under the economic point of view. For the study, inputs used for both cultivation processes, are equal in quantity.

Climate controlled chambers, have higher demand of energy, therefore, energy consumption is considerable higher compared to traditional processes. Furthermore, the Heating, Ventilating and Air Conditioning system (HVAC) needs to be disinfected and maintained continuously. As a result, the investment required for this process is considerable higher than traditional systems (see Figure 5).

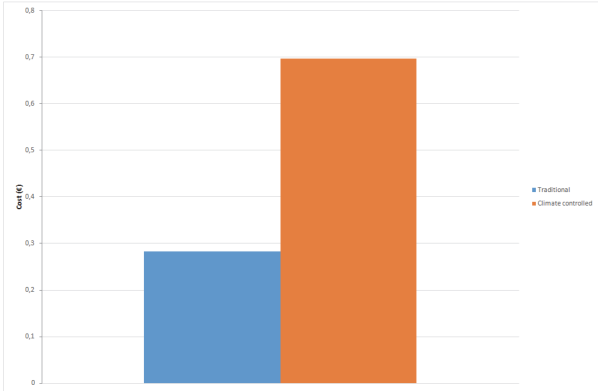

Figure 5: Cost of a kg of Agaricus Bisporus cultivation process

Figure 5 shows that the expenses for the climate controlled cultivation process is remarkably higher than the traditional process. The average cost to produce a kg of Agaricus Bisporus using the climate controlled cultivation process is 0.7€/kg. On the contrary, the average cost in the traditional cultivation process is less than half, 0.28€/kg.

5. CONCLUSIONS

The climate controlled cultivation process provides greater control of the temperature and relative humidity inside the cultivation chambers throughout the process. The climate controlled process allows to carry out the process at any time of year, because it does not depend on external conditions of temperature and humidity. However, energy demand is greater than the traditional cultivation process. In contrast, the traditional process is directly dependent on environmental conditions. As a result, the climate controlled process is faster, requiring less time to complete the cultivation process than the traditional process.

Conversely, the traditional cultivation process is much productive than the climate controlled system. Additionally, the investment needed is much lower in the traditional process for the ventilation system.

ACKNOWLEDGMENTS

This paper has been partially supported by the ADER Project: “Producción sostenible del champiñón de La Rioja y mejora de la protección ambiental, a través de la investigación de Ecoindicadores del Análisis de Ciclo de Vida (ACV)”.

REFERENCES

Evans W.A., 1994. Approaches to intelligent information retrieval. Information Processing and Management, 7 (2), 147–168.

Akinyele, J.B., Fakoya, S., Adetuyi, C.F., 2012. Anti-growth factors associated with Pleurotus ostreatus in a submerged liquid fermentation. Malaysian Journal of Microbiology 8, 135-140.

Beetz A, Kustudia M (2004) Mushroom cultivation and marketing. Horticulture production guide.

Burton, K.S., Smith, J.F., Wood, D.A., Thurston, C.F. (1997). Extracellular proteinases from the mycelium of the cultivated mushroom Agaricus bisporus. Mycological Research. Volume 101, Issue 11, 1997, Pages 1341-1347.

Donini, L.P., Bernardi, E., Do Nascimento, J.S., 2006. In vitro development of Agaricus brasiliensis in media supplemented with different brans. Pesq. Agrop. Brasileira 41, 995–999.

Durrant, A.J., Wood, D.A., Cain, R.B. (1991) Lignocellulose biodegradation by Agaricus bisporus during solid substrate fermentation. Journal of General Microbiology. Volume 137, Issue 4, 1991, Pages 751-755.

Dutta, S., 2013. Role ofmushrooms as nutraceutical an overview. Int. J. Pharma. Biol. Sci. 4, B59–B66.

Foulongne-Oriol, M., Navarro, P., Spataro, C., Ferrer, N., Savoie, J.M., 2014. Deciphering the ability of Agaricus bisporus var. burnettii to produce mushrooms at high temperature (25°C). Fungal Genetics and Biology 73, 1-11.

González-Matute, R., Rinker, D.L.(2006). Compatibility of ammonia suppressants used in poultry litter with mushroom compost preparation and production. Bioresource Technology. Volume 97, Issue 14, September 2006, Pages 1679-1686.

Gülser, C., Pekşen, A. (2003). Using tea waste as a new casing material in mushroom (Agaricus bisporus (L.) Sing.) cultivation. Bioresource Technology. Volume 88, Issue 2, June 2003, Pages 153-156

Leiva, F., Saenz-Díez, J.-C, Martínez, E, Jiménez, E, Blanco, J. (2016). Environmental impact of mushroom compost production. Journal of the Science of Food and Agriculture.

Leiva, F.J., Saenz-Díez, J.C., Martínez, E., Jiménez, E., Blanco, J. (2015). Environmental impact of Agaricus bisporus cultivation process. European Journal of Agronomy. Volume 71, November 01, 2015, Pages 141-148.

Leiva-Lázaro F.J., Blanco-Fernández J., Martínez-Cámara E., Latorre-Biel J.I., Jiménez-Macías E. (2015). Mushroom cultivation process, agaricus bisporus variety: comparison between traditional and climate controlled cultivation and identification of environmental impacts of the production processes. The 3nd International Workshop On Simulation For Energy, Sustainable Development & Environment SESDE 2015, Bergeggi, Italy. 21 – 23 September 2015.

Ma, Y., Guan, C.Y., Meng, X.J., 2014. Biological characteristics for mycelial growth of Agaricus bisporus, Applied Mechanics and Materials, pp. 297-302.

Moon, B., Lo, Y.M., 2013. Conventional and Novel Applications of Edible Mushrooms in Today's Food Industry. Journal of Food Processing and Preservation 38, 2146-2153.

Narayanasamy, P., Suganthavel, P., Sabari, P., Divya, D., Vanchinathan, J., Kumar, M.S., 2010. Cultivation of mushroom (Pleurotus florida) by using two different agricultural wastes in laboratory condition. Int. J. Microbiol. 7.

Pardo-Giménez, A., Pardo-González, J.E., Zied, D.C. Evaluation of harvested mushrooms and viability of Agaricus bisporus growth using casing materials made from spent mushroom substrate (Article). International Journal of Food Science and Technology. Volume 46, Issue 4, April 2011, Pages 787-792.

Rathee, S., Rathee, D., Rathee, D., Kumar, V., Rathee, P., 2012. Mushrooms as therapeutic agents. Braz. J. Pharmacogn. 22, 459–474.

Royse, D.J., Chalupa, W. (2009). Effects of spawn, supplement and phase II compost additions and time of re-casing second break compost on mushroom (Agaricus Bisporus) yield and biological efficiency. Bioresource Technology. Volume 100, Issue 21, November 2009, Pages 5277-5282.

Sanchez, J.E., Royse, D.J. (2009). Scytalidium thermophilum-colonized grain, corncobs and chopped wheat straw substrates for the production of Agaricus bisporus. Bioresource Technology. Volume 100, Issue 4, February 2009, Pages 1670-1674.

Saravanan, R., et al., Analysis of nutrients and minerals content in commercially purchased Agaricus bisporus. Research Journal of Pharmacy and Technology, 2013. 6(7): p. 765-768.

Straatsma, G., Gerrits, J.P.G., Thissen, J.T.N.M., Amsing, J.G.M., Loeffen, H., Van Griensven, L.J.L.D. (2000). Adjustment of the composting process for mushroom cultivation based on initial substrate composition. Bioresource Technology. Volume 72, Issue 1, March 2000, Pages 67-74.

Straatsma, G., Sonnenberg, A.S.M., van Griensven, L.J.L.D. (2013) Development and growth of fruit bodies and crops of the button mushroom, agaricus bisporus. Fungal Biology. Volume 117, Issue 10, October 2013, Pages 697-707.

Tautorus, T.E., 1985. Mushroom fermentation. Advances in Biotechnological Processes 5, 227-273.

Wani, B.A., R.H. Bodha, and A.H. Wani, Nutritional and medicinal importance of mushrooms. Journal of Medicinal Plants Research, 2010. 4(24): p. 2598-2604.

Xu, T., Beelman, R.B., Lambert, J.D., 2012. The cancer preventive effects of edible mushrooms. Anti Cancer Agents Med. Chem. 12, 1255–1263.

ANALYSYS OF SPANISH SELF-CONSUMPTION NORMATIVE: PROFITABILITY BASED ON CONSUMPTION PROFILES

Escobar-Forján, P.[(a)] , Jiménez-Macías, E.[(b)], Martínez-Cámara, E.[(c)] , García-Alcaraz, JL.[(d)], Sáenz-Díez, J.C.[(e)]

[(a,c)] Department of Mechanical Engineering. University of La Rioja. Logroño. Spain.
[(b,e)] Department of Electrical Engineering. University of La Rioja. Logroño. Spain.
[(d)] Autonomous University of Ciudad Juarez. Chiuhauha. Mexico.

[(a)] pescobarforjan@gmail.com, [(b)] emilio.jimenez@unirioja.es, [(c)] e.camara@eolicas.com,
[(d)] jorge.garcia@uacj.mx, [(e)] juan-carlos.saenz-diez@unirioja.es

ABSTRACT

This paper analyses the new Spanish normative on self-consumption (Royal Decree 900/2015) and its effects and profitability depending on the consumption profiles. A model based on the discounted cash flows over the life cycle of the plant model is used to analyze the feasibility of a photovoltaic system of self-consumption. The impact of the Royal Decree in the return on investment of a solar photovoltaic system of self-consumption is discussed for three different types of consumers, analysing the effect of the charges associated with the costs and services of the electrical system. In each case solutions are proposed to improve the viability and they are simulated with alternative regulatory schemes such as net metering. Finally, the effect of the difference in electricity production between two Spanish cities like Seville and Oviedo with very different climatic conditions is analyzed.

Keywords: self-consumption, Spanish power normative, viability, profitability analysis

1. BACKGROUND

This paper analyses the new Spanish normative on self-consumption (Royal Decree 900/2015) and its effects and profitability depending on the consumption profiles. First of all, most relevant issues are analysed in relation to different regulatory schemes existing in self-consumption to understand the most important aspects of Royal Decree. A model based on the discounted cash flows over the life cycle of the plant model will be used to analyze the feasibility of a photovoltaic system of self-consumption.

The impact of the Royal Decree in the return on investment of a solar photovoltaic installation of self-consumption is discussed for three different types of consumers, analysing the effect of the charges associated with the costs and services of the electrical system. In each case solutions are proposed to improve the viability and they are simulated with alternative regulatory schemes such as net metering. Finally, the effect of the difference in electricity production between two Spanish cities like Seville and Oviedo with very different climatic conditions is analyzed.

1.1. Self-consumption Support Methods

Historically, lawmakers have given special importance to develop rules on photovoltaic systems in the residential sector. As a result, various schemes have been introduced that are based on methods of support, may be indirect or direct [1].

Indirect methods include funding for research and development of technology, and regulations as affirmative obligation to make a photovoltaic system in new buildings. Other systems supporting the indirect self-consumption are so-called "net-metering" or "net-billing". This system compensates in their bill the energy spilled to network by electricity producers.

Direct methods provide financial support and can be based on quantity or quality.

An example of quantitative support is green certificate (GC), received by the owner of a photovoltaic system for the generation of a certain amount of energy. This system was used in the past decade in a few European countries such as Belgium, United Kingdom, Poland or Romania.

The main direct support schemes are based on the price. The most common policy is "feed-in tariff", which pays producers a specific price for each unit of energy produced and fed into the grid.

Other direct support schemes can be subsidies, tax rebates, and green loans.

1.2. Self-consumption scheme

There is a great diversity of models of electric consumption in the world with schemes and various parameters. In a simplified manner, it can be considered that there are five representative models [2]:

-Self-consumption with limitations. The savings in electricity bills are reduced by some additional fees or taxes. In addition, the excess electricity is fed into the grid but no compensation is obtained and it is lost by the self-consumer. This type of consumption is implemented in Spain.

- Self-consumption with electricity excess premium ("feed-in tariff"). The consumption saves on electricity bills and energy excess is sold under a defined rate that can be fixed or indexed to the retail price of electricity.

This mode is implemented in Germany and other countries.
- Net-billing. There are two streams of energy that could have two different prices. Costs related to the two flows are offset to calculate the reduction in the self-consumer bill. This mode is implemented in Italy.
- Net-metering. The electricity excess is compensated by the energy consumed during a particular time period; usually one year. In this case the price of the exported electricity has the same value as the price of electricity purchased from the grid. This implies a passive subsidy, since this price includes not only the cost of electricity, but also the associated system costs and other fees. This mode is implemented in Belgium.
- Self-consumption with bonus. Self-consumption is stimulated with a price above the market for energy self-consumed or through a certain value for the energy excess fed into the grid, higher than market price.
Website [3] at the initiative of the European Commission contains a database of all legal support mechanisms for renewable energy of 28 member countries and 4 countries of the European Free Trade Association (EFTA countries).

1.3. Self-consuption parameters

The most important parameters of the normative on self-consumption are presented bellow:
- Income from self-consumed electricity. It may be for savings in the bill, or premium, or green certificates.
- Charges to finance the costs of distribution and transportation. This parameter indicates whether the self.consumer have to pay the costs of the network.
- Value of electricity excess. It may be the same price of electricity but reduced by charges or fees. This is what is called "net-metering". This is often described as some energy credits that can be used for a predefined period to reduce the bill. It may be a premium payment or green certificates regulated by legislation. In other instances it may consist in the payment of the price of wholesale market or even it could not be entitled to any payment and therefore it supposes an energy lose.
- Maximum period of time for compensation. It is the time period during which it compensates the energy injected into the network. It can be real-time, 15 minutes, an hour, a day, a month, or indefinitely.
- Geographical compensation. It indicates whether the consumption and generation can be compensated in different locations.
- Duration of regulation. It indicates the period of validity of the regulation of self-consumption.
- Third party rights. It indicates whether a third party is allowed to own generation facilities under leasing schemes, PPAs, etc.
- Limitations on the system size. Regulations often impose limit generation capabilities.

1.4. State of the art

After three years of discussion of all sectors involved, on October 9 2015, the Royal Decree 900/2015 was approved.
Lopez et al. [4] evaluated the profitability of investors in different segments with particular emphasis on charges for costs and system services ("backup charge") and the effect of financing costs. Three alternative regulations dealing with selling energy excess were analyzed: pure self-consumption, net metering, and net billing. The study results show that the regulation will restrict the dissemination of photovoltaic systems of self-consumption, and therefore net billing scheme is proposed, which promotes the dissemination of photovoltaic systems at minimal cost for the system. This scheme is recommended by the European Commission.
De Boeck et al. [1] conducted an evaluation of the regulation of photovoltaic systems in the residential sector of the main European markets (Flanders in Belgium, Germany, Italy, Spain, and France). The feasibility of using an investment based on discounted cash flows from the plant during its life cycle was studied. The results indicated that the system of Italy has been the most profitable of all countries surveyed since 2010. It also indicates that most regulations make investing in a photovoltaic installation in a home to be profitable except in the case of Spain.
Prior to the publication of Royal Decree under study, Talavera et al. [5] conducted a study of profitability of a photovoltaic system installed at the University of Jaen. Levelized Cost of Electricity (LCOE), a payback period of 17.5 years and an internal rate of return of 8.48% in the worst case were calculated. In addition to this, the analysis included a sensitivity analysis of the factors that influence the profitability of the systems, as the initial investment, photovoltaic production, additional fees, and changes in the price of the electricity market.
Rabaza et al. [6] conducted a feasibility study of a network connected to different oil mills photovoltaic systems in Andalusia (southern Spain). The results of this study contemplated a reduction in spending power between 2% and 37%.
Marin-Comitre [7] conducted a feasibility study of several photovoltaic systems in the region of Extremadura (Spain), which is a region with high levels of solar radiation. The results indicate that the consumption without selling surplus energy is not profitable in the domestic sector. Moreover, if the Spanish government aproves the charge for costs and services of the electrical system, profitability would be seriously damaged.
Garcia-Trivino [8] analyzed the feasibility of net metering scheme in small power systems in homes, considering that could help them be feasible. This study was conducted after the publication of two draft Royal Decrees of self-consumption by the Spanish Government.
Colmenar-Santos et al. [9] assessed the potential profitability of self-sufficiency of a house and concluded that self-sufficiency can be achieved at prices of energy discharged to grid below the Feef-in Tariffs (FITs), available at that time but eliminated in 2012 through renewable moratorium with Law 1/2012.

Dufo-Lopez and Bernal-Augustin [10] analyzed the first two drafts and two reports by the National Energy Commission (CNE), concluding that the PV system could be profitable under the first proposed regulation and not in the draft 2015 where a charge on the self-consumed electricity was included (backup charge). This work evaluated the profitability comparing the LCOE of a photovoltaic system under the regulations proposed in the reports with the net value of the purchase of electricity for a home located in Saragossa (Spain), where irradiation is close to the average from Spain.
This work assesses the Royal Decree 900/2015 of self-consumption by analyzing the feasibility of a solar photovoltaic system for three consumer profiles and two different climatic conditions in Spain. The profitability of these systems is valued by payback time, Net Present Value (NPV), and Internal Rate of Revenue (IRR). Besides, the incidence of the net metering scheme on the aforementioned economic parameters is valued.

2. ROYAL DECREE 900/2015

Royal Decree 900/2015 creates two types of self-consumers". Self-consumption type 1 must meet that the contracted power consumer does not exceed 100 kW, that the sum of generation installed power is equal to or less than the power contracted by the consumer, and the holder of the supply is the same as the one of the generation facilities. Therefore, the subject is legally considered as a mere consumer, and electricity injected to the grid is unpaid. Moreover, in self-consumption type 2 it must be satisfied that the sum of installed power generation is equal to or less than the power contracted by the consumer, and all generation facilities must have the same owner. In this case there are two legal subjects: consumer and producer. Therefore, the producer must become an entrepreneur and PV self-consumption is considered as an economic activity, which will be taxed. This does not recognize the net metering scheme nor the figure of the "prosumer". It is unlikely that a residential system becomes type 2 and sells electricity excess to the grid due to administrative barriers and the need to become an entrepreneur. Most often, thus, is that it becomes self-consumer Type 1 exporting surplus energy without receiving compensation. In many cases, in the commercial and industrial segment, they will become self-consumers type 2 thus being able to sell energy as any other producer- This sale is a wholesale market price and paying the grid-access charge (0.5€/MWh) and the generation tax (7%). In case that the contract is in medium or high voltage, requirements by distribution companies for connection are much higher.
Facilities of self-consumption type 1 with less than or equal to 10 kW contracted power and installing a device to prevent the instantaneous energy discharge, shall be exempt from costs of access study and conexion by the distribution company.
Self-consumption type 2 facilities that are hiring in medium or high voltage and install a device to prevent the instantaneous energy discharge shall also simplify the connection requirements (this is not contained in Royal Decree but in the distribution rules).
The Royal Decree establishes fees for costs and system services (backup charge) divided into two parts: on the one hand by the difference between application power positions and power to charge for the purposes of access fees (€/kW) and on the other hand the self-consumed electricity (€/kWh). In a simplified way we can say that the fixed charge shall apply only if the photovoltaic system has a storage element.
These costs and service charges of the electricity system depend on the type of rate and tariff period in which energy is self-consumed.
The facilities of self-consumption type 1 below 10 kW are exempt from the variable charges for self-consumed electricity.
Geographical compensation and self-consumption for several clients are not allowed. Compensation is in real time and the duration of the regulatory scheme is unlimited.

3. METHODOLOGY

The purpose of this work is to determine the profitability of an investment for a solar photovoltaic system of self-consumption at the time that this decision is taken. Retroactive adjustments are not taken into account since they are not known.
The main factors that determine the profitability of photovoltaic installations are weather conditions, consumption profiles, the rate of consumption and self-sufficiency, installation costs, and electricity prices.

3.1. Weather conditions

The annual average global solar radiation on a horizontal surface can range from about 1,220 kWh/m2 in Asturias up to 1,800 kWh/m2 in Andalusia [11], that is, there exists a difference of about 47%. Simplifying, for calculating the energy produced, it is to be considered that the photovoltaic system is mounted and oriented in the optimal way. Let us consider on the one hand the city of Oviedo (capital city of Asturias) with 1,210 kWh of electricity production (35° tilt and 0° azimuth) and Seville (capital city of Andalusia) with 1,600 kWh (33º tilt and 0° azimuth) according to database Climate-SAF PVGIS [12].

3.2. Consumption profiles

Three ordinary consumer profiles are considered:
- Housing of 2 people with job. As shown in Figure 1, Monday through Friday during business hours. 9: 00h - 19:00 there is only residual consumption due to the refrigerator and stand-by of appliances and electronic equipment. Saturday and Sunday electricity consumption exist throughout the whole day.
- Industrial Company nº 1. As shown in Figure 2, there is consumption Monday to Friday during business hours from 6:00-18:00 h. The rest of the time, including Saturday and Sunday, there is only a residual consumption of about 3.5 kW.

- Industrial Company nº 2. As shown in Fig 3, there is increased consumption from Monday to Friday during working hours (6:00-18:00 h) but the rest of the time, including Saturdays and Sundays, there is considerable consumption because of the cold rooms.

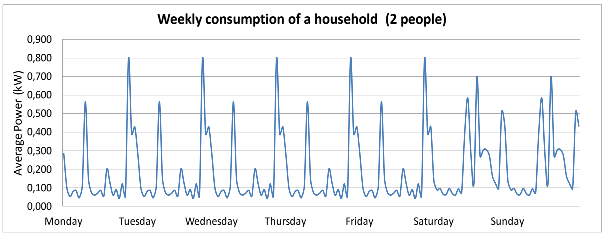

Fig. 1. Weekly consumption of a housing of two people

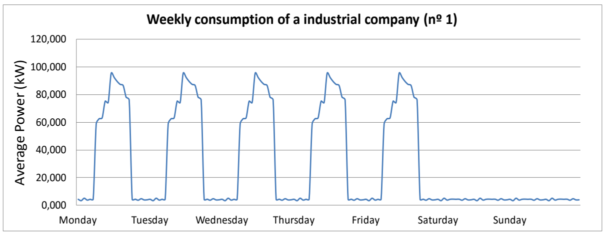

Fig. 2. Weekly consumption of industrial company nº 1

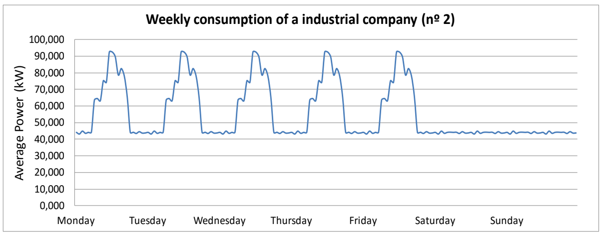

Fig. 3. Weekly consumption of industrial company nº 2

3.3. Self-consumption and self-sufficiency rates

These two rates are very important in the study of the feasibility and dependent consumption profile and the time curve of photovoltaic generation.

The self-consumption rate is the percentage of produced energy which is self-consumed. The self-sufficiency rate is the percentage of self-consumed energy in the total energy consumed.

The overall objective should be that these two rates are as high as possible.

3.4. Costs of photovoltaic solar system

System costs depend on its size and the execution way. For this study, conservative costs have been considered, estinating that the photovoltaic modules are installed in structure with optimal tilt and azimuth, and distance between photovoltaic modules, inverters, electrical panels and module counters are not excessive. A table of costs of facilities ranging from 1 kWp to 100 kWp has benn generated, which is summarized in Table 1. That table shows that in small powers, the costs of inverter, electrical panels and counter modules have much impact. As power increases the cost of photovoltaic modules increases, and therefore total cost decreases.

Table 1. Cost estimations of PV systems of different sizes (VAT not included)

Installation size (kWp)	Cost (€/kWp)
1	3,67
3	2,55
5	1,97
10	1,65
50	1,35
100	1,31

3.5. Electricity prices and charges

In this suty, housings have a tariff type 2.0A with 5kW contracted power, and companies nº 1 and nº 2 have a tariff 3.0 A with 100 kW contracted power. Electricity prices considered for the study are as shown in Table 2.

Table 2. Prices of electricity (VAT not included)

	Tariff period P1 (€/kWh)	Tariff period P2 (€/kWh)	Tariff period P3 (€/kWh)
Housing	0,1210	-	-
Company nº 1 and nº 2	0,1204	0,0996	0,0709

For the housing feasibility study it is taken into account the 21%VAT because it is owned by a person. In the case of the two companies it is not taken into account because this tax is compensated.

As seen in that table, the Royal Decree 900/2015 establishes fees for costs and system services (backup charge) that can be fixed or variable. As the facilities do not have storage elements, it is considered that there are no fixed charges. The housing of this study is exempt from variable charge because its contracted power is less than or equal to 10 kW. Therefore variable charges considered according to Royal Decree are the ones shown in table 3.

Table 3. Variable charges according to Royal Decree 900/2015

	Tariff period P1 (€/kWh)	Tariff period P2 (€/kWh)	Tariff period P3 (€/kWh)
Housing	0,000000	-	-
Company nº 1 and nº 2	0,029399	0,019334	0,011155

3.6. Economic model

The total costs of a photovoltaic system consist of three elements:

-Initial Investment: Composed of the sum of net investment cost and applicable VAT (only applicable in the case of housing, as previously seen). These two costs depend on the capacity of the facility.

$$C_{inv} = C_{net} \times (1 + VAT)$$

-Cost of inverter replacement. It is considered that the replacement of the inverter is held at half the lifetime of the system and therefore the value is deducted in year 12 [13],

$$C_{replace} = \frac{CAP \times replaceC}{(1+d)^{12}}$$

being *CAP* the system size in kWp, *replaceC* the cost of replacing the inverter kWp and *d* the discount rate.

The discount rate applicable to an investment is dependent on the rate of long-term inflation and investment risk in the country. In our case, in Spain, 5% will be considered [14].

- Present value of the total annual cost of maintenance and insurance,

$$C_{main\&insu} = m \times C_{net} \times \frac{1-(1+d)^{-25}}{d}$$

where m is considered equal to 1% and consists of the sum of annual maintenance cost of 0.5% and an annual insurance cost of 0.5%.

The first type of income of a photovoltaic system is through a direct payment via premium (feed-in tariff),

$$Rev_{FIT} = \sum_{i=1}^{I} \frac{FIT \times [(1-s) \times ((Y \times CAP)(1-(i-1)l))]}{(1+d)^{i}}$$

where FIT is the money received for each kWh fed into the grid, s is the ratio of consumption, Y is the production of photovoltaic electricity kWp, i is the number of year, I the number of years of the scheme after investment, and l is the degradation of the photovoltaic module. In this study, this term is not taken into account.

The second type of income is a direct payment through a green certificate,

$$Rev_{GC} = \sum_{i=1}^{I} \frac{GC \times \frac{((Y \times CAP)(1-(i-1)l))}{1000}}{(1+d)^{i}}$$

being GC the price at which users of the PV plant can sell their certificates per 1,000 kWh production. This term is negligible in the self-consumption facilities discussed in this article, and therefore it is not taken into account.

The third entry is a direct payment by tax deduction,

$$Rev_{TD} = \sum_{j=1}^{J} \frac{\frac{t \times C_{net}}{j}}{(1+d)^{j}}$$

being J the period during which tax deductions are active, and t is the percentage of the investment that can be deducted. In this type of facilities in Spain, it does not exist a national tax deduction, and therefore it is not taken into account.

The fourth entry is a savings bill for consumption, because there is less demand on the power grid,

$$Rev_{Selfc} = \sum_{n=1}^{25} \frac{[(Y \times CAP)(1-(n-1)l)] \times s \times [P_1(1+g)^{n-1} + Z]}{(1+d)^{n-1}}$$

where n is the year of operation, $P1$ the price of electricity, g the annual increase in electricity price, and s is the consumption rate. Z represents potential incentives to self-consumption.

Finally, the net-metering scheme is modeled. If the energy fed into the grid is less than the electricity purchased from the network,

$$Rev_{NetMetering} = \sum_{n=1}^{25} \frac{Efed_n \times r_n}{(1+d)^{n}}$$

$$Efed_n = (1-s) \times ((Y \times CAP)(1-(n-1)l))$$

where $Efedn$ is energy injected into the grid and rn is the rate of reimbursement for it. This formula will be introduced in an alternative model to the existing Royal Decree 900/2015.

If fed into the grid power is greater than the amount of power purchased from the grid, all the energy is bought with rn rate, and in some countries such as Italy it may receive a rate hn by injection excess compared to the acquired power.

$$Rev_{Netmetering} = \sum_{n=1}^{25} \frac{(Edrawn_n \times r_n) + [(Efed_n - Edrawn_n) \times h_n]}{(1+d)^{n}}$$

$$Edrawn_n = U - ((Y \times CAP)(1-(n-1)l))s$$

where $Edrawnn$ is the energy acquired from grid and U is the annual energy consumption. This formula is not taken into account.

The first parameter of performance is the payback period, which indicates the number of years required to recover the investment. From the economic point of view it is an imprecise parameter since it does not account for the value of money and does not account for income once the initial investment is recovered. Anyway it is the most understandable and simple concept for homeowners.

The second parameter is the net present value and gives a more accurate view. It calculates the total return on investment through its life cycle taking all incoming and outgoing cashflows. Future cashflows are discounted in order to represent the present value of money.

The third parameter is the internal rate of return. It is a percentage value for which the net present value of all cash flows resulting from investment is zero. If the internal rate of return is higher than the discount rate, investment worthwhile.

4. RESULTS AND DISCUSSION

Figure 4 shows the adaptation of the housing consumption curve with the horly curve of average daily production of electrical energy from a solar photovoltaic installation of 1 kWp in Seville and Oviedo. The curve of electricity production is displayed for July (maximum) and December (minimum).

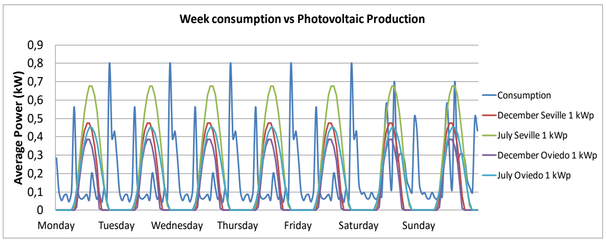

Fig. 4. Weekly consumption of housing vs photovoltaic production with 1 kWp installation, in two months and two different locations

As can be seen, the hours of maximal production of electrical energy coincide with the hours of lest consumption. This suggests that it can be interesting to introduce a system of energy storage and/or demand management system, but this is not the subject of this study. Table 4 shows the results of a simulation with various ranges of photovoltaic power in Seville.

Tolls are not considered because the contracted power is less than 10 kW. It is clear that with Royal Decree 900/2015 makes not viable photovoltaic systems in housings with this profile of consumption. With a self-consumption system of 1 kWp, only 36.31% of the power generated will be self-consumed, and the rest (63.69%) will be injected to the network without any remuneration. As a result, values have negative NPV and payback period exceeding 25 years. If the power of the PV system is increased, the rate of self-consumption and self-sufficiency hardly increases, and therefore the economic results worsen.

Power (kWp)	IRR (%)	NPV (€)	Payback (years)	Self-Consumption	Self-sufficiency
1	-	-3.630	> 25	36,31%	35,49%
2	-	-5.526	> 25	20,01%	39,12%
3	-	-7.595	> 25	13,58%	39,81%
4	-	-9.779	> 25	10,32%	40,33%
5	-	-12.214	> 25	8,32%	40,67%

Table 4. Simulation of photovoltaic installation of a housing in Seville according to Royal Decree 900/2015

A simulation has been developed with a net metering model with a payment of reimbursement for electricity fed into the grid (rn) whenever the poured energy into the grid is less than the acquired network Table 5).

Power (kWp)	IRR (%)	NPV (€)	Payback (years)	Self-Consumption	Self-sufficiency
1	5,74%	27	16	36,31%	35,49%
2	1,26%	-2.924	22	20,01%	39,12%
3	-0,57%	-5.023	>25	13,58%	39,81%
4	-1,98%	-7.229	>25	10,32%	40,33%
5	0	-9.679	>25	8,32%	40,67%

Table 5. Simulation of PV housing in Sevilla with net-metering

Results improve, but not enough to make the investment viable. The best system is theone of 1 kWp. As the power is increased, more energy is generated annually than is consumed and therefore energy excess is injected to network without any compensation.
It could be thought therefore that to achieve viability with this type of consumption profile it is necessary a primed tariff (FIT) with a value above the market, or, similarly as in the Ilatian case, an *hn* rate for the energy excess to the grid compared to the acquired. Table 6 shows the results with Royal Decree 900/2015 in Oviedo.

Table 6. Simulation of photovoltaic installation in housing in Seville according to Royal Decree 900/2015

Power (kWp)	IRR (%)	NPV (€)	Payback (years)	Self-Consumption	Self-sufficiency
1	-	-3.772	> 25	42,91%	31,99%
2	-	-5.566	> 25	25,58%	38,13%
3	-	-7.626	> 25	17,46%	39,04%
4	-	-9.806	> 25	13,30%	39,66%
5	-	-12.234	> 25	10,78%	40,17%

Results are worse compared to Seville. The rate of self-consumption increases because there are fewer photovoltaic production but the self-sufficiency rate decreases. Table 7 presents the results with net metering in Oviedo.

Table 7. Simulation of photovoltaic installation housing in Seville with net-metering

Power (kWp)	IRR (%)	NPV (€)	Payback (years)	Self-Consumption	Self-sufficiency
1	3,39%	-1.272	19	42,91%	31,99%
2	1,26%	-2.922	22	25,58%	38,13%
3	-0,56%	-5.021	26	17,46%	39,04%
4	-1,97%	-7.228	26	13,30%	39,66%
5	0	-9.678	26	10,78%	40,17%

The results worsen in economic terms over Sevilla. Figure 5 shows the rate of self-consumption and self-sufficiency in terms of the power of the photovoltaic solar installation in the company nº 1 in Seville.

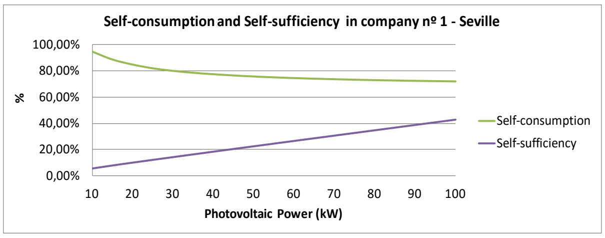

Fig. 5. Self-consuption and self-sufficiency in industrial company nº 1 in Seville

As the system size of the PV increases, the rate of self-consumption decreases in an important way among other factors because Saturday and Sunday there are only residual consumption.
Figure 6, Figure 7 and Figure 8 show the simulation of economic parameters with charges related to the costs and services of the system (according to Royal Decree 900/2015) and without charge.

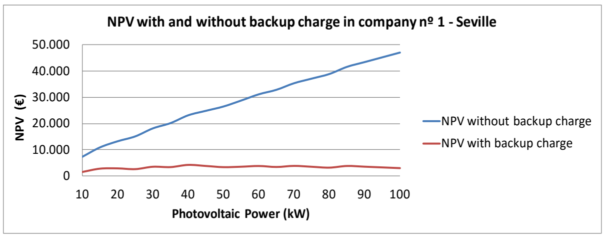

Fig. 6. NPV NPV of photovoltaic installation of self-consumption in industrial company nº 1 in Seville according to Royal Decree 900/2015 (with charges) and without charge

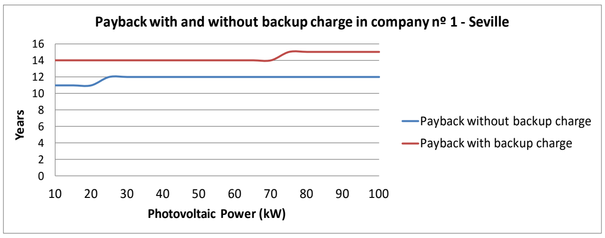

Fig. 7. Payback time consumption of photovoltaic installation in industrial company nº 1 in Seville according to Royal Decree 900/2015 (with charges) and without charge

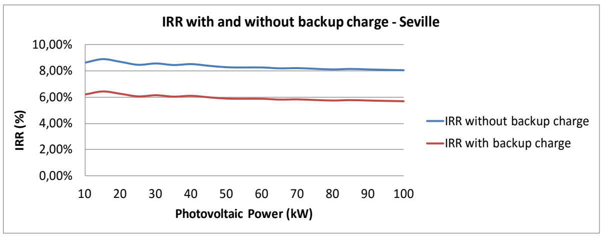

Fig. 8. IRR of photovoltaic installation of self-consumption in industrial company nº 1 in Seville according to Royal Decree 900/2015 (with charges) and without charge

With the application of charges the NPV is practically constant in all powers with a slight negative slope. This is because although the cost per kWp decreases as increases in power, it is offset by the decrease in the rate of consumption. The payback period is 14 years until 70 kW, and from there up it is 15 years. The IRR starts at 6.23% and remains more or less constant with a slight negative slope to reach 5.72% at 100 kW. Therefore solar photovoltaic self-consumption, according to Royal Decree 900/2015, for companies that only have a residual consumption during the weekend, have a very fair return.
Demand management could be interesting to increase the rate of self-consumption, but is not the subject of this study.
If no charges are considered, the NPV shoots-up as the power of the PV system increases, while the payback period and IRR follow parallel paths. The payback period improves between 2 and 4 years, resulting between 10 and 12 years depending on the power and IRR improves around 2 percentage points. This suggests that therefore simply removing charges can make these investments viable.
However, results varie in next Figures with the same case simulated with charges but with net metering to compensate for the energy produced on Saturday and Sunday.

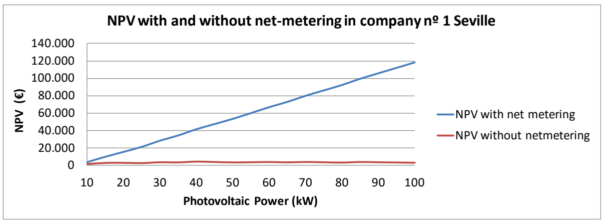

Fig. 9. NPV of photovoltaic installation of self-consumption in industrial company nº 1 in Seville according to Royal Decree 900/2015 (with charges) and net metering

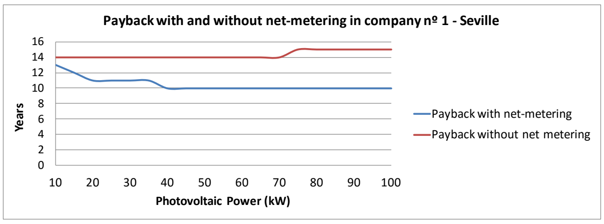

Fig. 10. Payback of photovoltaic installation of self-consumption in industrial company nº 1 in Seville according to Royal Decree 900/2015 (with charges) and net metering

It can be seen how the NPV with net-metering shoots-up compared to that achieved with Royal Decree 900/2015. The payback period decreases 1 year with a power of 10 kWp, but as power increases, and therefore the rate of self-consumption decreases, this difference grows, until achieving five years of difference in 100 kWp. That would mean 10 years of payback.

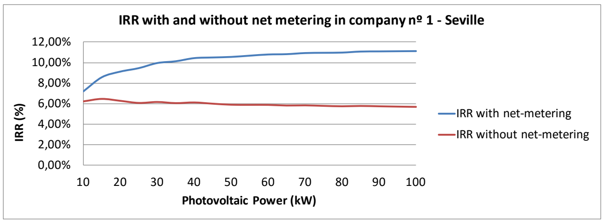

Fig. 11. IRR of PV installation of self-consumption in industrial company nº 1 in Seville according to Royal Decree 900/2015 (with charges) and net metering

Regarding the IRR, in 10 kWp there is only a difference of 1% but as the power increases, the difference increases up to a difference of about 4.5%. The IRR reaches 11.11% in 100 kWp, which results very interesting.
Now the photovoltaic solar system of company nº 2 in Seville will be analyzed.

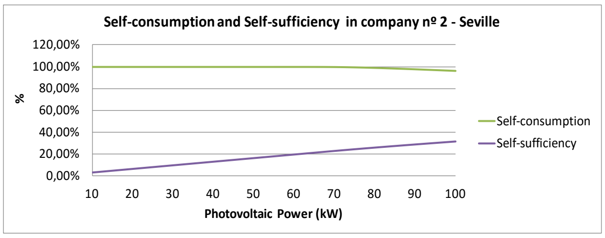

Fig. 12. Self-consumption and self-sufficiency of PV installation of self-consuption in industrial company nº 2 in Seville

In this case (Figure 12) the consumption is almost 100% since there is a significant consumption 24 hours 365 days a year due to cold storage. It just seems to go down something when reaching 80 kWp. The self-sufficiency rate rises in proportion to the increase in power. Figure 13, Figure 14 and Figure 15 show respectively NPV, IRR and payback period of the company nº 2 in Seville with and without charge.

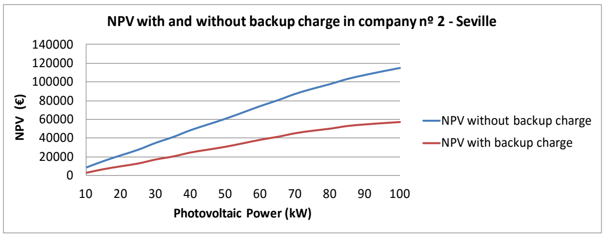

Fig. 13. NPV of self-consumption PV installation in industrial company nº 2 in Seville according to Royal Decree 900/2015 (with charges) and without charge

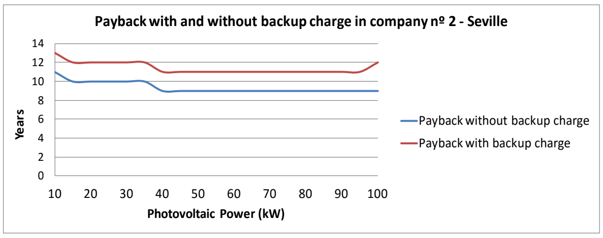

Fig. 14. Payback of of self-consumption photovoltaic installation in industrial company nº 2 in Seville according to Royal Decree 900/2015 (with charges) and without charge

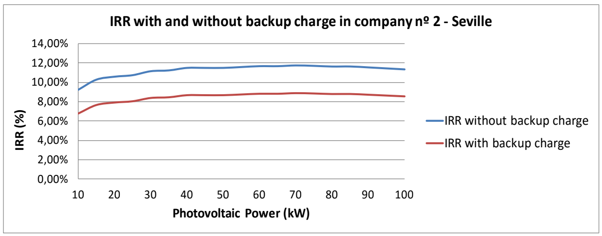

Fig. 15. IRR of self-consumption photovoltaic installation in industrial company nº 2 in Seville according to Royal Decree 900/2015 (with charges) and without charge

Now the NPV is incrementing in both cases, because if the power is increased the rate of consumption is almost equal to 100%. Best NPV is achieved in the case of not having charges.
The payback period is represented by two parallel lines with a distance of 2 years. With charges the payback period is about 11 years, and without charge it is about 9 years.
The IRR with and without charge are two parallel lines with a difference of 3%. A maximum of 11.70% and 8.90% can be reached, with an output of 70 kWp.
In this case the net metering regulatory scheme does not provide a significant improvement because all the energy is consumed.
Finally the effect of less solar radiation will be analysed observing Oviedo results.

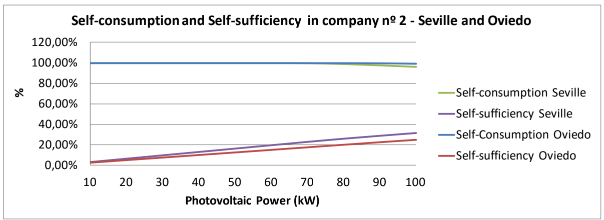

Fig. 16. Self-consumption and self-sufficiency of photovoltaic installation of self-consumption in industrial company nº 2 in Seville and Oviedo.

The rate of self-consumption is similar, except from 80 kWp where self-consumption is higher in Oviedo, because electricity production is lower. Regarding self-sufficiency, it is clear that the increase in the rate of self-sufficiency in Seville is greater, because electricity production is higher. Figure 17, Figure 18, and Figure 19 present NPV, Payback, and IRR respectively.

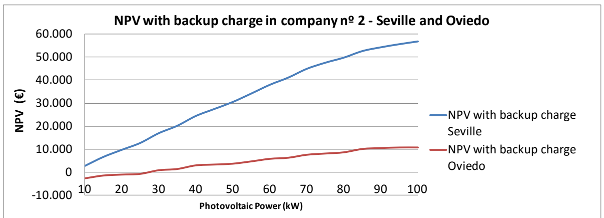

Fig. 17. NPV of self-consumption photovoltaic installation in industrial enterprise nº 2 according to Royal Decree 900/2015 (with charges) in Seville and Oviedo.

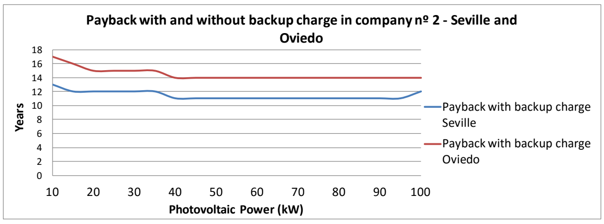

Fig. 18. Payback of photovoltaic installation of self-consumption in industrial enterprise nº 2 according to Royal Decree 900/2015 (with charges) in Seville and Oviedo.

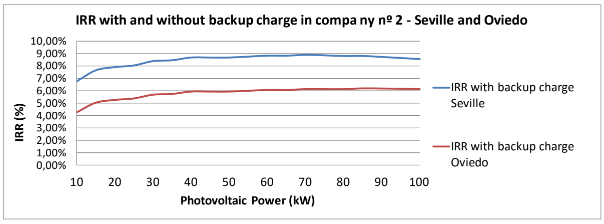

Fig. 19. IRR of self-consumption photovoltaic installation in industrial company nº 2 according to Royal Decree 900/2015 (with charges) in Seville and Oviedo.

NPV is much greater in Seville and the payback may present average differences of 3 years. Oviedo presents a minimum payback of 14 years.
The IRR are two parallel lines with a gap between them of about 2.5%. Therefore, IRR in Oviedo is about 6%, which is a very fair rate.
Therefore the weather affects strongly the investment profitablility, and for instance a profitable system in Seville can be unprofitable in Oviedo.

5. CONCLUSSIONS

This article has analyzed the impact of Royal Decree 900/2015 on the profitability of a photovoltaic solar system of self-consumption for three consumer different profiles and two climatic conditions.
In the case of housing in Seville with 2 people working, is not profitable in any case because the rate of consumption is very low.
The period of the day on which the photovoltaic production is higher is precisely when less energy is consumed. It is estimated that the payback period can be more than 25 years. Even with a net metering scheme limited to the case of energy transferred being than or equal to the acquired network, it does not give a very interesting payback (16 years).
It is estimated that for an interesting investment it is necessary a scheme of self-consumption with FIT rate with a value above the market price or *hn* rate by excess to the grid compared to acquired power.
In addition installation of storage elements or load management systems could be assessed, especially in homes with more consumption.
In Oviedo, with electricity production 24% lower than in Seville, results a considerably worse.
In the case of industrial company nº 1 in Seville, which does not work Saturdays or Sundays or has significative

consumption 24 hours, the results of profitability with Royal Decree are very fair (about 14 years of payback and 6% IRR). Especially relevant are charges associated to costs and services of the system, which impact in a negative way. Without charges a payback of approximately 12 years and 8% IRR could be obtained. Therefore, the charges decrease by 2 years payback and 2 percentage points IRR. As a result, a net-metering scheme could have a very positive influence on this facility compared to the current Royal Decree, providing an average of four years less of payback and 4 percentage points more of IRR.
Finally, results shown that the industrial company nº 2 in Sevilla, with has 24 hours a day, 365 days a year consumption of importance, presents the best economic results obtained. It can reach about 9% IRR and 11 years payback, which are interesting results. Anyway, if there were no charges, 3 years less payback and 3% more of IRR would be obtained. Oviedo worsens results in a very important manner with a payback of 14 years and an IRR of 6%.

REFERENCES

[1] L. De Boeck, S. Van Asch, P. De Bruecker, A. Audenaert. Comparison of support policies for residential photovoltaic systems in the major EU markets through investment profitability. Renewable Energy 87 (2016) 42-53.

[2] IEA PVPS TASK 1- Review and analysis of PV self-comsumption policies. (2016).

[3] Renewable energy policy database and support legal sources on renewable energy http://www.res-legal.eu/home/

[4] Javier López Prol, Karl W Steininger. Photovoltaic self-consumption regulation in Spain: profitability analysis and alternative regulation. Graz Economics Papers 2015.07.Stability analysis and alternative regulation schemes. (2015)

[5] D.L. Talavera, J. de la Casa, E. Muñoz-Cerón, G. Almonacid. Grid parity and self-consumption with photovoltaic systems under the present regulatory framework in Spain: The case of the University of Jaén Campus. Renewable & Sustainable Energy Volumen: 33 (2014) Páginas: 752-771.

[6] Rabaza, Ovidio ; Contreras-Montes, Jesus Garcia-Ruiz, Maria ; Delgado-Ramos, Fernando; Gomez-Lorente, D. Techno-Economic Performance Evaluation for Olive Mills Powered by Grid-Connected Photovoltaic Systems. Energies (2015)

[7] Marin-Comitre, Ubaldo; Anastasio Mulero-Diaz, Angel ; Miranda Garca-Cuevas, Maria Teresa. Feasibililty analysis of photovoltaic facilities for household electricity self-consumption in Extremadura. Dyna. Volumen: 89 Número: 4 (2014) Páginas: 413-421

[8] Garcia-Trivino, Pablo; Llorens-Iborra, Francisco; Garcia-Pichardo, Eloy; Andres Garcia-Vazquez, Carlos; Miguel Fernandez-Ramirez, Luis. Economic viability of small power photovoltaic facilities for dwellings by using the net metering mode. DYNA (2014) Volumen: 89 Número: 2 Páginas: 229-235

[9] Colmenar-Santos, Antonio; Campinez-Romero, S; Perez-Molina, Clara; Castro-Gil, Manuel. Profitability analysis of grid-connected photovoltaic facilities for household electricity self-sufficiency. Energy Policy. Volumen: 51 (2012) Páginas: 749-764

[10] Dufo-López and Bernal-Agustín. A comparative assessment of net metering and net billing policies. Study cases for Spain. 2015. Energy 84 (2015):684-694.

[11] Marcel Šúri, Thomas Huld, Ewan D. Dunlo1, Michel Albuisson, Mireille Lefèvre, Lucien Wald. Uncertainties in photovoltaic electricity yield prediction from fluctuation of solar radiation. Proceedings of the 22nd European Photovoltaic Solar Energy Conference, Milano, Italy 3-7.9.2007.

[12] Photovoltaic Geographical Information System (PVGIS). European Commission, Joint Research Centre, Institute for Energy and Transport (IET). http://re.jrc.ec.europa.eu/pvgis/

[13] R. Haas, G. Resch, C. Panzer, S. Busch, M. Ragwitz, A. Held, Efficiency and effectiveness of promotion systems for electricity generation from renewable energy sources - Lessons from EU countries, Energy 36 (2011), 2186-2139.

[14] Creara Energy Experts. Pv Grid Parity Monitor. Residencial Sector 3rd issue (2015).

BUILDING STRUCTURE MODELS. IMPACT ON CUMULATIVE ENERGY DEMAND AND CARBON FOOTPRINT

Esteban Fraile-García[(a)], Javier Ferreiro-Cabello[(b)], Francisco J. Marrodán-Esparza[(c)], Emilio Jiménez-Macías[(d)]

[(a,c)] University of La Rioja (Spain), Department of Mechanical Engineering
[(b)] Qualiberica SL., and University of La Rioja (Spain), Department of Mechanical Engineering
[(d)] University of La Rioja (Spain), Department of Electrical Engineering

[(b)] javier.ferreiro@unirioja.es , [(a)] esteban.fraile@unirioja.es , [(c)] francisco.marrodan@unirioja.es , [(d)] emilio.jimenez@unirioja.es

ABSTRACT
This paper assesses the impact of the arrangement of pillars and building height and its effect on the environmental impacts for the structural solution. Impacts are analyzed in the elements of the structure: foundations, pillars, and slabs. By embodied energy and carbon footprint, both, the manufacturing process of materials and the process of implementation of the proposed structure are measured. The results are obtained per executed square meter. The analysis provides the optimal arrangement for the pillars and the height of the building; the increase in separation of the pillars causes greater impacts, and the design of tall buildings also drives to an important increase of resource consumption.

Keywords: Reinforced concrete. Cumulative energy demand (CED). Carbon footprint. Building structure models.

1. INTRODUCTION
Today's society is fully aware of the need to limit the environmental impacts. The activities to be carried out in industrial processes are responsible for unavoidable environmental impacts. Building projects have a long implementation time and imply a series of necessary activities for their implementation. This work focuses on assessing the environmental impacts of different structural solutions through the use of reinforced concrete.
Building activities using reinforced concrete has its own characteristics. On the one hand it is necessary to know the amounts of the materials incorporated permanently in the structural solution. These materials mostly consist of reinforcing steel and structural concrete. In addition, to favor the construction process, a series of auxiliary materials for the forms are required on the construction site, which are also consumed. This work focuses on the valuation of both groups of materials and the corresponding impact generated.
The life cycle analyses present an important number of indicators. For this work we opted for two very representative indicators: embedded energy and carbon footprint. These two variables have been used in previous studies as indicators in scientific and technical literature. Both will be used to estimate both, the impacts generated in the manufacture of materials, and the construction of the project structure. To assess the execution of the structure, an average distance from the fixed manufacturing facilities to the location of the work has been estimated.
The impact of manufacturing and construction phases in structures dedicated to residential buildings are representative today, as the use phase represents zero impact. In the future, if the objectives of achieving virtually zero consumption buildings are reached, these two phases will record most of the impact generated by the buildings.
The number of columns or supports and the building height have been considered as representative geometric variables in defining building. For the structural solution of the floors a bidirectional slab of recoverable coffer with a constant structural depth of 30 centimeters has been implemented. The paper presents a range of solutions and assesses the impacts generated by each proposal. These impacts have been divided into two phases: production phase of the necessary materials in fixed industrial installations and transportation, and construction phase at the location of the work.

2. METHODOLOGY
The proposed methodology focuses on assessing the environmental impact incurred in the process of building a reinforced concrete structure. This paper assesses the entire structure, including the foundation. For horizontal reticular structure of recoverable coffer and 80 centimeters interaxis is used. All structural elements are made in reinforced concrete. Prefabricated elements are not used, and assembly operations are developed in the work area but with the support of a fixed industrial facility of steel. Thus, materials permanently incorporated into the structure are only two in this case: B-500S steel and HA-25/P/20/IIa concrete.
To execute these structures, once consolidated the pillars, a provisional structural framework of floorboard is used to hold the caissons (Figure 1). Once the

structure is consolidated, these elements are retrieved and used in subsequent structures.

Figure 1 Provisional floorboard framework.

Obviously the environmental impact associated with the implementation of a structure will be lower when the material consumption is optimized (reducing the amounts of concrete and steel) as well as the use of formwork materials and labor.

This research is to model a building of square floor of dimensions 24x24 meters with different column layouts and number of floors (Figure 2). For the column layout three values of the grid have been selected: a situation of short span of 4x4 meters, another common situation in building of 6x6 meters, and an alternative with overhead span of 8x8 meters. The modeled cases include 4 slabs, 6 slabs, 8 slabs, and 10 slabs. The buildings all have a height on the ground floor of 4 meters and the other floors with heights of 3 meters, devoting the last floor to a flat roof.

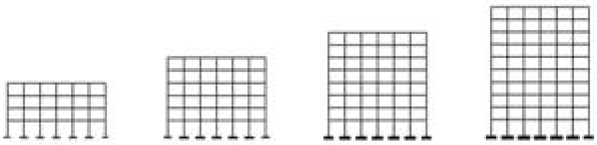

Figure 2 Section of buildings from 4 to 10 slabs 10.

The loads considered are selected from the usual building, based on the guidelines of the Technical Building Code (CTE) of Spain. In this way, facade loads are modeled as uniform loads, with a value of 7 kN/m in the perimeters of the slabs, and on the deck this value is reduced to 3kN/m. For surface loads on the various intermediate levels, 2kN/m2 have been estimated for permanent loads and also 2kN/m2 for use overload; in the flat desk these values have changed to 3 kN/m2 for permanent loads and 1kN/m2 for use overload. Wind loads have been implemented considering the Spanish legislation and snow loads are included in overload considered in use. For foundation dimensioning, an average performance of land bearing capacity has been considered, with a maximum permissible pressure of 0.2 N/mm2.

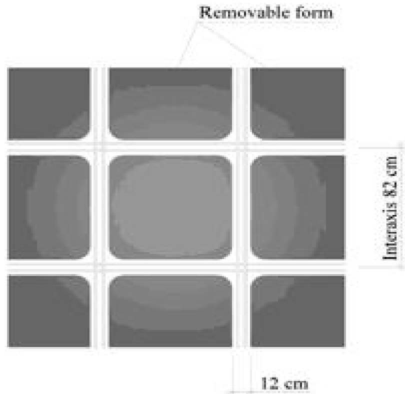

Figure 3 features of the selected slab

All the slabs have been solved using a structural depth of 30 centimeters (25 cm of caisson plus 5 cm of compression layer) and 80 centimeters of interaxis, 12 centimeters of nerve width, and constant coating (Figure 3). Thus the weight of the implemented slab is 4.03 kN/m2. This weight and dimensions are common in the structures of residential buildings and parking.

The structural analysis was carried out following the Spanish legislation and using a structural calculation software tool: CYPECAD. This structural analysis provides data relating to the consumption of materials, which in the selected typology represent the significant values to be used for the comparison. By using a construction database that is implemented in the own CYPECAD the impacts generated by each material used for the execution of each of the items are obtained. The phases covering this LCA range from cradle to grave. The reinforced concrete structure during the use phase does not require maintenance or energy inputs. The future regulation, which imposes almost zero consumption buildings, drives the focus to the impacts generated in the production phase. In the case of in situ concrete structures of this study we focus on the A1-A2-A3 and A4-A5 phases. The identification of the phases and scope of this study can be seen in Table 1.

The structure is divided into three sections: foundation, columns and slabs, following the construction process.

For the case of foundation four representative items are set: square meters of framework for foundation, cubic meters of cleaning concrete, cubic meters of structural concrete, and kg of reinforcing steel. Data of the considered steps are observed in Table 2. For cleaning concrete, a thickness of 10 centimeters and shrinkage in the execution of 5% have been considered. Columns consist of the materials used for formwork (considering 50 applications), structural concrete, and reinforcing steel. In the case of slabs, in addition to the materials permanently incorporated to the structure (steel and concrete) it is considered the materials used for the total framework and the recoverable caissons. In the case shown in the table, a repercussion of a caisson per square meter has been estimated, with fifty uses. For the proportional part of the materials used in the construction process the impact generated in its manufacture is also recorded.

Table 1 Considered phases of the LCA

	Product Stage			Construction process Stage		Use Stage							End of life Stage				Supplementary information beyond building life cycle
	Raw material supply	Transportation	Manufacturing	Transportation	Construction-installation process	Use	Maintenance	Repair	Replacement	Refurbishment	Operational energy	Operational water	De-construction demolition	Transportation	Waste processing	Disposal	Reuse-Recovery-Recycling Potential
	A1	**A2**	**A3**	**A4**	**A5**	**B1**	**B2**	**B3**	**B4**	**B5**	**B6**	**B7**	**C1**	**C2**	**C3**	**C4**	**D**
CYPE	X	X	X	X	X												

Table 2 Impacts of representative items.

			A1-A2-A3 Production of the materials used		A4 Transport Construction Zone A5 Placement and Execution.	
			Embodied energy (MJ)	Emissions CO_2 eq.(kg)	Embodied energy (MJ)	Emissions CO_2 eq.(kg)
m² framework for foundation	Materials	Weight (kg)				
	Steel	1,14	39,900	3,192	0,080	0,006
	Galvanized steel	0,05	1,950	0,140	0,017	0,001
		Auxiliary elements			0,081	0,012
		Transport to landfill			0,046	0,003
		Total:	**41,850**	**3,332**	**0,224**	**0,022**
m³ cleaning concrete in foundation	Materials	Weight (kg)				
	Concrete	2.300	2392,000	224,848	40,848	3,019
		Auxiliary elements			0,027	0,004
		Transport to landfill			0,106	0,008
		Total:	**251,160**	**23,609**	**42,114**	**3,133**
m² framework for m³ of columns	Materials	Weight (kg)				
	Steel	14,222	497,770	39,822	4,793	0,355
		Auxiliary elements			0,231	0,033
		Transport to landfill			1,643	0,122
		Total:	**497,770**	**39,822**	**6,670**	**0,510**
m² framefork for slab	Materials	Weight (kg)				
	Wood	0,599	1,797	0,052	0,027	0,002
	Plastic and steel	10,475	36,663	5,427	2,134	0,159
		Gasoil			10,488	0,776
		Auxiliary elements			0,108	0,016
		Transport to landfill			0,685	0,051
	Total:	**11,07**	**38,460**	**5,479**	**13,442**	**1,004**
m³ concrete	Materials	Weight (kg)				
	Concrete	2.530	2.631,200	247,333	44,931	3,325
	Total:	**2.530**	**2.631,200**	**247,333**	**44,931**	**3,325**
kg steel B500S for reinforc.	Materials	Weight (kg)				
	Steel	1,1	35,000	2,800	0,337	0,025
	Total:	**1,1**	**35,000**	**2,800**	**0,337**	**0,025**

These results combined with consumption impacts allow us to obtain the full impacts of the proposed solutions. Two different consumptions are made, the materials incorporated permanently to the structure and materials consumed in execution. Table 3 identifies the items that are consumed in each block with the units used.

Table 3 Items incorporated for each block of the structure

	Items	Units
Fundation	Cleaning Concrete foundation HL-15/P/20	m^3
	Reinforcing steel B 500 S	kg
	Concrete HA-25/P/20/IIa	m^3
	Framework for fundation	m^2
Columns	Framework for columns	m^2
	Reinforcing steel B 500 S	kg
	Concrete HA-25/P/20/IIa	m^3
Slabs	Framework for slabs	m^2
	Reinforcing steel B 500 S	kg
	Concrete HA-25/P/20/IIa	m^3
	caissons	Ud

3. OBJECTIVE

The focus is to have a vision of the environmental cost of the entire structure using two indicators: the embodied energy and the generated carbon footprint. The inclusion of two variables that change will allow to compare different alternatives and select the one that is most feasible from an environmental standpoint.

The inclusion of variations in the geometry of the building (arrangement of the columns and building height) allows us to observe the impacts generated in the different proposals. To facilitate monitoring the impact generated, the structure has been divided into three blocks with different treatment. The foundation with four corresponding headings: cleaning concrete, steel foundation, structural concrete, and formwork. The columns with: formwork, structural concrete, and reinforcing steel. And finally slabs, in which the definition of the form and the materials must be incremented with the placement and rental of the caissons.

4. CASESTUDY

Performing calculations by regulations currently in use in Spain the technically viable alternatives are determined. Steel, concrete and auxiliary elements (formwork and caissons) at different values for each block of the structure are found for the viable alternatives. The model analysis allows to control the deformations and adjust the arrangement of the reinforcements, all rigorously complying with current regulations.

Once data consumption are known and the impacts of each item are established, we can determine the environmental cost of each alternative. Obtaining the impact through two indicators (CED and CO2 equivalent) and in two distinct phases (production of necessary materials, and transport / placement / execution on site) requires us to present the results in four figures. Figures 4 and 5 show the corresponding phase production of materials (A1-A2-A3) displaying the corresponding impact to each of the blocks studied (foundation, columns and slabs).

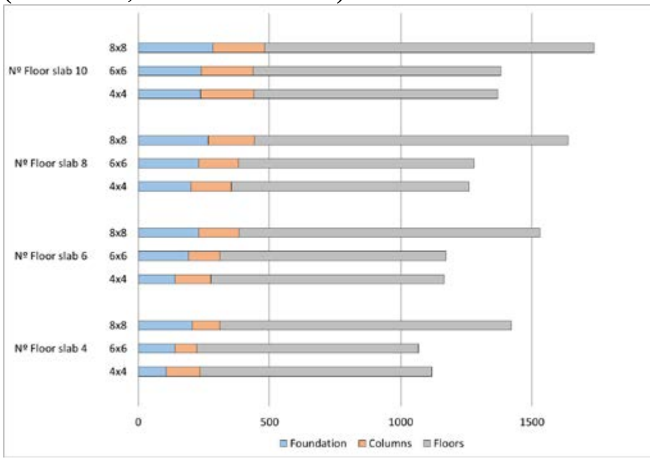

Figure 4 Embodied energy for the manufacture of materials (MJ/m2).

In order to compare the results, the ratio for each square meter of structure has been obtained. Values corresponding to the CED range from 1066.75 to 1735.97 MJ / m2 which is a variation of 62.73%. If we look at each of the blocks, biggest oscillation occurs in the foundation, with 165.01%, and the lowest in the slabs, with a total of 48.69% variation. The most attractive option is found in a building of four floors and with the grid of 6x6 meters. In this case the foundation represents 13.04%, columns 7.81%, and slabs the 79.15%, presenting the absolute minimum in the last two blocks.

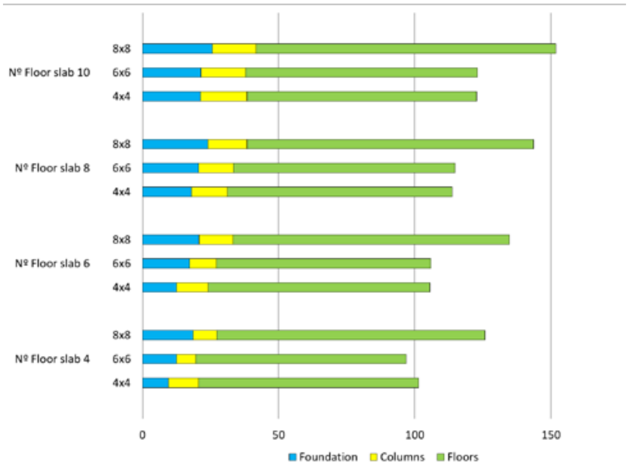

Figure 5 CO2 emissions for the manufacture of materials (kg CO2 Eq/m2).

For the ratio of equivalent CO2 emissions, results vary from 96.76 to 151.70 kg CO2 Eq/m2 which is a variation of 56.78%. The variation in emissions is lower than in embodied energy. If we look at each of the blocks, the biggest is again in foundations with 166.74%, and the lowest in slabs, with a total variation of 42.61%. The most attractive option is located again by a solution of four floors and with the grid of 6x6 meters. In this case the foundation represents 12.96% columns 7.31%, and slabs 79.73%.

Figures 6 and 7 show the corresponding phase transport of materials definitively incorporated into the structure (steel, concrete) as well as the necessary for the mounting (formwork) and execution in work (A4 -A5) displaying the corresponding impact to each of the blocks studied (foundation, columns and slabs). The transports are counted from the fixed industrial installations to the place of execution. This result records labor consumption and materials required for formwork and concrete placement. Its environmental impact is much lower than that recorded in the production phase.

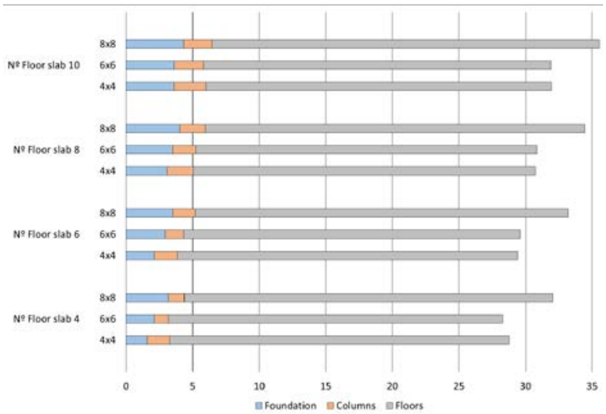

Figure 6 Embodied energy to transport of elements and execution on site (MJ/m2).

Now we assess the results of the energy embodied in the implementation process for each square meter of structure. Corresponding ratio values range from 28.29 to 35.54 MJ / m2, which is a variation of 25.63%. If we look at each of the blocks, the biggest oscillation occurs in the foundation, with 171.70%, and the lowest in the slabs, with a total variation of 15.76%. The most interesting option is achieved by solving a building of four floors and with the grid of 6x6 meters. Analyzing the impact of blocks for this case, the foundation represents 7.53%, columns 3.68%, and slabs the 88.79%, presenting the absolute minimum in columns and slab.

If we value the transportation and execution of the structure in the work based on equivalent CO2 emissions, results vary from 2.10 to 2.64 kg CO2 Eq / m2, which is a variation of 25.71%. In this case the variation in the output is slightly higher than that produced in the indicator of embodied energy. If we look at each of the blocks, the biggest variation occurs in the foundations, with 166.67%, and the lowest in the slabs, with a total variation of 15.51%. The most attractive option again is found by using four floors and 6x6 meters grid. In this case the foundation represents 7.58%, columns 3.79%, and slabs 89.63%.

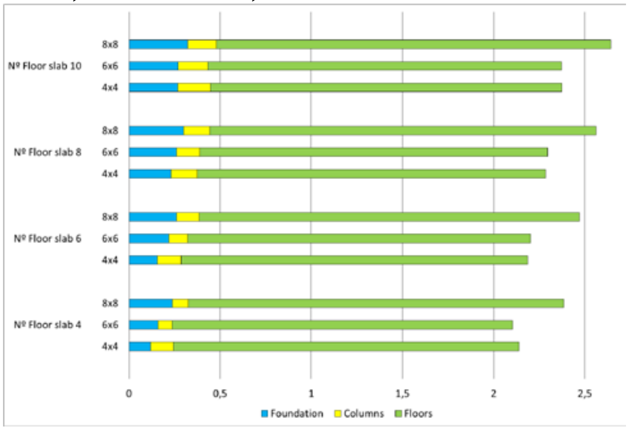

Figure 7 CO2 emissions for the transport of elements and execution on site (kg CO2 Eq/m2).

5. CONCLUSIONS

As a preliminary conclusion, it is important to note that variations make the results present significant oscillations. These oscillations are most important in the production phase of materials.

The production phase (A1-A2-A3) has a much higher impact than transport and execution stages (A4-A5). For the optimal case this value is 37 times higher. This is because the production of materials includes those definitively incorporated and also the ones consumed during the construction process.

The blocks in which the structures (foundations, columns, and slabs) were fractionated have different weights. The block most representative is slabs, hovering around 80% compared to 7% of the columns and 13% of the foundation. The starting volume is higher and therefore also impacts are. The greatest variations occur in column and foundations blocks. These items suffer the greatest variations in the ratio per square meter. The columns represent for example in 4x4 grid 49 units per slab, compared to 16 used in the 8x8 grid. In this aspect also the foundation is conditioned due to the number of elements. In both cases the change of heights affects the amounts of the materials used.

With the contemplated structural thickness, the option of 8 meters for slabs represents an increased generated impact around 20% compared to options of 6 meters. This situation is generated in part by the high stresses to which the slabs are subjected and consequently the necessary amounts of reinforcing steel increase.

The increased height in buildings drives to an increase of impact per square meter of the implemented structural solution, while the slab block has small variation compared with variations in the foundation and column blocks. In the latter, impact double the value because of the effect of height.

Since slab is the most representative block, optimal solutions are found for a grid of 6x6 by using low-rise buildings (four floors).

On the horizon, regulations promoted by institutions to achieve almost zero consumption buildings are presented. This situation will make tools like the one proposed here in combination with the use of Building Information Modeling (BIM) allow assess constructive alternatives and locate those representing the lowest environmental impact.

REFERENCES

Camp 2013 “CO2 and cost optimization of reinforced concrete frames using a big bang big crunch algorithm” Engineering Structures 48 363-372.

CTE “Código Técnico de la Edificación”. Real Decreto 314/2006, de 17 de marzo, del Ministerio de Vivienda (España).

CYPECAD (2015) ”CYPE Ingenieros Software para Arquitectura, Ingeniería y Construcción”. CYPE Ingenieros S.A.

Dolan 2014 “A comparison of the embodied energy and embodied carbon of a timber visitor centre in Ireland with its concrete equivalent” WCTE 2014 World Conference on Timber.

EHE-08 “Instrucción de Hormigón Estructural”, Real Decreto 1247/2008, de 18 de julio, del Ministerio de Fomento (España).

Goggins 2010 “The assessment of embodied energy in typical reinforced concrete building structures in Ireland” Energy and Buildings 42 735-744.

Lenzen 2002 “Embodied energy in buildings Wood versus concrete. Reply to Börjesson and Gustavsson” Energy Policy 30 249-255.

Lim 2015 “Embodied energy and CO2 emission reduction of a column beam structure with enhanced composite precast concrete members” Journal of Asian Architecture and Build.

McGrath 2012 “Embodied energy and carbon footprinting of concrete production and use” Proceedings of the 3rd International Conference on the Durability of Concrete Structures.

Miller 2015 “Concrete slab comparison and embodied energy optimization for alternate design and construction techniques” Construction and Building Materials 80 329-338.

Muigai 2012 “The role of the structural engineer in the design of low embodied energy concrete frame buildings Concrete Repair, Rehabilitation and Retrofitting” III Proceedings.

Park 2014 “Evaluation of the influence of design factors on the CO2 emissions and costs of reinforced concrete columns” Energy and Buildings 82 378-384.

Paya Zaforteza 2009 “CO2 optimization of reinforced concrete frames by simulated annealing” Engineering Structures 31 1501-1508.

Porwal, A., Hewage, K.N., (2012) "Building information modeling-based analysis to minimize waste rate of structural reinforcement", Journal of Construction Engineering and Management, Vol. 138, Num. 8, Pag. 943-954.

Shuai 2010 “Embodied energy and resources consumption impact to concrete” Wuhan Ligong Daxue Xuebao Journal of Wuhan University of Technology 32 143-146+151.

Stumpf 2014 “Un estudio de caso sobre la energía contenida en construcciones con estructuras de hormigón y de mampostería estructural” Revista de la Construccion 13 9-14.

Tempest 2009 “Compressive strength and embodied energy optimization of fly ash based geopolymer concrete” 3rd World of Coal Ash, WOCA Conference Proceedings [volume] [first].

Yeo 2011 “Sustainable design of reinforced concrete structures through embodied energy optimization” Energy and Buildings 43 2028-2033.

Yeo 2015 “Sustainable design of reinforced concrete structures through CO2 emission optimization” Journal of Structural Engineering (United States) 141.

Yepes 2015 “Cost and CO2 emission optimization of precast prestressed concrete U beam road bridges by a hybrid glowworm swarm algorithm” Automation in Construction 49 123-134.

A DECISION SUPPORT SYSTEM FOR DISASTER PREVENTION IN URBAN AREAS

Agostino G. Bruzzone[(1)], Marina Massei[(2)], Matteo Agresta[(3)], Giuseppina Murino[(4)]

[(1) (2)] DIME, University of Genova, Italy – URL: www.itim.unige.it

[(3) (4)] Simulation Team– URL: www.simulationteam.com

[(1)] agostino@itim.unige.it, [(2)] massei@itim.unige.it,
[(3)] agresta@simulationteam.com, [(4)] giuseppina.murino@simulationteam.com

ABSTRACT
This paper proposes an overview of floods simulation models linked to Decision Support Systems focused on disaster prevention in urban areas. The preliminary solution proposed consists of a system of models simulating different layers. The authors developed human behavior models able to reproduce the reactions of the population in this context.

Keywords: Flood Simulation, Mega-Cities, Smart Government, Intelligent Agents, Decision Support Systems

1. INTRODUCTION
Prevention from risks is one of the biggest challenges for modern societies indeed politicians and decision makers constantly need to face strategic decisions to ensure a good quality of life and a high level of safety and security to their citizens.
Disasters are frequent and may happen for natural causes (i.e. extreme natural events such as heart quakes, Tornadoes, Tsunami, Floods) or can be provoked by men (i.e. chemical or nuclear accidents, terroristic attacks etc..). These events happen in rural areas or in high density populated zones and they usually create humanitarian emergencies even with critical logistics problems (Diaz et al. 2013-a). Obviously when they happen inside a high populated city the magnitude of the disaster increases exponentially and nowadays there is the rise of the urbanization process.
It is important to note that urbanization is changing the world and a growing number of people is moving from the countryside to the city: it has been calculated that in 2014 for the first time more than 50% of global world population was living in urban areas and this trend is expected to grow and to overcome the 60% within the 2050. (World Urbanization Prospects, 2014).
In Fig. 1 is reported the percentage of population living in urban area: North America and Latin America have the higher value with, respectively, 81,8% and 80%while Europe the urban population is 73 %. Only Africa and Asia are now below the 50% (with 40,8% and 48,8%), but there is the perspective to overcome this quota in the next years.

Table 1: Percentage of Urban Population Data, elaborated from UN "Department of Economic and Social Affairs"

Percentage of Urban population	2016	2020	2030	2040	2050
WORLD	54,48%	56,22%	60,04%	63,23%	66,37%
AFRICA	40,87%	42,64%	47,12%	51,48%	55,93%
ASIA	48,83%	51,24%	56,32%	60,34%	64,16%
EUROPE	73,82%	74,65%	77,00%	79,55%	81,95%
LATIN AMERICA AND THE CARIBBEAN	80,05%	81,01%	83,04%	84,68%	86,19%
NORTHERN AMERICA	81,81%	82,50%	84,24%	85,90%	87,42%
OCEANIA	70,78%	70,88%	71,32%	72,18%	73,51%

The rise of urban population also directly associated to an other global phenomena: the proliferation of the megacities, that are usually defined as *"cities with more than 10 Millions of inhabitants"*. The number of such mega urban centers is growing: in 1990 there were only 10 megacities worldwide and in 2014 such cities were already 28 with a population living there of 453 Million. Such number represent the 12% of the total world's urban population. (Un, D. E. S. A., 2015). By 2030, the world is projected to have 41 mega cities (Cohen, 2006).
In this context, one of the big challenges for the future generations is to preserve the harmonized growth of urban centers, guaranteeing a good balance between urbanization, development, and welfare and healthcare (Fujita et al.1999; Hoornweg, 2011, Diaz et al. 2013-b). The high density of people living and consuming energy in the same area lead to several challenges such as guaranteeing a sustainable growth preserving Safety & Security and the Environment.
Indeed it is important to underline that the cities and urbanized areas have more than 50% of total global population, use 75% of global resources (Bugliarello, 1999), but represent only 2% of earth's surface.
Mayors and decision makers constantly need to face with strategic decisions, but making the "right" choice is more related to "art" than to quantitative optimization; indeed, even this process cannot be the pure result of a mathematical computation, it is evident that the use of simulation model provide an opportunity for a more reliable decision making. It is also possible t

consider to use these models for supporting the crowdsourcing approach and to engage in the process directly the population.

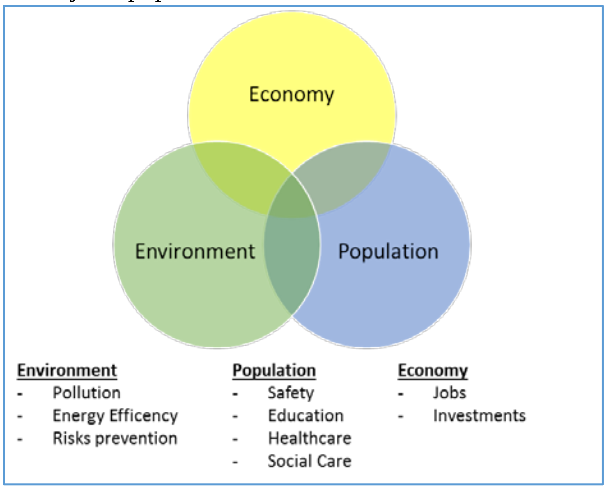

Figure 1: Main driver for decision makers

Obviously this requires also a cultural evolution of political decision makers and public opinion .
In this context the possible sources of complexity includes among the others:

a) Correlation between different Goals: different priorities are often in contrast:

- **Economy:** keeping high the number of jobs, and the income of the citizens, increasing the economic development, increasing the number of industries etc..
- **Environment**: keep low the pollution, increase the energy efficiency and prevent natural risks
- **Population and Welfare :** improve the welfare, increase the education level, improve safety and security, improve social care

b) Limited Resources: decision making process for public authorities is an hard task since it is necessary to balance the limited resources available (for example in terms of money, people and time).

c) Political constraints: decision makers need also to keep high the political consensus among their citizens.
For example the pedestrization of a road can appear a wrong choice and it can receive several negative opinions, but after a certain time people is happy and will never change such choice.

d) "Chicken and Egg" Problem
Defining some priorities to certain projects or certain activities and operas imply the exclusion or the procrastination of other actions.
It is important to note that decision makers often need to take also unpopular decision that can be "right" or decisions that can be "costly", but with no direct impact on popularity: for example cleaning a river is a costly action, it require time and it can also lead disturbance to commercial activities and lead disturbance to the traffic
Indeed there are some decision that require time for being effective and others that are more appealing and can provide immediate results with less effort. An example is a wrong urban planning and land use, with an uncontrolled urban growth.
Indeed each choice have a potential impact on the future of the city on different time scales: sometimes a choice may be unpopular, but extremely useful for the future and it may require time for being accepted and appreciated by the population.

e) Complexity in Predicting the Behaviour of the System
The decision making process is often the result of an intuitive solutions based on a qualitative estimation. Indeed considering and predicting all the possible effects of each set of possible choices in a quantitative way is not possible for human brain if the number of variables becomes high.
In addition it is important to note that many variables and process are stochastic and the secondary effects generated among the different entities and events may have a high impact on the final result. (Bruzzone et al, 2015a).
Historically, the pioneer in simulating complex system was Jay W. Forrester, that introduced the concept of System Dynamic and Urban Dynamics (Forrester 1961; Forrester,1969). Urban systems are described as *"complex systems"* and the governance of these systems is obviously extremely challenging. In this sense simulation provides a strong support in this area providing numerical results derived from an analytic analysis. Such analytical results may be available only by using a computer simulation, that is a fundamental instrument to study complex systems (McLeod 1982; Gould et al, 1988; Bar-Yam, 1997).

2. FLOODS OVERVIEW

In this paragraph the authors focus the attention on floods that are one of the most common natural disasters and one of the most dangerous.
Floods have strong impact in safety and economy; in literature it is possible to find several studies related to human losses (Neumayer et Barthel,2011;Doocy et al., 2013) and quantification of economical ones. (Cochrane,2004). Looking for a possible definition of flood the authors decide to use *"a situation in which water temporarily covers land where it normally doesn't"* (Martini, & Loat, 2010). Rainfall rate is generally the direct responsible of the rise in water level; a possible classification of rains is provided by Spanish National Meteorological institute, see Table 2.

Table 2: Rain Classification

Type of Rain	***mm/h***
Light Rain	< 2.0
Moderate Rain	2 – 15
Heavy Rain	15 - 30
Very Heavy Rain	30-60
Torrential Rain	> 60

After a first analysis, such values seems to be slightly different in Europe among different Nations and Institutes and the authors were not able to find a common standard for them.

Before focusing on simulation techniques and achievements of the previous researches it is important to understand the flood phenomena and clarify what are the different type of floods and understand their causes and their effects. In the Table 3 the different types of floods are described and summarized. Floods can be divided into five different typologies: Flash Floods, Coastal Floods, Urban Floods, River or Fluvial Floods and Ponding (or Pluvial) Floods based also on previous works on this topic (Jha, et. al., 2012) and (Anonymus, A. 2007). The main differences are summarized in Table 3.

- **Flash flood**

Flash floods are distinguished by the rapid rate of rise in the water level, they provide a short warning lead time, resulting in very little time to respond to the threat. (Davis, 2001).

It is a direct response to rainfalls; it has a really high intensity, but it is normally concentrated in a small area. The amount of water involved can be lower compared to other types of floods, but the energy of the flow drags big objects like trees and cars. A flash flood occurs usually in conjunction with heavy rains, with a minimum average value of 20mm/h (Bluestein, 1993) and such phenomena normally covers a period of less than 6 hours.(Gaume et al., 2009).

The short notice, huge flows and high velocities of flash floods make these types of floods particularly dangerous. Examples of flash floods in the recent year are documented in several papers, for example in Italy by Faccini et al. (2015) and Borga et al. (2007) and in France by Delrieu et. al, (2005).

- **Coastal floods:** a coastal flood, or tsunami-like phenomenon, happens when the coast is flooded by the sea, this could be caused by an intense storm or a big
- natural event such as a hearth-quake or a hurricane that creates high waves in the sea.
- **Urban floods**

Urban floods are a growing issue both for developing and developed countries. They are frequent in particular in rapidly expanding towns that often are characterized by a wrong land use that usually is correlated to a lack of urban drainage of the water.

The speed of the water depend on the orography of the city.

- **River (or fluvial) floods**

Such phenomena are caused by rainfall over extended period. In this case the river could overflow its banks and create flooding. This kind of flooding involve huge quantities of water.

- **Ponding (or pluvial flooding)**

Such type of floods happens in quite flat areas: when the rain water falling that is normally stored and absorbed by the ground cannot be more absorbed; in these case the flooding occurs. This event is similar to an urban flooding, but it happen in rural areas.

*Table 3: Floods Classification * data elaborated from (Jha, et. al., 2012), (Anonymus, A. 2007).*

Type	Natural causes	Human induced	Area Covered	Lead time	Capability to predict the area involved	People potentially involved	Duration	Intensity of water	Relevant Parameters
Flash floods	- Fluvial - Cost - River - Pluvial	Insufficient drainage system	Low	Short	Low	Low	Few hours	High	Intensity duration of rainfalls and prediction of the most affected area
Coastal floods	Storm Tsunami Volcanic eruptions	Development of coastal zone Destruction of natural flora	Medium/ high depending on local topography	Medium	High	Medium	Long	Medium	Strength, intensity, direction and speed of the hurricane or storm.
Urban floods	Rainfalls Coastal Fluvial	Saturation of drainage Lack of permeability due wrong land use planning Lack of management	Medium	Medium	Low/Medium	High	Few hours to days	Low	Intensity of rainfalls, Elevation profile, Urban drainage system condition
River (or fluvial) floods	Intensive rainfall Ice jam clogging Collapse of dikes	Lack of river manteinance Wrong Urbanization	Depending on terrain elevation	Medium/High	Medium/High	Medium/High	days/weeks	High	Water level prediction
Ponding (or pluvial flooding)	Rainfalls	Terrain saturation	High	High	High	Long	Varies	Medium	Intensity of rainfalls, Elevation profile, Urban drainage system condition

As it possible to see in Table 3, each type of flood have different characteristics and it is clear that facing with these different phenomena require different strategies and different countermeasures. For example, if we compare pluvial floods with flash floods it is evident that they need different preventive actions: the flash floods are faster and have a low lead time while the pluvial flood are slower but they involve a higher territory. Indeed, it is obvious that the model required for the analysis should be different according to the different flood risk type and, consequently there is a need for different type of simulators.

3. FLOODS SIMULATION AND ITS POTENTIAL

The number of mobile phones, sensors, cameras and other devices that are present in urban area is huge. Potentially these data can be used for several applications in real time; tweets and post contents in the web, variation of data traffic etc. are already used for several application such as traffic jams monitoring or emergency detections.

E-government is also correlated to new ways of taking measures, for example river level with telemetry cameras or the use of drones for acquiring real time information and measures (Changchun et al. 2010). Real time Decision Support Systems is a potential instrument for the future, but if we consider floods, it is important to note that the hydrological models that are needed to calculate the level of water are often really computational heavy since they are based on Saint Venant equation and finite element techniques. That's why many existing models and simulators cannot be used in real time and they need a pre-simulated scenario. Hereafter it is described a possible classification of real time flood forecasting systems into three main categories (Henonin et. al., 2013):

- **Empirical Scenario Based**: it is based on real time flood forecasting without any hydraulic-hydrogeological model. Such tool is based on historical data and past events, which are tested by Subject Matter Experts. The warning is attributed based on the past data, the current level of rainfalls, and the predicted one. It can be extended with an automatic system of alerts to key people and citizens by mail/SMS/website and can be completed with a specific web page where citizens can connect and take information on the appropriate measures to avoid the damage.
- **Pre-simulated scenario**: it is a real time flood forecasting system based on previous hydraulic simulation. In this case, the input of the system is still the rainfall intensity prediction and its actual value; the system will match the pre-simulated scenario that is closer to such values.
- **Real time simulation;** it is a flood forecasting model with a real time hydraulic simulation. In this case it is important to balance the model complexity with the computational power that is needed.

Obviously the complexity of the simulation that is needed for a comprehensive reproduction of the phenomena should be different according each type of floods. The floods happening in rural areas are "easier" to be analysed, in a certain way, because the presence of human is lower than in the city and men made structures are not intensively present within the area; for example the "artificial" drainage system is often not present, and urban structures are rare; such situation make the hydraulic model simpler. On the contrary, modelling floods inside a city, such as urban flash floods is particularly difficult due to the absence of natural flow paths and the presence of man-made structures. (Snell & Gregory, 2002; Hapuarachchi et al. 2011); in these cases the errors are inherent both the process of estimating rainfall from radar and the modelling of the rainfall–runoff transformation (Hossain et al., 2004). In addition the dataset available to calibrate the model comes from cities that are different. (Viglione et.al., 2010) For this reason in the past years have been developed the HYDRATE Project, founded by European Commission, to develop a harmonized dataset of European flash food data (www.hydrate.tesaf.unipd.it) that represents a valuable source.

4. HUMAN BEHAVIOUR MODELLING

Human Behavior Modelling (HBM) is a challenging task and it is the subject of ongoing researches even because of the emergent behaviors and properties due to the presence of multiple complex interactions among humans (Oren and Longo, 2008). Indeed it has a great potential in different contexts such as military, economic, political, and emergency or evacuation. The continuous evolution of interoperable simulation reinforce the opportunity to combine different models to create federation based on Modelling & Simulation in new areas; an example is the possibility to support strategic decision making and to face complex humanitarian scenario (Simulation Team and NATO M&S COE, 2013). In facts the Simulation Team have developed different solutions based on Intelligent Agents to address in this context the HBM (Bruzzone et.al.,2015a; Bruzzone et. al.,2014); a good example are the Intelligent Agent Computer Generated Forces (IA-CGF) for simulating intelligent behavior in defence and humanitarian crisis.

HBM is often based on micro-simulation, that means that each different human correspond to a single entity; in some other case the HBM are based on social and economic group interactions; currently IA-CGF operates on these different layers concurrently; indeed in reproducing human factor for computer simulation, it is quite common the necessity to address different layers such as:

- Individual layer including Rational Decision making and Emotional and Irrational;
- Social layer including Crowd Behavior, Social Networks and Families.

For instance these two layers could be simulated by means of Intelligent Agents (IA) able to reproduce the following different aspects (Wooldrige & Jennings, 1995):

- Autonomy: ability to operate without external control
- Reactivity: capability to respond to any stimulus
- Social Ability: Capability to interact with other agents
- Proactivity: capability to take the initiative

Focusing the attention on urban context, the simulation of the population behavior results a powerful instrument for decision makers. Indeed it provides a quantitative feedback of the reaction of the citizens to the different political choices on different time-scales:

- **short term behavior** (i.e. pedestrian evacuation swarm behavior etc.)
- **long term reactions** (i.e. simulation of political consensus, trustiness level

5. TRAFFIC SIMULATION DURING EMERGENCY SITUATION

There are interesting studies carried out on the impact of flooding on road transportation systems; for instance simulations have been carried on by integrating a flood simulator, (MIKE) with a traffic model (SUMO) by means of a microscopic simulation: in case of a flood the trips that have an origin or destination in the flooded area are cancelled and the routes that pass through a flooded area are rerouted to unfavourable routes; furthermore, the speed of the vehicles is reduced in function of the intensity of the rainfalls.(Pyatkova, 2015). Another example, have been developer for quantifying and spatially map the flood characteristics by integrating GIS data. The estimated flood volume is used to estimate a hazard factor of each road (Dawod et. al., 2012). The authors developed in the past a demonstration based on IA-CGF and interoperable simulation to reproduce flooding covering an entire State respect the transportation layer; the case was inspired to Katrina and demonstrated the effectiveness of this context (Bruzzone & Massei 2006).

6. SIMULATION MODEL DESCRIPTION

Based on the above mentioned consideration it is evident that Modeling & Simulation is fundamental to test the feasibility of complex systems such as a decision support system for flooding in urban areas; indeed this approach support the adoption of an holistic view of the system and the assessment of the scenario awareness before making important choices; this allows to evaluate risks of alternative decision and it is fundamental to prevent problems and errors. The adoption of an interoperable simulation framework is the key to support decision making, in facts the adoption of HLA (High Level Architecture) allows to interoperate also with external systems to guarantee dynamical update on the situation.
Indeed this framework could be dynamically connected through the High Level Architecture supported by the RTI (Run Time Infrastructure) with real systems such as C2 (Command and Control systems), Sensor Networks, web mining to update the situation and provide a real time representation of the scenario (Srivastava et al.2000). Another important aspect is related to the necessity to integrated Dbase covering the complex description of the urban area and providing all the boundary conditions necessary for processing the flooding dynamic evolution.
In the following, the overall architecture and nature of the proposed system is summarized:

- **Meteo forecasting Model**: this model simulates the weather forecasting. The output of such model provide the probability of rain that is associated to each zone of the city and the dynamic evolution of it along time as well as other boundary conditions that influence the situation (e.g. wind, luminosity, ect.).
- **Catchment Model:** this model simulate the water catchment by the soil. The model is quite complex because it need to consider the actual drainage network in the city and the different composition of the soil (green areas, building etc.).
- **Hydrological Model:** this model is strictly correlated to the catchment model, it determines the water level inside the city; the simulation of the rivers could be based on this model or it could be incorporated in the catchment model depending on the resolution applied; in general this model address simulation of water streams and flooding flows.
- **Town Model:** this model reproduce the rainfall on the urban area**;** for instance the falling on the roofs is conveyed in drainage system, therefore the different buildings are characterized by pumping systems located in different part that could be subjected to block in different ways during the flooding (e.g. hospitals with pumps in the basement and hospital with pumps on the roof).
- **Human Behavior Model:** this model simulate the human behavior of individuals and groups that compose the city. The model allows to consider multi resolution entities corresponding to aggregated people objects allowing to reproduce individuals as well as groups. This model provides as output the feelings of the population and of different aggregations such as consensus level, fear, trustiness to a political group in charge of the government of the city. This mode reproduces also the entities and units devoted to apply countermeasures to the flooding.
- **Environmental Framework:** this model provide access to the Dbases representing the different elements; indeed in large urban areas the size of this Dbase suggests to create a scalable access potentially distributed, therefore the computational aspects shoul drive the specific implementation to guarantee quick access to the information required by the different simulators; the Dbases include the different urban layers and data of the town, the population demographics as well as terrain characteristics and digital elevation mapping.

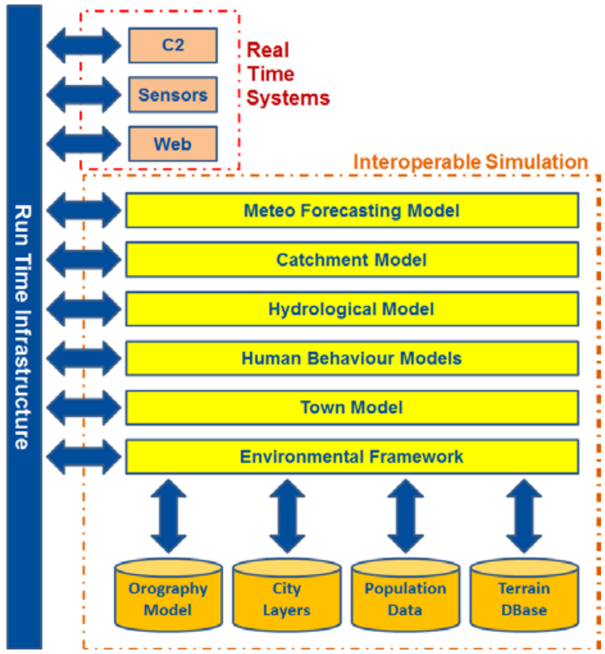

Figure 2:General Architecture

The simulator proposed in this case is designed to adopt the HLA IEEE1516 (High Level Architecture) standards and guarantees interoperability; the Federates could be based on stochastic models adopting combined simulation continuous and discrete events combined together.

7. CONCLUSIONS

In this paper the general architecture of a Decision Support System for urban disaster prevention is presented with special attention to flooding; the analysis outline the complexity to reproduce the dynamics of both physical and social phenomena in this context, but also the potential of adopting innovative approaches (e.g. HLA, IA) to address these issues. The analysis on the experimental results of previous researches confirms the feasibility of the approach and it is used to support the design of the general architecture of the simulator to be used. The authors provides here a synthetic proposal for the structure of an interoperable simulator devoted to address this issue and, currently, further development are on-going for the implementation and the Verification and Validation of the model.

REFERENCES

Alcrudo, F. (2002). A state of the art review on mathematical modelling of flood propagation. In First IMPACT project Workshop, Wallingford, UK

Anonymus, A. (2007). Handbook on good practices for flood mapping in Europe. Excimap (European exchange circle on flood mapping).

Atiya, A. F., El-Shoura, S. M., Shaheen, S. I., & El-Sherif, M. S. (1999). A comparison between neural-network forecasting techniques-case study: river flow forecasting. IEEE Transactions on neural networks, 10(2), 402-409.

Bar-Yam, Y. (1997). Dynamics of complex systems (Vol. 213). Reading, MA: Addison-Wesley.

Bluestein, H. B., (1993) "Observations and Theory of Weather Systems, Vol.II, Synoptic–Dynamic Meteorology in Midlatitudes, Oxford Univ.Press

Borga, M., Boscolo, P., Zanon, F., & Sangati, M. (2007). Hydrometeorological analysis of the 29 August **2003 flash flood in the Eastern Italian Alps. Journal of hydrometeorology, 8(5), 1049-1067.

Changchun, L., Li, S., Hai-bo, W., & Tianjie, L. (2010) "The research on unmanned aerial vehicle remote sensing and its applications", Proc. of the 2nd IEEE ICACC, Shenyang, China, March, Vol. 2, pp. 644-647

Bruzzone A.G., M. Massei, M. Agresta, A. Tremori, F. Longo, G. Murino, F. De Felice, A. Petrillo, (2015b) Human behavior simulation for smart decision making in emergency prevention and mitigation within urban and industrial environments, proc of 27th EMSS European Modeling & Simulation Simposium

Bruzzone A.G., Massei M., Longo F., Nicoletti L., Di Matteo R., Maglione G., Agresta M. (2015a) "Intelligent agents & interoperable simulation for strategic decision making on multicoalition joint operations. Proc. of 5th International Defense and Homeland Security Simulation Workshop, DHSS

Bruzzone, A., Massei, M., Longo, F., Poggi, S., Agresta, M., Bartolucci, C., & Nicoletti, L. (2014). Human behaviour simulation for complex scenarios based on intelligent agents. In Proceedings of the 2014 Annual Simulation Symposium (p. 10). Society for Computer Simulation International.

Bruzzone A.G., Massei M., (2006) "Modelling for Estimating Impact on Road Transportation of Regional Emergencies & Disasters", Proceedings of I3M2006, Barcelona, October

Bugliarello, G., (1999) "Megacities and the developing world," The Bridge, Volume 29

Butler, H. L. (1978). Coastal flood simulation in stretched coordinates. Coastal Engineering Proceedings, 1(16).

Campbell, S. (1996). Green cities, growing cities, just cities?: Urban planning and the contradictions of sustainable development. Journal of the American Planning Association, 62(3), 296-312.

Cohen, B. (2006) "Urbanization in developing countries: Current trends, future projections, and key challenges for sustainability", Technology in society, 28(1),63-80

Campolo, M., Andreussi, P., Soldati, A. (1999) "River flood forecasting with a neural network model", Water Resources Research,35(4),1191-1197.

Chau, K. W., Wu, C. L., & Li, Y. S. (2005). Comparison of several flood forecasting models in Yangtze River. Journal of Hydrologic Engineering, 10(6), 485-491.

Cochrane, H. (2004). Economic loss: myth and measurement. Disaster Prevention and Management: An International Journal, 13(4), 290-296.

Davis, R. S. (2001). Flash flood forecast and detection methods. In Severe Convective Storms (pp. 481-525). American Meteorological Society.

Dawod, G. M., Mirza, M. N., & Al-Ghamdi, K. A. (2012). GIS-based estimation of flood hazard impacts on road network in Makkah city, Saudi Arabia. Environmental Earth Sciences, 67(8), 2205-2215.

Delrieu, G., Nicol, J., Yates, E., Kirstetter, P. E., Creutin, J. D., Anquetin, S., & Payrastre, O. (2005). The catastrophic flash-flood event of 8-9 September 2002 in the Gard region, France: A first case study for the Cevennes-Vivarais Mediterranean Hydrometeorological Observatory. Journal of Hydrometeorology, 6(1), 34-52.

Diaz R., Behr J., Toba A.L., Giles B., Manwoo N., Longo F., Nicoletti L. (2013-a). Humanitarian/emergency logistics models: A state of the art overview. Simulation Series, 45 (11), pp. 261-268.

Diaz, R., Behr, J.G., Longo, F., Liu, H. (2013-b). A systems framework for modeling health disparities in the prevalence in chronic conditions following a natural disaster event. Crisis Management: Concepts, Methodologies, Tools, and Applications, 1-3, pp. 497-513.

Doocy S, Daniels A, Murray S, Kirsch TD. (2013). The Human Impact of Floods: a Historical Review of Events 1980-2009 and Systematic Literature Review. PLOS Currents Disasters. Edition 1

Faccini, F., Luino, F., Sacchini, A., & Turconi, L. (2015). Flash flood events and urban development in Genoa (Italy): lost in translation. In Engineering Geology for Society and Territory-Volume 5 (pp. 797-801). Springer International Publishing.

Gaume, E., Bain, V., Bernardara, P., Newinger, O., Barbuc, M., Bateman, A., ... & Daliakopoulos, I. (2009). A compilation of data on European flash floods. Journal of Hydrology, 367(1), 70-78.

Glossary of Meteorology (2000). "Rain". American Meteorological Society. Retrieved 2010-01-15.

Gould, H., Tobochnik, J., & Christian, W. (1988). An introduction to computer simulation methods (Vol. 1). New York: Addison-Wesley.

Hapuarachchi, H. A. P., Wang, Q. J., & Pagano, T. C. (2011). A review of advances in flash flood forecasting. Hydrological Processes, 25(18), 2771-2784.

Henonin, J., Russo, B., Mark, O., & Gourbesville, P. (2013). Real-time urban flood forecasting and modelling–a state of the art. Journal of Hydroinformatics, 15(3), 717-736.

Hoornweg, D. (2011). Cities and climate change: responding to an urgent agenda. World Bank Publications.

Hossain, F., Anagnostou, E. N., Dinku, T., & Borga, M. (2004). Hydrological model sensitivity to parameter and radar rainfall estimation uncertainty. Hydrological Processes, 18(17), 3277-3291.

Jay W. Forrester, (1961), Industrial Dynamics, Pegasus Communications, ISBN 1-883823-36-6.

Jay W. Forrester, (1969), Urban Dynamics, Pegasus Communications, ISBN 1-883823-39-0.

Jha, A. K., Bloch, R., & Lamond, J. (2012). Cities and flooding: a guide to integrated urban flood risk management for the 21st century. World Bank Publications.

Jonkman, S. N. (2005). Global perspectives on loss of human life caused by floods. Natural hazards, 34(2), 151-175.

Maaten, R. (2007). Review of flood event management Decision Support Systems. Deltares.

Martini, F., & Loat, R. (2010). Handbook on good practices for flood mapping in Europe. European exchange circle on flood mapping (EXCIMAP), Paris/Bern

Martini, F., & Loat, R. (2010). Handbook on good practices for flood mapping in Europe. European exchange circle on flood mapping (EXCIMAP), Paris/Bern.

McLeod J. (1982) "Computer Modeling and Simulation: Principles of Good Practice", SCS, San Diego

Merkuryeva, G. V., & Kornevs, M. (2013). Water Flow Forecasting and River Simulation for Flood Risk Analysis. Information Technology and Management Science, 16(1), 42-46.

Met Office (August 2007). "Fact Sheet No. 3: Water in the Atmosphere". Crown Copyright. p. 6. Retrieved 2011-05-12.

Moriarty, K. D., Ni, D., & Collura, J. (2007). Modeling traffic flow under emergency evacuation situations: Current practice and future directions.

Nash, J. E., & Sutcliffe, J. V. (1970). River flow forecasting through conceptual models part I—A discussion of principles. Journal of hydrology, 10(3), 282-290.

Neumayer, E., & Barthel, F. (2011). Normalizing economic loss from natural disasters: a global analysis. Global Environmental Change, 21(1), 13-24.

Ören, T., Longo, F. (2008). Emergence, anticipation and multisimulation: Bases for conflict simulation. Proceedings of the 20th European Modeling and Simulation Symposium, EMSS 2008, pp. 546-555.

Pyatkova, K., Chen, A. S., Djordjevic, S., Butler, D., Vojinović, Z., Abebe, Y. A., & Hammond, M. J. (2015). Flood impacts on road transportation using microscopic traffic modelling technique.

Qi, H., & Altinakar, M. S. (2011). A GIS-based decision support system for integrated flood management under uncertainty with two dimensional numerical simulations. Environmental Modelling & Software 26(6), 817-821.

Simulation Team and NATO M&S COE (2013) "Strategic Decision Making Training Through Serious Games: NDC Report", NATO ACT Report, Norfolk, VA

Srivastava, J., Cooley, R., Deshpande, M., & Tan, P. N. (2000). Web usage mining: Discovery and applications of usage patterns from web data. Acm Sigkdd Explorations Newsletter, 1(2), 12-23.

Snell S, Gregory K. (2002). A Flash Flood Prediction Model for Rural and Urban Basins in New Mexico. Technical report, New Mexico Water Resources Research Institute

Un, D. E. S. A. (2015). World Urbanization Prospects: The 2014 Revision.

Viglione A., Borga, M., Balabanis and G. Blöschl,(2010) Barriers to the exchange of hydrometeorological data across Europe – results from a survey and implications for data policy. J. of Hydrology, 394, issue 1-2, 63-77. doi:10.1016/j.jhydrol.2010.03.023.

Wooldrige M., N.R. Jennings (1995). "Intelligent Agents, Theory and Practice"

World Urbanization Prospects (2014) Economic and Social Affairs, United Nations ISBN 978-92-1-151517-6

WIND FARM PERFORMANCE ASSESSMENT UNDER DIFFERENT WAKE MODELS: A CASE STUDY IN COMPLEX TERRAIN

Duilio Curcio[(a)], Giuseppe Filardo[(b)]

[(a),(b)] CAL-TEK Srl

[(a)]curcioduilio@libero.it, [(b)]filardogiuseppe@libero.it

ABSTRACT
The focus of this paper is a wind farm located in Calabria (Italy). The objective is to implement a support tool (a simulator) to be used for carrying out specific analyses in order to test system performance in terms of energy production under different wake models. After the modeling phase, the simulation model has been validated. Three different wake models are introduced to evaluate system power loss due to near and far wake effects in complex terrain.

Keywords: wind farm Modeling & Simulation, wake models, wind farm performance analysis, complex terrain

1. INTRODUCTION

According to Shakoor *et al.* (2016), during the last decade energy production from non-conventional resources (wind, solar, biogas, etc.) have registered an outstanding increase due to the forthcoming sale of all conventional stocks.

In particular, wind energy has had a growth of 27% in the last five years for a total installed capacity of about 230 GW at the end of 2011 with an overall turnover of 50 billion Euro (Grassi *et al.* 2014). In addition, the Global Wind Energy Council Report in 2012 stated that wind energy has become the most rapidly rising source of energy in the world, having a steep increase in development from 2009.

Energy from wind is generally obtained through wind farms (WFs), which consist of hundreds of turbines (WTGs). A WTG aims at extracting the kinetic energy from wind, converting it into mechanical energy at the rotor axis and then into electrical energy (Vermer *et al.* 2003; Shakoor *et al.* 2015). During the first phase (when WTG extracts energy from wind), the rotation of wind turbine rotor cause a reduction of the wind speed behind it and swirls the air flow, i.e. the Wake Effect (WE) of a wind turbine: the area behind the wind turbine is characterized by a modified wind flow both in terms of mean velocity and turbulence intensity. A wind speed decrease causes a reduction of the WF energy production while a turbulence intensity increase produces dynamic mechanical loadings on downwind WTGs (which are said to be *shadowed* by the turbine generating the wake), see Gonzalez-Longatt *et al.* (2012).

As a consequence, wake effects evaluation plays an important role in the WF design in order to maximize the energy production and WTGs lifetime (Kiranoudis and Maroulis 1997). In order to describe WEs, several models have been developed which can be classified in:

- *analytical/explicit* or *kinematic* wake models: these are the earliest and use self-similar velocity profiles determined semi-empirically; they evaluate the velocity in a wake through a set of analytical expressions and are based on the conservation of mass and empirical relations of wake decay, which are mainly used for micro-siting and WF output predictions, see Lissaman (1979), Jensen (1983) and Voutsinas *et al.* (1990);
- *computational/implicit* wake models: developed as alternatives to the explicit models, these are based on approximations of either the Navier-Stokes or vorticity transport equations, see Zervos *et al.* (1988); Smith and Taylor (1991); Crasto and Gravdahl (2008).

According to Kozmar *et al.* (2016), several studies on WEs of wind turbines at the flat terrain and open sea have been carried out. However, little is known about WEs in *complex terrain*, see Yang *et al.* (2015).

In particular, the contribution proposed by authors aims at extending research knowledge on this topic. The main objective of this paper is to present a simulation model used as support tool for carrying out specific analyses for testing wind farm performance in terms of energy production under three different wake models in a complex terrain environment. Simulation model development, validation and preliminary analysis are presented. It is worth mentioning that Simulation has been extensively used in many sectors for complex systems design, decision support and training, from Industry to Logistics, from Defense to Environmental Sustainability (e.g. Longo, 2012-a; Longo 2012-b; Bruzzone et al. 2011). More recently Modeling & Simulation based approaches, have been also used to support design of sustainable energy production systems (Perez et al. 2015). The paper is organized as follows: Section 2 reports a description of the existing wind farm; Section 3 presents the simulation model as well as validation results while Section 4 describes the preliminary analysis and simulation results. Finally, Conclusions summarize critical issues and main results of the study.

2. THE WIND FARM

As before mentioned, the wind farm considered in this research work is located in Calabria, south part of Italy, in a complex terrain which rises from sea level to a maximum altitude of 340 m.

In particular, terrain complexity is due to the succession of hills and increasing slope areas, i.e. *complex orography*, with trees of variable height, low greenery and cultivated plots of land, i.e. *complex roughness*, as reported in Figure 1.

The wind farm on this complex terrain is made up by 27 WTGs located at different altitudes: the base of the lowest turbine is located at 280 m above sea level while the highest is at about 340 m. The remaining WTGs are arranged within the altitude range.

All the three blades WTGS have a rated power of 2.0 MW: 17 of them are mod. *Vestas V90* with a rotor diameter of 90 m and a hub height of 80 m; the others 10 are mod. *Repower MM92* with a rotor diameter of 92.5 m and a hub height of 80 m.

Table 1 reports for each WTG its longitude and latitude in UTM-WGS 84 coordinate system, altitude above sea level and model.

Table 1: WTGs of the on-shore wind farm

WTG	***Long. East***	***Latitude North***	***Alt. (m)***	***Mod.***
WTG1	627232	4304548	337.5	*Vestas V90*
WTG2	626763	4304481	319.8	" "
WTG3	626308	4304660	337.5	" "
WTG4	625986	4305421	334.3	" "
WTG5	625550	4304266	307.7	" "
WTG6	625571	4303990	310.0	" "
WTG7	626221	4303380	324.9	" "
WTG8	626079	4303841	321.3	" "
WTG9	625913	4303353	314.8	" "
WTG10	626033	4303598	286.9	" "
WTG11	626900	4302881	339.1	" "
WTG12	626233	4303064	325.4	" "
WTG13	627238	4302928	336.3	" "
WTG14	627290	4303239	339.6	" "
WTG15	627287	4303418	324.4	" "
WTG16	626799	4303117	318.5	" "
WTG17	627041	4303548	323.8	" "
WTG18	626195	4304791	340.8	*REpower MM92*
WTG19	625904	4305054	336.1	" "
WTG20	625750	4304662	318.8	" "
WTG21	625297	4304561	311.4	" "
WTG22	625160	4304067	309.6	" "
WTG23	625524	4303778	309.0	" "
WTG24	625395	4303330	309.0	" "
WTG25	625685	4303140	304.0	" "
WTG26	625451	4302881	285.0	" "
WTG27	624982	4303112	289.0	" "

Figure 1: Wind Farm terrain complexity

3. THE SIMULATION MODEL

According to authors experience, simulation is the most effective tool for designing and analyzing systems behavior under internal/external changes, see Curcio and Longo (2009) and Longo et al. (2012).

In fact, the simulation model presented in this research work aims at reproducing system performance in terms of energy production under three different *analytical/explicit* or *kinematic* wake models, i.e. Jensen, Larsen, Ishihara.

The software tools adopted for the simulation model implementation and climatology data analysis are:

- *Minitab 14.0*, *WindRosePro3*, *MS Excel* for probability plots, Weibull distribution parameters and wind roses from available climatology data;
- *WindSim Express 7.0* in the pre-processing step for digital terrain model (DTM) definition, WF layout (including WTGs technical specifications), masts with climatology data;
- *WindSim 7.0* as a post-processor for average wind speed at each WTG estimation, wake effects, full load hours evaluation, wind farm power assessment.

3.1. Wake models description

Three different *analytical/explicit* or *kinematic* wake models are investigated in this research work: Jensen, Larsen and Ishihara.

Table 2 lists all the factors considered in each wake model while the following subsections describe more in detail each wake model.

Table 2: Wake models parameters

Parameter	***Jensen***	***Larsen***	***Ishihara***
Incoming wind speed	•	•	•
Downstream distance from the WTG	•	•	•
Radial distance from the WTG		•	•
Rotor diameter	•	•	•
Hub height		•	
Turbulence intensity		•	•

3.1.1. Jensen wake model

The analytical wake model developed by N.O. Jensen is one of the oldest analytical wake models.

According to N.O Jensen, the wake behind the wind turbine has a linear expansion and the velocity deficit is only dependent on the distance downstream from the turbine.

The wake increase is described by the following equation:

$$D_{wake} = D(1 + 2ks) \tag{1}$$

while velocity deficit u_{def} due to wake effects is defined as follows:

$$u_{def} = U_{\infty}\left[\frac{1-\sqrt{1-C_T}}{(1+2ks)^2}\right] \tag{2}$$

where:

- D: rotor diameter (m);
- D_{wake}: wake diameter (m);
- k: *wake decaying constant* (it represents how the wake breaks down by specifying the growth of the wake width per unit length in the downstream direction);
- s: normalized downstream distance (with respect to the rotor diameter) from the turbine;
- U_{∞}: undisturbed wind speed (m/s);
- C_T: thrust coefficient.

3.1.2. Larsen wake model

Larsen wake model is based on Prandtl turbulent boundary layer equations.

The wake flow is assumed to be incompressible, stationary and asymmetric. The wake increase is described by the following equation:

$$D_{wake} = 2\left(\frac{35}{2\pi}\right)^{\frac{1}{5}}(3c_1^2)^{\frac{1}{5}}[C_T A(x+x_0)]^{\frac{1}{3}} \tag{3}$$

while velocity deficit u_{def} due to wake effects is:

$$u_{def} = -\frac{U_{\infty}}{9}[C_T A(x+x_0)^{-2}]^{\frac{1}{3}}\left\{r^{\frac{3}{2}}[3c_1^2 C_T A(x+x_0)]^{\frac{-1}{2}} - \left(\frac{35}{2\pi}\right)^{\frac{3}{10}}(3c_1^2)^{\frac{-1}{5}}\right\}^2 \tag{4}$$

where:

- r: radial distance from the turbine (m);
- x: downstream distance from the turbine (m);
- A: rotor swept area (m^2);
- x_0: constant that denotes the turbine's position with respect to the applied coordinate system;
- c_1: constant representing the non-dimensional mixing length (related to Prandtl mixing length).

3.1.3. Ishihara wake model

In this model turbulence effects on the wake from both the ambient turbulence and the mechanical generated turbulence are considered.

The wake increase is described by the following equation:

$$D_{wake} = \frac{k_1 C_T^{\frac{1}{4}}}{0.833}D^{\left(1-\frac{p}{2}\right)}x^{\frac{p}{2}} \tag{5}$$

The velocity profile of Ishihara model is assumed to have a Gaussian profile and the velocity deficit is given by:

$$u_{def} = \frac{\sqrt{C_T}}{32}U_{\infty}\left(\frac{1.666}{k_1}\right)^2\left(\frac{x}{D}\right)^{-p} exp\left(-\frac{r^2}{D_{wake}^2}\right) \tag{6}$$

with

$$p = k_2(I_a + I_w) \tag{7}$$

where I_a and I_w are respectively the ambient turbulence and the turbine-generated turbulence while $k_1 = 0.27$ and $k_2 = 6$.

3.2. Wind data analysis

Before simulation model implementation, wind data of two different on-site masts, i.e. MAST1 and MAST2, have been analyzed.

Table 2 shows for each MAST its longitude and latitude in UTM-WGS 84 coordinate system and height.

Each mast consists of 5 wind anemometers at different heights, a pressure detector and a thermometer. Two years of wind speed, wind direction and temperature data are available for each mast. In the following pages, the data will be analyzed and filtered by using Minitab 14.0, WindRosePro3, MS Excel in order to evaluate for each wind anemometer:

- prevailing wind directions, see Figure 2-3;
- main wind speed statistics and percentage distribution for different wind speed classes, see Figure 4;

- Weibull distribution plots and parameters as reported in Figure 5.

Table 2: On site masts

MAST	*Long. East*	*Latitude North*	*Alt. (m)*
MAST1	626938	4304099	50
MAST2	625829	4304814	66

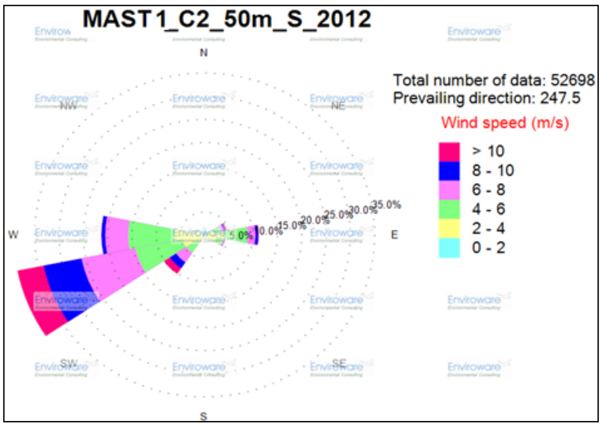

Figure 2: Prevailing wind direction for MAST1 at 50 m height

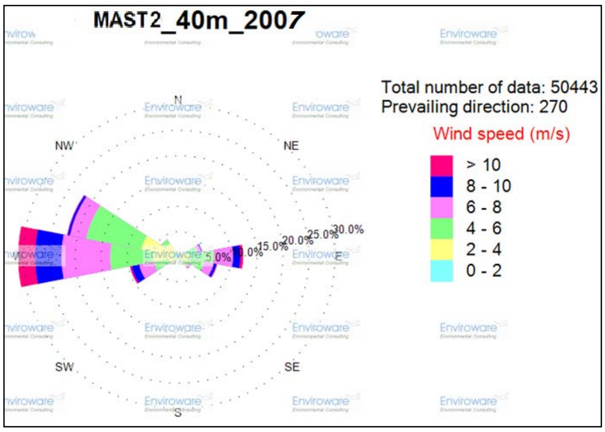

Figure 3: Prevailing wind direction for MAST2 at 40 m height

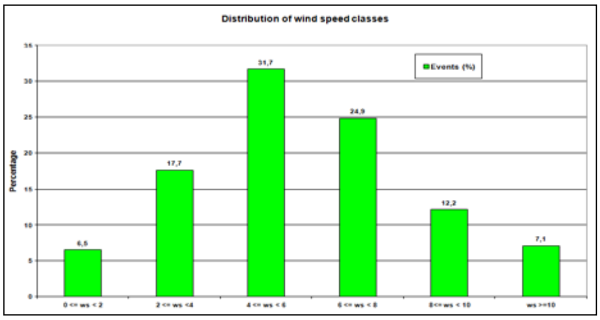

Figure 4: Distribution of wind speed classes for MAST2 at 40 m height

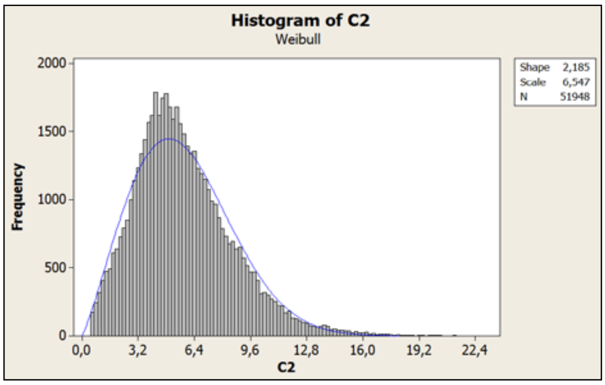

Figure 5: Weibull data distribution for MAST1 at 50 m height

Wind data analysis highlights that input data available for the simulation model are:

- MAST1: data from 01/01/2012 to 01/01/2013 registered at 50 m;
- MAST2: data from 01/01/2007 to 01/01/2008 registered at 40 m.

3.3. Digital Terrain Model (DTM)

As before mentioned, a digital terrain model has been generated through the software tool WindSim Express 7.0 by using the following on-line available resources:

- *ASTER GDEM v2 Worldwide Elevation Data (1 arc-second Resolution)* for elevation;
- *VCF Tree Cover Worldwide 2005 (500 m Resolution)* for roughness maps.

Table 3 reports DTM position, size and resolution in UTM-WGS 84 coordinate system while Figures 6 shows DTM elevation and roughness. Finally, in Figure 7 the WF layout (27 WTGs) including masts is represented.

Table 3: DTM size

	Min. (m)	*Max. (m)*	*Size (m)*	*Resol. (m)*
Easting (m)	620374	631950	11576	38.1
Northing (m)	4297892	4309469	11578	38.1

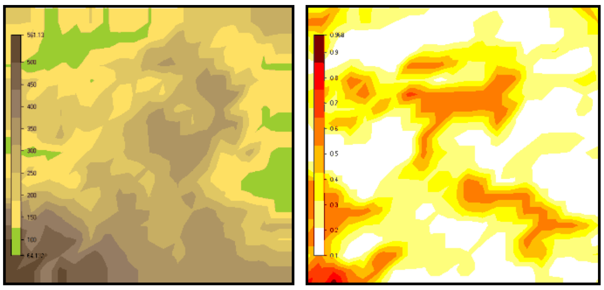

Figure 6: DTM elevation (left) and roughness (right)

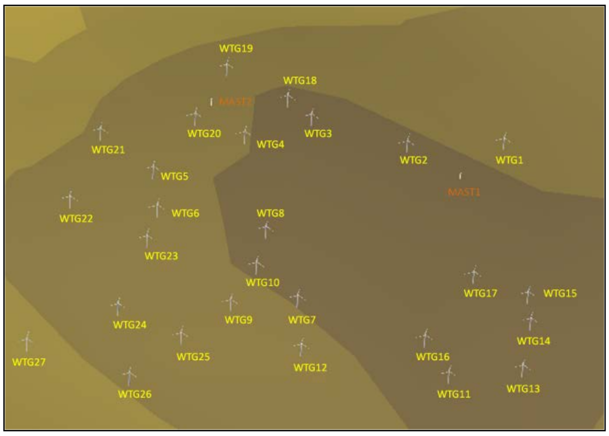

Figure 7: Wind Farm layout

4. SIMULATION MODEL VALIDATION

The digital terrain model is then introduced in the post-processor tool WindSim 7.0 in order to evaluate average wind speed at each WTG, wake effects, wind farm power assessment, full load hours.

Before carrying out specific analyses in order to test system performance in terms of energy production under different wake models, the simulation model was validated.

According to Balci (1998), validation is the process of determining the degree to which a model is an accurate representation of the real world from the perspective of the intended use of the model.

Data used for simulation model validation are wind farm annual energy production (AEP) from January 2011 to December 2015, see Table 4.

Table 4: Wind Farm real AEP (MWh)

	Real AEP
2011	97816,08
2012	110321,15
2013	109349,25
2014	102214,99
2015	98655,53
Av.	***103671,4***

The smallest estimated AEP given by the simulation model implemented is 111445 MWh/year which becomes 103643,85 MWh/year if a reduction of 7% related to technical losses (i.e. turbines internal/ external losses, machines availability, etc.) is considered.

Comparing the real AEP of the wind farm (which average value from 2011 to 2015 is 103671,4 MWh/year) with the simulated one (103643,85 MWh/year), they are quite similar. As a consequence, the simulation model implemented is an accurate representation of the real wind farm and wind input data chosen for each mast represent accurately the terrain and climatology complexity of the wind farm site.

5. SIMULATION RESULTS ANALYSIS

As before mentioned, the objective is of this research work is to implement a support tool (a simulator) to be used for carrying out specific analyses in order to test system performance in terms of energy production under different wake models. More in detail, three different scenarios corresponding to wake models considered, i.e. Jensen, Larsen, Ishihara, have been implemented; for each wake model wake losses, net AEP and full load hours have been monitored as system performance parameters.

In addition, according to Gonzalez-Longatt *et al.* (2012), the authors for evaluating the overall impact of wake effects on the output AEP of the wind farm, introduce a wake coefficient parameter (WCP) defined as follows:

$$WCP = \frac{Net\ AEP}{Gross\ AEP} \quad (8)$$

This parameter combines all the local wake effects at each WTG into a single measure of the overall wake effects of the wind farm.

Table 5 shows for each wind turbine generator its simulated Gross annual energy production (Gross AEP), i.e. not affected by wake effects, estimated in 124,483 GWh/year for the whole wind farm.

Table 5: Gross AEP (GWh/year)

WTG	***No Wake Model***
WTG1	4,123
WTG2	4,678
WTG3	4,813
WTG4	4,645
WTG5	4,438
WTG6	4,408
WTG7	4,463
WTG8	4,543
WTG9	4,278
WTG10	4,472
WTG11	4,794
WTG12	4,309
WTG13	5,024
WTG14	5,045
WTG15	4,962
WTG16	4,786
WTG17	4,81
WTG18	5,379
WTG19	4,749
WTG20	4,893
WTG21	4,419
WTG22	4,482
WTG23	4,736
WTG24	4,467
WTG25	4,461
WTG26	4,224
WTG27	4,082
Tot.	**124,483**

Tables 6 – 7 – 8 report respectively simulation results for each WTG related to wake losses (%), Net AEP (GWh/year), i.e. gross AEP with wake losses, and full load hours (hours) respectively for Jensen, Larsen and Ishihara wake models implemented.

Table 6: Wake losses (%)

WTG	*Jensen*	*Larsen*	*Ishihara*
WTG1	9,733	4,14	10,04
WTG2	9,583	4,263	9
WTG3	18,872	7,862	18,07
WTG4	17,743	6,374	17,38
WTG5	6,043	3,067	5,52
WTG6	11,92	4,912	12,29
WTG7	22,669	8,585	24,95
WTG8	10,969	4,682	11,38
WTG9	17,427	6,379	17,27
WTG10	9,386	4,213	8,39
WTG11	6,657	3,069	6,92
WTG12	13,787	5,467	13,64
WTG13	15,755	5,858	16,17
WTG14	8,349	3,744	8,16
WTG15	8,305	4,431	7,58
WTG16	11,661	4,831	10,92
WTG17	7,291	3,281	7,07
WTG18	12,111	5,583	10,93
WTG19	3,122	1,396	3,3
WTG20	12,451	4,799	12,58
WTG21	4,051	1,779	3,78
WTG22	4,42	1,785	4,66
WTG23	8,169	3,283	8,21
WTG24	8,92	3,476	8,47
WTG25	13,568	5,606	12,71
WTG26	5,521	2,571	4,72
WTG27	3,276	1,298	3,09
Av.	**10,435**	**4,323**	**10,266**

As showed in Table 6 and Figure 8, Jensen and Ishihara wake models estimate similar wake losses while Larsen model predicts the smallest ones.

According to Equation 3, Larsen wake model predicts a larger initial wake expansion than that evaluated by the other two models; in addition this model introduces all the climatology parameters at the WTG hub height.

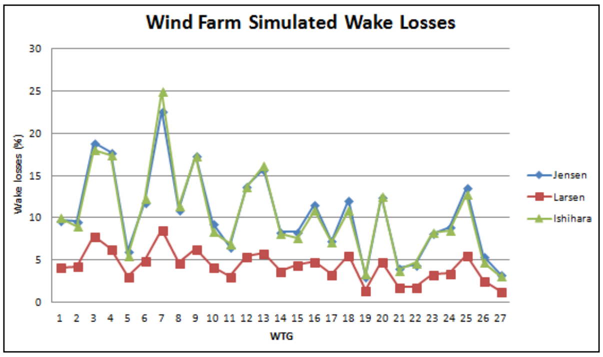

Figure 8: Wind Farm wake losses for each WTG

As a consequence, annual net AEP and full load hours reflect the same trend, see Tables 7 – 8 and Figures 9 – 10. In addition, wake coefficient parameters (WCP) for Jensen and Ishihara models are quite similar and smaller than Larsen, see Equations 9 – 10 – 11.

Table 7: Net AEP (GWh/year)

WTG	*Jensen*	*Larsen*	*Ishihara*
WTG1	3,722	3,953	3,709
WTG2	4,23	4,479	4,257
WTG3	3,905	4,435	3,943
WTG4	3,821	4,349	3,837
WTG5	4,17	4,302	4,193
WTG6	3,882	4,191	3,866
WTG7	3,452	4,08	3,349
WTG8	4,045	4,33	4,026
WTG9	3,533	4,005	3,539
WTG10	4,053	4,284	4,097
WTG11	4,475	4,647	4,461
WTG12	3,715	4,074	3,721
WTG13	4,232	4,729	4,211
WTG14	4,624	4,856	4,633
WTG15	4,55	4,742	4,586
WTG16	4,228	4,555	4,263
WTG17	4,459	4,652	4,469
WTG18	4,728	5,079	4,791
WTG19	4,601	4,683	4,592
WTG20	4,284	4,658	4,277
WTG21	4,24	4,34	4,252
WTG22	4,283	4,402	4,272
WTG23	4,349	4,581	4,347
WTG24	4,069	4,312	4,088
WTG25	3,856	4,211	3,894
WTG26	3,991	4,116	4,024
WTG27	3,948	4,029	3,955
Tot.	**111,445**	**119,074**	**111,663**

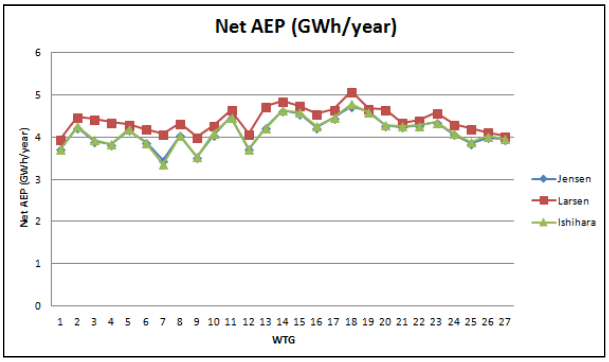

Figure 9: Wind Farm Net AEP for each WTG

$$WCP^{Jensen} = \frac{Net\ AEP^{Jensen}}{Gross\ AEP} = \frac{111{,}445}{124{,}483} = 0{,}895 \qquad (9)$$

$$WCP^{Larsen} = \frac{Net\ AEP^{Larsen}}{Gross\ AEP} = \frac{119{,}074}{124{,}483} = 0{,}95 \qquad (10)$$

$$WCP^{Ishihara} = \frac{Net\ AEP^{Ishihara}}{Gross\ AEP} = \frac{111{,}663}{124{,}483} = 0{,}897 \quad (11)$$

Table 8: Full load hours (hours)

WTG	*Jensen*	*Larsen*	*Ishihara*
WTG1	1860,95	1976,25	1854,6
WTG2	2114,85	2239,3	2128,6
WTG3	1952,35	2217,3	1971,6
WTG4	1910,55	2174,6	1918,9
WTG5	2084,95	2151	2096,5
WTG6	1941,25	2095,7	1933
WTG7	1725,8	2040,1	1674,9
WTG8	2022,3	2165,1	2013,1
WTG9	1766,4	2002,75	1769,8
WTG10	2026,3	2142	2048,6
WTG11	2237,25	2323,25	2230,9
WTG12	1857,55	2036,8	1860,7
WTG13	2116,15	2364,75	2105,7
WTG14	2311,95	2428,1	2316,7
WTG15	2275,1	2371,2	2293,2
WTG16	2114	2277,45	2131,8
WTG17	2229,65	2326,1	2234,9
WTG18	2306,24	2477,56	2337,2
WTG19	2244,43	2284,43	2240,3
WTG20	2089,61	2272,24	2086,6
WTG21	2068,29	2117,26	2074,1
WTG22	2089,46	2147,07	2084,3
WTG23	2121,51	2234,39	2120,6
WTG24	1984,82	2103,46	1994,6
WTG25	1880,87	2054,14	1899,5
WTG26	1946,82	2007,61	1963,4
WTG27	1925,90	1965,26	1929,6
Av.	**2044,64**	**2185**	**2048,65**

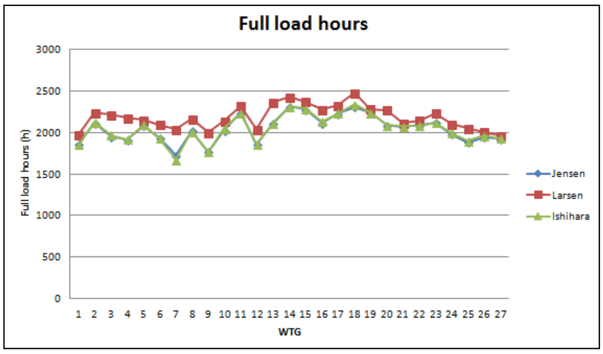

Figure 10: Wind Farm Full load hours for each WTG

6. CONCLUSIONS

This research work focuses on a wind farm located in Calabria (Italy) characterized by complex terrain.

A simulation model is implemented to test system performance in terms of energy production under three different wake models, i.e. Jensen, Larsen, Ishihara.

After the modeling phase, the simulator has been validated by using annual energy production data of the existing wind farm from January 2011 to December 2015.

Three different scenarios corresponding to wake models considered have been implemented; for each model wake losses, Net AEP, full load hours have been monitored as system performance parameters.

REFERENCES

Balci O., (1998). Verification, Validation and Testing. In: J. Banks, Handbook of Simulation, John Wiley & Sons, Inc., 335–393.

Bruzzone, A.G., Tremori, A., Tarone, F., Madeo, F. (2011). Intelligent agents driving computer generated forces for simulating human behaviour in urban riots. International Journal of Simulation and Process Modelling, Volume 6, Issue 4, pp 308-316

Crasto G., Gravdahl A.R., (2008). CFD wake modeling using a porous disc. Proceedings of the European Wind Energy Conference Exhibition.

Curcio, D. , Longo, F. (2009). Inventory and internal logistics management as critical factors affecting the Supply Chain performances. International Journal of Simulation and Process Modelling, Volume 5, Issue 4, pp. 278-288

Gonzalez-Longatt F., Wall P., Terzija V., (2012). Wake effect in wind farm performance: Steady-state and dynamic behavior. Renewable Energy.

Grassi S., Junghans S., Raubal M., (2014). Assessment of the wake effect on the energy production of onshore wind farm using GIS. Applied Energy, in press.

Jensen N.O., (1983). A note on wind generator interaction. Technical report Riso-M-2411.

Kiranoudis C.T., Maroulis Z.B., (1997). Effective short-cut modelling of wind park efficiency. Renewable Energy, 11, 439–457.

Kozmar H., Allori D., Bartoli G., Borri C., (2016). Complex terrain effects on wake characteristics of a parked wind turbine. Engineering Structures, 110, 363–374.

Lissaman P.B.S., (1979). Energy efficiencies of arbitrary of wind turbines. Journal of Energy, 3.

Longo, F., (2012-a). Sustainable supply chain design: An application example in local business retail. Simulation, Volume 88, Issue 12, pp 1484-1498.

Longo, F. (2012-b). Supply chain security: An integrated framework for container terminal facilities. International Journal of Simulation and Process Modelling, Volume 7, Issue 3, pp 159-167.

Longo F., Massei M., Nicoletti L. (2012). An application of modeling and simulation to support industrial plants design. International Journal of Modeling, Simulation, and Scientific Computing Volume 3, Issue 1, Article number 1240001

Pérez E., Ntaimo L., Ding Y. (2015). Multi-component wind turbine modeling and simulation for wind farm operations and maintenance. Simulation, Volume 91, Issue 4, pp 360-382

Shakoor R., Hassan M.Y., Raheem A., Rasheed N., (2015). The modelling of wind farm layout

optimization for the reduction of wake losses. Indian Journal of Science and Technology, 8 (17), 69817.
Shakoor R., Hassan M.Y., Raheem A., Wu Y., (2016). Wake effect modeling: A review of wind farm layout optimization using Jensen's model. Renewable and Sustainable Energy Reviews, 58, 1048–1059.
Smith D., Taylor G.J., (1991). Further analysis of turbine wake development and interaction data. Proceedings of 13th BWEA Conference, pp. 280–292. Swansea (Wales).
Vermeer L.J., Sorensen J.N., Crespo A., (2003). Wind turbine wake aerodynamics. Progress in Aerospace Sciences, 39 (6–7), 467–510.
Voutsinas S., Rados K., Zervos A., (1990). On the analysis of wake effects in wind parks. Wind Engineering, 14.
Yang X., Howard K.B., Guala M., Sotiropoulos F., (2015). Effects of a three-dimensional hill on the wake characteristics of a model wind turbine. Physical Fluids, 27.
Zervos A., Huberson S., Hermom A., (1988). Three-dimensional free-wake calculation of wind turbine wake. Journal of Wind Engineering and Industrial Aerodynamics, 27–65.

AUTHORS BIOGRAPHIES

DUILIO CURCIO was born in Vibo Valentia (Italy), on December the 15th, 1981. He took the degree in Mechanical Engineering from University of Calabria in 2006 and he received the PhD in Mechanical Engineering at the same University in February 2010. Now he collaborates with Public Authorities for technical consulting.

GIUSEPPE FILARDO was born in Lamezia Terme (Italy), on March the 9th, 1981. He took the degree in Energy Engineering from University of Calabria in 2008. He is currently a freelance engineer operating in the field of renewable energy plants design and management.

Author's Index